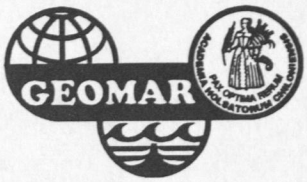

RAINER ZAHN

NORTH ATLANTIC THERMOHALINE CIRCULATION DURING THE LAST GLACIAL PERIOD: EVIDENCE FOR COUPLING BETWEEN MELTWATER EVENTS AND CONVECTIVE INSTABILITY

GEOMAR
Forschungszentrum
für marine Geowissenschaften
der Christian-Albrechts-Universität
zu Kiel

Kiel 1997

GEOMAR REPORT 63

GEOMAR
Research Center
for Marine Geosciences
Christian Albrechts University
in Kiel

Habilitationsschrift / Habilitation Thesis
zur Erlangung der venia legendi
im Fach Geologie
vorgelegt der
Mathematisch-Naturwissenschaftlichen Fakultät
der Christian-Albrechts-Universität zu Kiel

Redaktion der Serie: Gerhard Haass
Umschlag: Kerstin Kreis, Harald Gross, GEOMAR Technologie GmbH

Managing Editor: Gerhard Haass
Cover: Kerstin Kreis, Harald Gross, GEOMAR Technologie GmbH

GEOMAR REPORT
ISSN 0936 - 5788

GEOMAR REPORT
ISSN 0936 - 5788

GEOMAR
Forschungszentrum
für marine Geowissenschaften
D-24148 Kiel
Wischhofstr. 1-3
Telefon (0431) 600-2555, 600-2505

GEOMAR
Research Center
for Marine Geosciences
D-24148 Kiel / Germany
Wischhofstr. 1-3
Telephone (49) 431 / 600-2555, 600-2505

TABLE OF CONTENTS

1.0 INTRODUCTION

1.1 The Marine and Ice Core Record of Ocean and Climate Change

The evolution of global climate is intimately tied to the mode and strength of the ocean's thermohaline circulation. The causal links between thermohaline forcing and climatic response are not understood in full detail, but there is general agreement that the ocean's thermohaline circulation may act as a catalyst for climatic change [Broecker and Denton, 1989; Boyle, 1990; Sarnthein and Altenbach, 1995]. Atmospheric circulation models suggest that thermohaline overturn in the glacial maximum North Atlantic may have held oceanic heat transport close to modern levels [Macdonald and Wunsch, 1996]. Enhanced mid-depth ventilation - at water depths above 2000 m - of the North Atlantic is indeed suggested by the distribution of paleoceanographic proxies that have been compiled from glacial-maximum sections of mid-depth sediment cores [Duplessy et al., 1988; Lehman and Keigwin, 1992; Yu et al., 1995; Sarnthein et al., 1995]. The lead of southern hemisphere climate relative to global ice volume has been linked to an early response of thermohaline overturn in the high-latitude North Atlantic to orbital forcing that is transmitted to the south by southward flowing deeper water masses [Crowley, 1992; Imbrie et al., 1992]. These conceptual models explain the long-term evolution of ocean and climate change in terms of varying planetary energy budgets that are driven by variations of the Earth's orbital parameters on time scales of 10^4-10^5 years, and associated changes in solar radiation - the so-called Milankovitch cycles of climate change [Milankovitch, 1941; Ruddiman and McIntyre, 1984; Berger et al., 1994].

Ice core proxy-records from the Greenland ice cap that monitor the variability of climate in the North Atlantic region have added considerably to our understanding of ocean and climate change in that they provide convincing evidence for significant climatic variability on sub-Milankovitch ($<10^4$ yr) time scales (Figure 1). The ice core data show that the last glacial period, and the subsequent glacial-interglacial climate transition, were punctuated by rapid and high-amplitude climatic variation - the Dansgaard-Oeschger oscillations - that resulted in annual mean temperature increases of up to 7°C, lasting for several

hundred years and then disappearing within decades [Dansgaard et al., 1993; Grootes et al., 1993; Taylor et al., 1993]. Similar variability - even though documented at a lesser resolution - is also seen in various sediment properties from North Atlantic sediment cores and in cores from the Norwegian-Greenland Seas (Figure 1) [Bond et al., 1992, 1993; Keigwin and Lehman, 1992; Grousset et al., 1993; Sarnthein et al., 1994; Fronval et al., 1995; Rasmussen et al., 1996 a, b].

1.2 'Heinrich' Events as Examples for Rapid Climatic Change

The most outstanding documentation of rapid climatic variation in marine records from the northern North Atlantic are sedimentary sequences that are faunally nearly barren and enriched in ice-rafted detritus (IRD) [Ruddiman, 1977; Heinrich, 1988; Broecker et al., 1992; Alley and MacAyeal, 1994; Broecker, 1994]. These so-called 'Heinrich' layers have been attributed to sporadic collapses of the Laurentide ice sheet in response to ice sheet instability that occurred episodically during the last glacial and triggered sudden surges of icebergs to the North Atlantic [Heinrich, 1988; Broecker et al., 1992; Alley and MacAyeal, 1994; Broecker, 1994]. Based on a conceptual model that invokes free ice sheet oscillation as a function of atmospheric and geothermal parameters, it has been predicted that the 'Heinrich'-IRD events were accompanied by a fresh water flux to the North Atlantic in the order of 0.16 Sv over a period of 250-500 years [MacAyeal, 1993]. Negative planktonic foraminiferal $\delta^{18}O$ excursions in conjunction with increased abundances of polar planktonic foraminiferal species which are characteristic features of the 'Heinrich' layers lend support to this hypothesis [Bond et al., 1993; Keigwin and Lehman, 1994; Bond and Lotti, 1995]. This evidence has been used to infer that the density of North Atlantic surface waters was lowered during these periods thus enhancing the buoyancy of the surface layer to an extent that vertical overturn spun down or was brought to a complete halt [Maslin et al., 1995]. This would be consistent with numerical simulations which have shown that freshwater forcing of much shorter duration and smaller magnitude may cause convective instabilities that weaken or temporarily even terminate deep convection in the North Atlantic [Paillard and Labeyrie, 1994; Rahmstorf, 1994; 1995; Weaver and Hughes 1994;

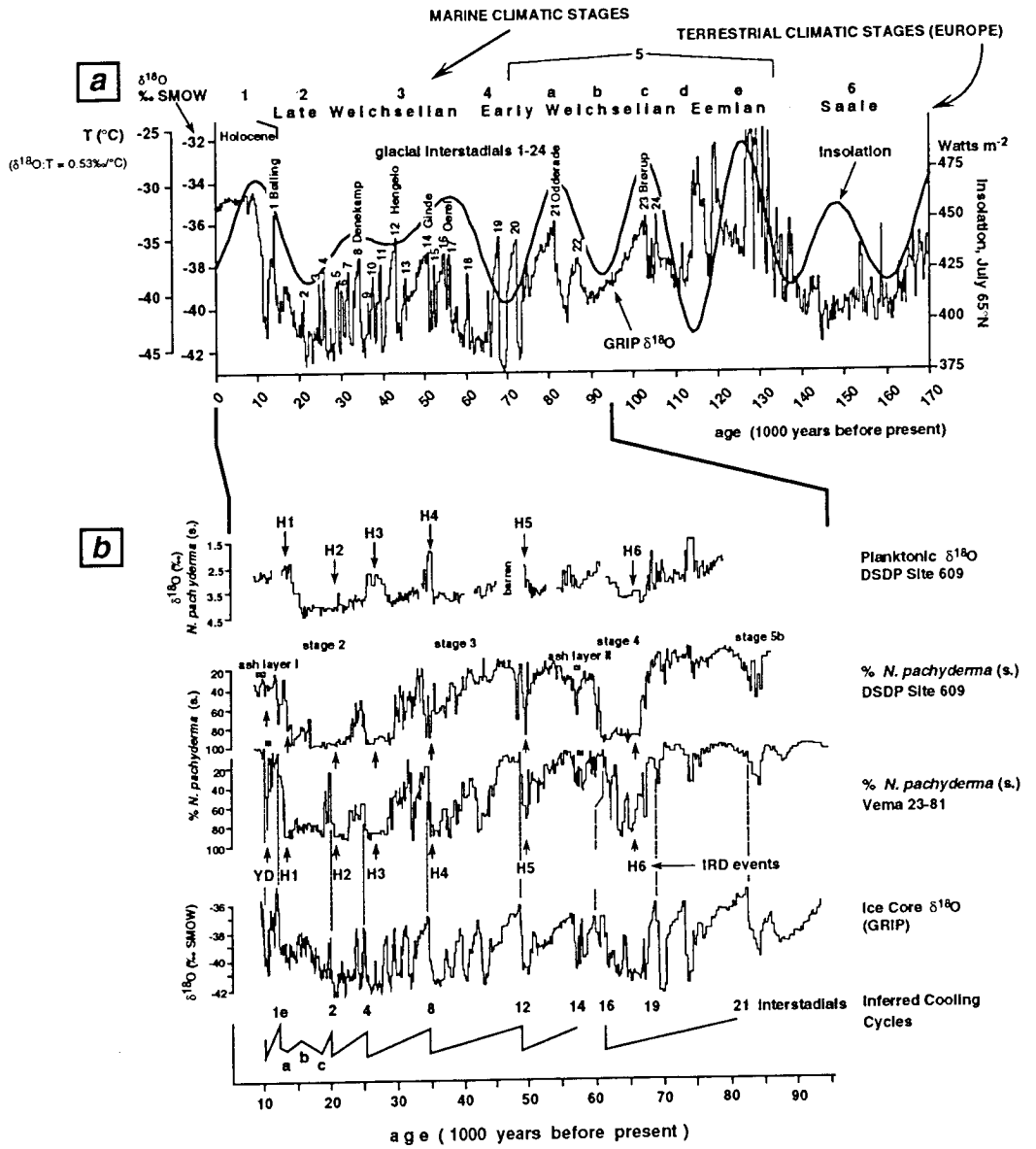

Figure 1. (a) The Greenland ice core record provides evidence for rapid oscillations of climate during the last glacial period (after Dansgaard et al. [1993]). (b) Similar oscillations are found in paleoceanographic proxy records at northern North Atlantic Sites 609 and V23-81 (Bond et al. [1993]). The correlation between the ice core and marine data are used to infer a close coupling between atmospheric and surface ocean forcing in the northern North Atlantic. Redrawn after Bond et al. [1993].

Manabe & Stouffer 1995].

1.3 Impact of 'Heinrich' Events on North Atlantic Thermohaline Circulation: Paleoceanographic Data and Modelling Approaches

Paleoceanographic research in the North Atlantic has long revealed the close relation between changing glacial-interglacial surface ocean conditions and the strength of thermohaline overturn [e.g., Mix and Fairbanks, 1985; Boyle and Keigwin, 1987], the so-called conveyor-belt circulation [Broecker et al., 1990]. Using changes of planktonic foraminiferal communities as indicators for changing surface conditions, CLIMAP [1981] inferred a southward shift of the North Atlantic polar front from the Norwegian-Greenland Seas to the northern North Atlantic, around 40°N. Convection of deep waters also shifted southward into the northern North Atlantic. The reduction in thermal disequilibrium between surface waters and overlying atmosphere that was associated with the southward shift of the polar front likely caused evaporation rates to decrease leading to lower salinities and densities of surface waters which ultimately should have resulted in reduced rates of convection in the North Atlantic [Boyle and Keigwin, 1987; Duplessy et al., 1988; Sarnthein et al., 1994].

Compilation of planktonic and benthic foraminiferal $\delta^{13}C$ along meridional transects documents in detail the changes in the North Atlantic's vertical water mass structure that went along with changes in surface ocean conditions [Duplessy et al., 1988; Sarnthein et al., 1994]. The principal change was a shift in depth of the core layer from 3000 m to around 2000 m during the last glacial in response to enhanced buoyancy of convecting water masses. Only in the immediate vicinity of convection, i.e. north of 45°N, did the influence of newly-convected deep waters reach water depths similar to today [Sarnthein et al., 1994]. Ocean general circulation models that were devised to test the sensitivity of North Atlantic thermohaline overturn to various freshwater and heat flux conditions confirmed the existence of a variety of stable modes of thermohaline circulation. Each mode is characterised by its own rates and depths of convection and imposes different states of climate upon the North Atlantic region [Bryan, 1986; Manabe and Stouffer, 1988; Mikolajewicz and Maier-Reimer, 1990;

Fichefet et al., 1994; Bintanja and Oerlemans, 1996; Rahmstorf, 1996; Seidov et al., 1996].

Evidence for rapid and high-amplitude climatic oscillations during the last glacial period and the last deglacial recorded in Greenland ice cores [Dansgaard et al., 1993; Grootes et al., 1993; Taylor et al., 1993] has provided new momentum to the search for links between climate change and the ocean's thermohaline circulation. Marine records from the North Atlantic region show some correlation with the ice core data from Greenland providing circumstantial evidence for changes of the North Atlantic's circulation in association with rapid fluctuations of the regional climate [Lehman and Keigwin, 1992; Sarnthein et al., 1992; Bond et al., 1993; Weinelt, 1993; Bond and Lotti, 1995; Fronval et al., 1995; Sarnthein et al., 1995; Jung, 1996; Rasmussen 1996 a, b].

Various models have been proposed to evaluate potential forcing factors that may have contributed to the climatic oscillations. The most striking result of the models [Rahmstorf, 1994; Paillard and Labeyrie, 1994; Weaver and Hughes, 1994; Rahmstorf, 1996] is that rapid and high-amplitude climatic changes that closely resemble those seen in the Greenland ice core record do not necessarily need to be linked to dramatic changes of thermohaline circulation e.g., a total collapse of convection in the North Atlantic and a shut-down and later resumption of the conveyor-belt circulation as has been proposed previously [Stommel, 1961; Broecker et al., 1985]. Instead, changes in northward heat transport may occur either through changes of the conveyor's mass transport or changes of its temperature. The former would be driven by various rates of freshwater flux in association with changes in the hydrological cycle resulting in a weaker conveyor [Weaver and Hughes, 1994]. The latter would be driven by shifts of convection sites from colder (higher) latitudes (e.g., Norwegian-Greenland Seas; NGS) to warmer (lower) latitudes (e.g., Labrador Sea) while convection continues at similar rates [Rahmstorf, 1994].

A further important feature of the models is that thermohaline overturn displays a hysteresis response to changes in external forcing in that convection and forcing are linked in a non-linear fashion [Stocker and Wright, 1991; Mikolajewicz and Maier-Reimer, 1994; Rahmstorf, 1995]. Convective overturn

first declines gradually as freshwater input to the North Atlantic increases, and then collapses abruptly once freshwater forcing exceeds a certain threshold value. After freshwater input has decreased to its initial value, a new stable mode is found with different convection rates. The response of thermohaline circulation to enhanced inputs of freshwater, either through varying rates of precipitation or meltwater flux, or through changes of surface circulation, does not depend so much on the total amount of freshwater input but more on whether or not the freshwater is targeted directly at the site of convection.

The general features of these theoretical considerations have been confirmed by 3-D model runs that use North Atlantic sea surface temperature and salinity reconstructed from paleoceanographic time series [Seidov et al., 1996]. In the 3-D model three different modes of circulation occur that are a function of glacial, deglacial, and post-glacial surface boundary conditions: (1) a glacial mode of convection where convection is reduced by some 30% relative to its modern value in response to a southward shift by 10° latitude of convection sites and resultant changes in surface temperature and salinity; the mode of circulation is similar to that of modern winter time circulation; (2) a meltwater mode of circulation in which a prominent freshwater incursion that is documented in marine records from the Norwegian-Greenland Seas during the early stages of the last deglaciation (14.2-13.2 ^{14}C-kyr; Weinelt [1993], Sarnthein et al. [1995]) leads to an intermittent shut-down of convection and a current reversal with a southward surface flow and a northward deeper flow; (3) a modern mode of circulation with meridional overturning, deep export of NADW to the south, and weaker abyssal AABW advection to the north [Seidov et al., 1996]. The early deglacial meltwater event undoubtedly was of much larger magnitude than the freshwater spikes used e.g., by Weaver and Hughes [1994] and Rahmstorf [1995] to produce convective instability, but it was targeted at the northernmost North Atlantic and the Norwegian-Greenland Seas i.e., areas where deep convection occurs and which are especially vulnerable to changes of surface conditions.

'Heinrich' events are thought of as intermittent periods of iceberg surges and meltwater flow from the Laurentide and Scandinavian ice sheets that occurred during the last glacial period [Bond and Lotti, 1995]. Iceberg drift and

associated meltwater flow during the events was largest in a belt between 40° and 50°N across the North Atlantic [Ruddiman, 1977; Bond et al., 1992], an oceanographically important region that was close to sites of convection during the last glacial [Duplessy et al., 1992; Sarnthein et al., 1994; Seidov et al., 1996]. Paleoceanographic studies at northern North Atlantic sites have suggested that 'Heinrich' events caused a significant drop of surface temperatures and salinities, and resulted in changes of surface circulation [Bond et al., 1993; Maslin, 1995; Maslin et al., 1995; Sarnthein et al., 1995]. Enhanced meltwater flux during the 'Heinrich' events in this area thus likely induced convective instabilities that would have slowed-down or even stopped thermohaline overturn. As such, 'Heinrich' events provide potentially valuable records of the sensitivity of thermohaline circulation to perturbations of external forcing.

2.0 SCIENTIFIC OBJECTIVES AND STRATEGIES

In this thesis I use benthic and planktonic stable isotope records in conjunction with records of IRD abundance and mineralogy along sediment cores from the southern Portuguese margin to monitor the North Atlantic's ventilation response to the 'Heinrich' events (Figure 2, Table 1). Special emphasis is given to the evolution of Mediterranean Outflow Water (MOW) in association with other North Atlantic mid-depth water masses, which are monitored at sediment cores from the upper Portuguese margin at water depths above 1500 m. Today, these cores are in the northward advection path of MOW that flows at water depths between 700 and 1400 m along the western Iberian margin [Zenk and Armi, 1990].

Because the Portuguese margin is outside the North Atlantic's belt of maximum IRD deposition, hemipelagic sedimentation continued during the 'Heinrich' events and abundances of planktonic and benthic foraminifers remained high enough to allow for continuous stable isotope records and detailed ^{14}C-AMS dating across the IRD layers. Furthermore, sedimentation rates at the upper Portuguese margin are higher by a factor of three compared to the open North Atlantic and allow to monitor ventilation changes during the

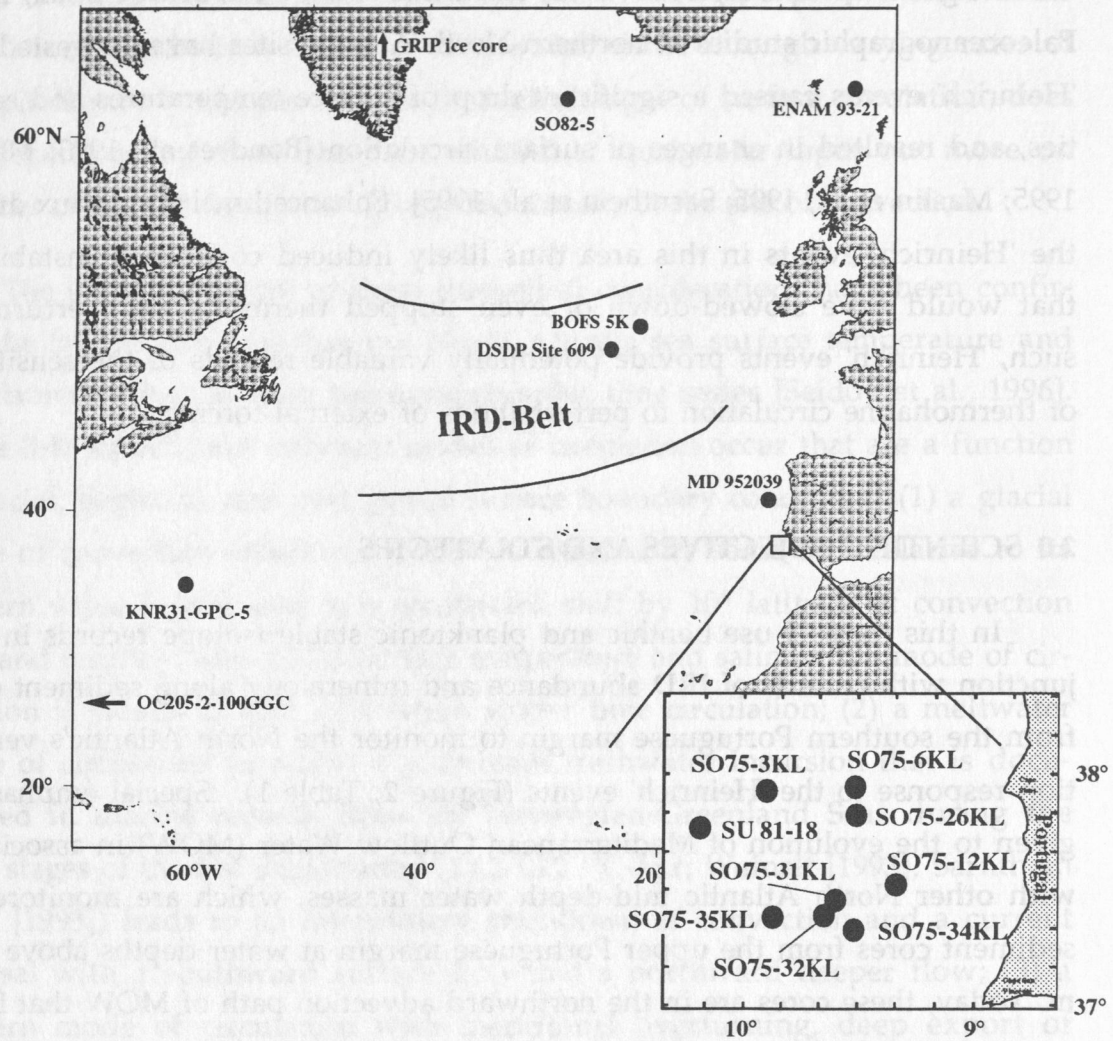

Figure 2. Location of sediment cores from the southern Portuguese margin and the subtropical and northern North Atlantic that are used in this thesis. See also Table 1.

Table 1. Location of sediment cores used in this thesis

Core	latitude	longitude	water depth	region	source
SO75-3KL	37°55.2'N	09°54.0'W	2430 m	Portuguese margin	this study
SO75-6KL	37°56.3'N	09°30.4'W	1281 m	Portuguese margin	this study
SO75-12KL	37°31.6'N	09°19.9'W	819 m	Portuguese margin	this study
SO75-26KL	37°49.3'N	09°30.2'W	1099 m	Portuguese margin	this study
SO75-31KL	37°27.8'N	09°36.0'W	1708 m	Portuguese margin	this study
SO75-32KL	37°23.0'N	09°38.2'W	1873 m	Portuguese margin	this study
SO75-35KL	37°21.8'N	09°52.1'W	3582 m	Portuguese margin	this study
MD95-2039	40°34.7'N	10°20.9'W	3381 m	Portuguese margin	this study
SO82-5	59°11.3'N	30°54.5'W	1416 m	Reykjanes Ridge	Jung [1996]
ENAM91-23	62°44.0'N	03°59.9'W	1020 m	Faeroe-Shetland Channel	Rasmussen et al. [1996a, b]
16004-1	29°58.7'N	10°38.8'W	1512 m	Moroccan margin	Zahn et al. [1987]
OC205-2-100GGC	26.061°N	78.028°W	1045 m	Bahamas	Slowey and Curry [1995]
BOFS-5K	50°41.3'N	21°51.9'W	3547 m	Rockall Plateau area	Maslin et al. [1995]
KNR31-GPC-5	34.3°N	57.9°W	4500 m	Bermuda Rise	Keigwin and Jones [1994]

'Heinrich' events at much higher resolution.

Planktonic $\delta^{18}O$ variation will be used to infer the timing and extent of surface ocean change off Portugal during the 'Heinrich' events. In conjunction with foraminiferal census counts, surface temperature and salinity changes will be deduced and compared to similar records from the northern North Atlantic. Benthic $\delta^{18}O$ will be used to monitor the variable contribution of Mediterranean Outflow Water to the upper Portuguese margin. The concept of $\delta^{18}O$ equilibrium fractionation in T-S fields will be applied to estimate possible contribution of cold and low-salinity mid-depth waters from the open North Atlantic - as opposed to warm high-salinity Mediterranean waters - to the Portuguese margin.

Benthic $\delta^{13}C$ records will provide insight into the degree of mid-depth ventilation during the 'Heinrich' events. The data are compared with marine records from the northern and subtropical North Atlantic and the Greenland ice core record to determine the relation between North Atlantic climate and thermohaline circulation. The benthic $\delta^{13}C$ data will also serve as proxies in an attempt to quantify water mass oxygen levels as a primary indicator of ventilation. Finally, the benthic $\delta^{13}C$ record from the upper Portuguese margin is compared to paleoceanographic proxy records from the shallow northern and deep subtropical North Atlantic and to the ice core records from Greenland and Antarctic to provide an interhemispheric perspective of rapid climate change and its effects on thermohaline circulation.

2.1 Relation to Submitted, Accepted and Published Manuscripts

The evolution of the Mediterranean Outflow and mid-depth ventilation at the upper Portuguese margin and its implications for thermohaline circulation is subject of a manuscript that has been recently accepted for publication in *Paleoceanography* [Zahn et al., 1997]. Central parts of the chapters on stratigraphy and the interpretation of benthic $\delta^{18}O$ and $\delta^{13}C$ in this thesis are either directly taken from or expand on the discussions in this manuscript. I provide the manuscript as an attachment to this thesis. The discussion of Mediterranean paleoceanography in this thesis is related to the review that is provided in

the *ODP Leg 161 Initial Reports* introductory chapter on western Mediterranean tectonics and paleoceanography [Comas, Zahn, Klaus et al., 1996].

Estimation of absolute water mass O_2 levels is part of the manuscript by J. Baass, J. Schönfeld and R. Zahn that has been submitted in December 1996 to the ENAM special issue of *Marine Geology* (guest editor J. Mienert, GEOMAR). This manuscript is currently under review. The O_2 estimates given in this manuscript deviate from those discussed in this thesis. They require revision in view of the revised T-S estimates from benthic $\delta^{18}O$ in Zahn et al. [1997] and in this thesis, and in view of glacial-interglacial changes of mean-ocean $\delta^{13}C_{\Sigma CO2}$. These revisions will be done after the reviews have been received from the editor of the *Marine Geology* ENAM special issue.

3.0 THE WESTERN IBERIAN MARGIN: OCEANOGRAPHIC SETTING AND PALEOCEANOGRAPHIC EVOLUTION

The surface hydrography at the Portuguese margin today is defined by equatorward advection of surface waters in the Portugal current that extends southward into the Canary Current and comprises the northern part of the North Atlantic's eastern boundary current [Wooster et al., 1976] . During autumn and winter, a nearshore northward surface current develops in response to weakened southward trade winds and is associated with a northward advection of warm saline surface waters along the western Iberian margin [Haynes and Barton, 1990]. This current is opposite to the summer-time surface circulation when the Portugal Current carries cold surface waters to the south that are derived from upwelling of subsurface waters in local upwelling patches which occur over the entire shelf and upper continental slope off Portugal [Fuiza, 1982 and 1983].

The hydrography of deeper water masses at the Portuguese margin is defined by the advection of North Atlantic Central Water (NACW), Mediterranean Outflow Water (MOW), upper and lower North Atlantic Deep Water (NADW), and Antarctic Bottom Water (AABW) (Figure 3) [Harvey and Theodorou, 1986; McCartney, 1992; Schmitz and McCartney, 1993]. MOW is the most outstanding

hydrographic component in that it comprises a prominent salinity maximum (Figure 4). MOW today enters the North Atlantic with temperature-salinity (T-S) values of 13°C/38.4 [Howe, 1982; Zenk, 1975; Ambar et al., 1976]. Potential density of this water is around 37.4 (s_2=density on 200 dbar surface), i.e. considerably higher than that of 36.7 for North Atlantic Deep Water (NADW). Rapid mixing with less saline North Atlantic Central Water (T-S=13°C/35.6; Zenk [1975]) and Labrador Sea Water (LSW, a component of upper NADW; T-S=3°C/34.85; Talley and McCartney [1982]) that both flow at the depth level of MOW reduces the density of MOW so that it flows northward along the upper Portuguese Margin in an upper (750 m) and lower (1250 m) core layer [Zenk and Armi, 1990] (Figure 4). Immediately west of the Gulf of Cadiz, T-S values for upper and lower MOW are around 12.5°C/36.2 and 11.5°C/36.4, respectively; northward advection (compared to the 2000 dbar surface) in the upper layer is highest, around 2.73 Sv (1 Sverdrup = 10^6 m^3 s^{-1}), compared to 1.24 Sv in the lower layer [Zenk and Armi, 1990].

Paleoceanographic research at the Portuguese margin has largely concentrated on the glacial-interglacial evolution of coastal upwelling and associated changes of microfossil assemblages. The Portuguese upwelling system is driven by northerly trade winds which change in intensity in conjunction with seasonal variations of the Azores anticyclonic cell and concomitant meridional migrations of the subtropical (atmospheric circulation) front [Fiuza et al., 1982; Fiuza, 1982]. During summer, the area of maximum upwelling shifts from south of Morocco to the western Iberian margin [Fiuza et al., 1982]. Faunal patterns along sediment cores from the Portuguese margin provide circumstantial evidence that coastal upwelling was increased off Portugal during the last glacial, either because of more intense upwelling or longer annual upwelling seasons [Abrantes, 1988]. Increased glacial upwelling conceivably resulted from enhanced trade winds and possible northward penetration of nutrient-enriched South Atlantic Central Waters that would have injected more nutrients into the Portuguese upwelling system [Abrantes, 1991]. Regional distribu-

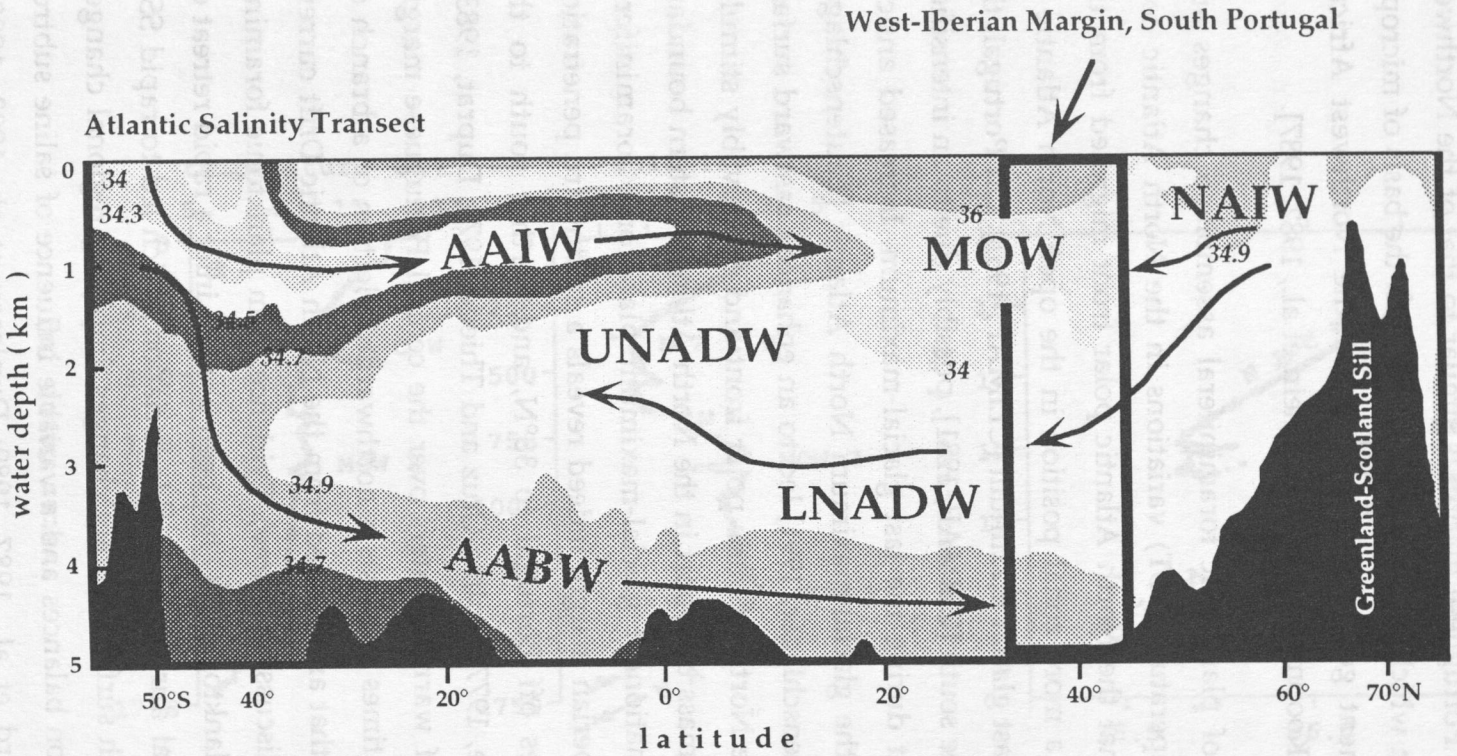

Figure 3. Atlantic water mass pattern as depicted from salinity distribution in the western Atlantic. The box marks the location and depth range of sediment cores from the southern Portuguese margin that are used in this thesis. Water masses are: Antarctic Intermediate Water (AAIW), North Atlantic Intermediate Water (NAIW), Mediterranean Outflow Water (MOW), Upper and Lower North Atlantic Deep Water (UNADW, LNADW), Antarctic Bottom Water (AABW). For the last glacial period, the paleoceanographic data presented in this thesis suggest a stronger contribution of UNADW and NAIW to the hydrography at the upper Portuguese margin, at the expense of MOW. During the 'Heinrich' meltwater events, thermohaline overturn in the North Atlantic was reduced.

ion patterns of diatom assemblages and diatom accumulation rates indicate that the upwelling front off Portugal migrated further offshore during the last glacial in response to coastline changes due to the glacially lowered sea level [Abrantes, 1991, 1995]. As such, the patterns of upwelling intensity and atmospheric circulation at the Portuguese margin is similar to that of the Northwest African upwelling system which has been documented on the basis of micropaleontological and sediment geochemical data from the Northwest African margin [Sarnthein, 1978; Koopmann, 1981; Sarnthein et al., 1982, 1987].

Synoptic mapping of planktonic foraminiferal assemblage changes and inferred sea surface temperature (SST) variations in the North Atlantic convincingly demonstrate that the North Atlantic polar front migrated from the Greenland Sea today to a more zonal position in the open North Atlantic at around 40°N during the last glacial maximum [CLIMAP, 1981]. Off Portugal, the polar front was bent to the south [CLIMAP, 1981], possibly due to an intensified eastern boundary current during the last glacial-maximum. Increased anticyclonic wind stress over the glacial-maximum North Atlantic [Lautenschlager and Herterich, 1990; Lautenschlager, 1991] led to an enhanced eastward surface water transport along the North Atlantic polar front and conceivably stimulated increased southward mass transport in the North Atlantic eastern boundary current. Detailed examination of glacial-maximum planktonic foraminiferal patterns at the western Iberian margin indeed reveals a southward penetration of polar-subpolar species off Portugal to 38°N, and further south to the Moroccan margin [Thiede, 1977; Molina-Cruz and Thiede, 1978; Duprat, 1983]. However, the presence of warmer waters over the central Portuguese margin during glacial maximum times suggests a northward deflection of a branch of warm subtropical waters that are derived from the North Atlantic Drift current (Duprat [1983]; see also discussion below). Evidence from planktonic foraminiferal census counts and planktonic $\delta^{18}O$ has been used to infer a rapid retreat of the polar front off Portugal during the last deglaciation which led to rapid SST changes that covaried with surface salinity changes, implying regional changes in evaporation-precipitation balances and a variable influence of saline subtropical surface waters [Bard et al., 1987, 1989; Duplessy et al., 1992, 1993].

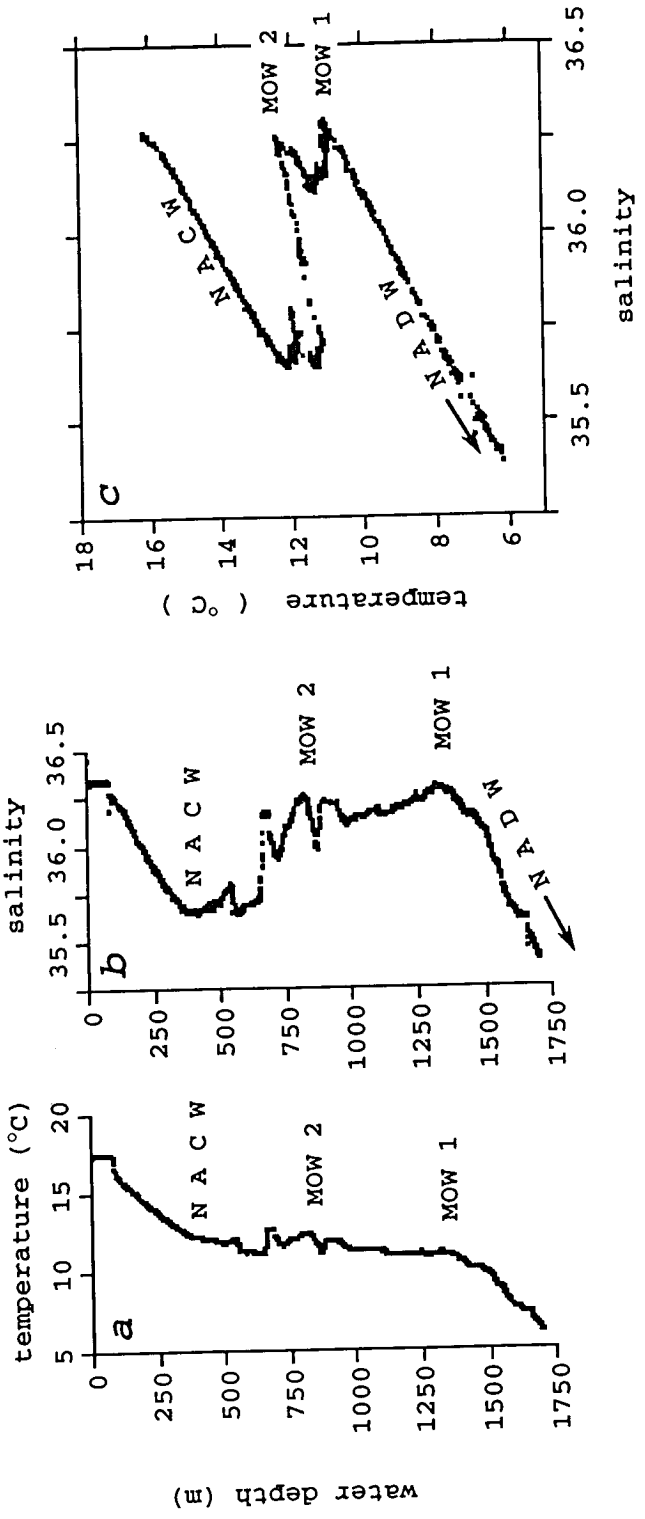

Figure 4. Vertical temperature and salinity profiles (a, b) at Station SO75-36WS (37°21.8'N, 09°52.1'W), southern Portuguese margin. Mediterranean Outflow Water (MOW) comprises a marked salinity maximum that is devided into a lower and an upper layer (c; MOW 1 and MOW 2) [Zenk and Armi, 1990]. NACW is North Atlantic Central Water, NADW is North Atlantic Deep Water.

The paleoceanographic evolution of deeper water masses in the Northeast Atlantic has been reconstructed by mapping benthic foraminiferal $\delta^{13}C$ from sediment cores at the Northeast Atlantic continental margin, the open North Atlantic, and the Norwegian-Greenland Seas [Boyle and Keigwin, 1987; Zahn et al., 1987; Duplessy et al., 1988; Veum et al., 1992; Oppo and Lehman, 1993; Sarnthein et al., 1994; Jung, 1996]. These studies infer enhanced ventilation of the mid-depth North Atlantic, in response to the formation of a Glacial North Atlantic Intermediate Water (GNAIW, *sensu* Duplessy et al. [1988]) or enhanced formation of Upper North Atlantic Deep Water at the expense of Lower North Atlantic Deep Water [Boyle and Keigwin, 1987; Sarnthein et al., 1994]. Northward advance of AABW far into the northern North Atlantic caused significantly decreased ventilation there at depths below 3500 m. The net result of the reorganization of vertical water mass architecture in the North Atlantic was a steeper vertical gradient of biologically cycled nutrients between nutrient depleted mid-depth and nutrient-enriched deep and bottom waters.

From this pattern it is concluded that during the last glacial the upper Portuguese margin, at water depth above 1500 m, was influenced by the presence of a well ventilated water mass. Enhanced glacial benthic $\delta^{13}C$ levels at the upper Moroccan continental margin have been inferred to document a stronger influence of MOW on the North Atlantic mid-depth hydrography. This hypothesis has also been used to explain enhanced benthic $\delta^{13}C$ further north, at the Portuguese margin and the Rockall Plateau area in the open northern North Atlantic [Sarnthein et al., 1994; Jung, 1996]. Evaluating benthic $\delta^{18}O$ in view of equilibrium δ_c fractionation as a function of ambient water temperature and salinity, I will show below that MOW contribution must have been reduced during the last glacial, and that enhanced mid-depth ventilation at the Portuguese margin must have come from a North Atlantic source, similar to today's North Atlantic Central Water.

An important aspect for this thesis is the occurrence of IRD layers on the Portuguese margin [Kudrass and Thiede, 1970; Kudrass, 1973]. The IRD layers indicate a flow of icebergs from the northern North Atlantic along the western Iberian margin during the last glacial and deglacial. Recently, Lebreiro et al. [1996] have reported on the occurrence of discrete IRD layers on Tore

Seamount off Portugal. Oxygen isotope stratigraphy and mineral composition of these layers revealed that they correspond to 'Heinrich' events 1, 2, 3, and 6. I.e., IRD deposition during the North Atlantic's 'Heinrich' events also occurred outside the area of maximum iceberg drift (the so-called 'Heinrich' belt, between 40° and 55°N; Bond et al. [1993], Broecker [1994]), on the Portuguese margin.

4.0 MATERIALS AND METHODS

4.1 Stable Isotopes

Benthic and planktonic foraminiferal isotope records were measured for 9 sediment cores from the southern Portuguese margin at water depths between 800 m and 3600 m (Figure 2; Table 1). The cores were routinely sampled at 10-20 cm intervals to establish a first oxygen isotope stratigraphy. Mid-depth cores between 1000 m and 2000 m water depth (SO75-6KL, -26KL, -31KL, -32KL) were then re-sampled at 2-5 cm across the last glacial-interglacial transition to enhance stratigraphic resolution for better paleoceanographic interpretation of intermediate water and upper deep water variability. IRD layers were sampled at 2 cm intervals to obtain higher stratigraphic resolution and check for hydrographic and sedimentologic fine structure during these intervals.

Benthic foraminiferal isotope measurements were carried out on 1 to 21 specimens of *Cibicidoides wuellerstorfi*, *C. pseudoungerianus*, and *C. mollis*. These species inhabit epibenthic microhabitats and are therefore assumed to reliably record $\delta^{13}C$ variations of ambient bottom water total dissolved carbon [Zahn et al., 1986; McCorkle et al., 1990]. Within the IRD layers, isotope measurements were carried out on a minimum of 6 benthic specimens per isotope sample. The foraminiferal tests were picked from the size fractions >250 µm. The planktonic isotope records were measured using 25 specimens of *Globigerina bulloides* from the 315-400 µm size fraction. Prior to isotope analysis, all foraminiferal shells were cracked open to release potential sediment fillings. They were then ultrasonically rinsed in methanol and transferred to a CARBO KIEL automated carbonate preparation device that is linked on-line to a FINNIGAN MAT 251 mass spectrometer. The measurements were carried

out at the isotope laboratories of the Universities of Bremen, Erlangen and Kiel. The mass spectrometers at these laboratories are intercalibrated with an internal laboratory standard (Solnhofen limestone) to insure compatibility of the isotope data. Long-term reproducibility was 0.08‰ for $\delta^{18}O$ and 0.05‰ for $\delta^{13}C$ as calculated from replicate analyses of the internal carbonate standard. The isotope data are referred to the PDB scale and are deposited at GEOMAR in an electronic data repository.

4.2 ^{14}C-AMS Dating

^{14}C ages were determined via accelerator mass spectrometry (AMS) using the 3MV Tandetron system at the Leibniz-Labor of Kiel University, and using the Tandetron Accelerator at the Centre des Faibles Radioactivités in Gif-sur-Yvette, Paris [Duplessy and Arnold, 1989] (Table 2). For core SO75-6KL, 11 samples containing 287 to 1549 specimens of *G. bulloides* from the size fraction >250 µm were analysed. For core SO75-26KL, dated were 15 monospecific samples of *G. bulloides* containing 590 to 1090 tests in the same size fraction (>250 µm) and two shell fragments. For core MD95-2039, ^{14}C-AMS datings were carried out on 13 samples containing 275-1,529 tests of *G. bulloides* (>250 µm) and 1,464-1,648 tests of *N. pachyderma* (sin.) (150-250 µm). All samples were ultrasonically rinsed in methanol. The shell fragments were treated with 10% H_2O_2 and dilute HCl to remove organic material and carbonate dust.

Ice-rafted detritus (IRD) was counted from the size fraction > 250 µm at 10 cm intervals. Discrete IRD maxima were found in all cores that correlate with the North Atlantic 'Heinrich' events H1, H2, and H4, as revealed by radiocarbon dating (see below). For cores SO75-6KL and SO75-26KL, detailed IRD countings were carried out at 2 cm intervals across the IRD maxima to check for IRD variability within the maxima. Bulk volume of the samples was 45 ccm on average. IRD grains were counted from the total sample, no split samples were used for the countings. Maximum countings reached 689 grains for IRD layer 3 in core SO75-26KL.

4.3 Planktonic Foraminiferal Census Counts

Planktonic foraminiferal counts were performed on samples from core SO75-26KL by Dr. Uwe Pflaumann (Geologisch-Paläontologisches Institut, Kiel) and Dr. Devesh Sinha (Varanasi University, India).[1] Supplementary counts were performed by Dipl.-Geol. Thorsten Kiefer (GPI, Kiel). The census matrix was then used as input to the SIMMAX Modern Analog Technique (MAT) routine to obtain estimates of surface paleo-temperatures. The SIMMAX MAT equation was calibrated using 738 analogue samples from the Atlantic between 60°W-30°E and 40°S-87°N [Pflaumann et al., 1996]. SST estimates are within 0.31°C (winter temperature) and 0.30°C (summer temperature) of the modern control. A detailed description of the SIMMAX-MAT and its relation to concurrent transfer function techniques is given by Pflaumann et al. [1996].

4.4 IRD Counting and X-Ray Diffractometry

The mineral composition of IRD layers in core SO75-26KL was determined by X-ray powder diffraction (XRD) scans on IRD samples [Park, 1994] using a Siemens D 5000 automated diffractometer with incident and diffracted beam monochrometer (CuKa radiation at 25 mA and 40 kV; scanning angle was 20°-50°). The d_{hkl} peaks were identified using the reference lists of Brindley and Brown [1984] and Bayliss et al. [1986]. Individual mineral percentages were determined from analogue records using Biscaye's [1965] planimetry factors. Additional XRD scans were run on samples immediately below and above the IRD layers to obtain the mineralogy of the sediments which were deposited prior to and after the IRD events. The XRD measurements were carried out at GEOMAR by Dipl.-Geol. Myong-Ho Park as part of his Diplom thesis [Park, 1994].

[1] Dr. Sinha worked at GEOMAR in August to October 1994 under a cooperational research grant of the Indian National Science Academy (INSA) and the Deutsche Forschungsgemeinschaft.

4.5 Stratigraphy

4.5.1 Cores SO75-6KL and SO75-26KL

Cores SO75-6KL and SO75-26KL that have been dated with ^{14}C-AMS serve as stratigraphic master series for the benthic and planktonic isotope records along the Portuguese margin cores that are used in this thesis. Age control on the last glacial-interglacial transition in core SO75-26KL was obtained by correlating the planktonic δ^{18}O record with the planktonic δ^{18}O record from nearby core SU81-18 that has been dated by ^{14}C-AMS in great detail [Bard et al., 1989]. A series of 17 ^{14}C-AMS ages was measured further down in core SO75-26KL (Table 2). One sample at 174-178 cm yields a ^{14}C-age (reservoir corrected, see Table 2) of 14.32 ka that fits well with the early phase of deglaciation which is documented by the initial decrease of benthic and planktonic δ^{18}O at this core depth (Figures 5a, b). Two samples bracketing the subtle benthic δ^{18}O minimum around 400 cm core depth yield ages of 22.95 ka and 24.87 ka, somewhat younger than the age of 25.4 ka that has been estimated by Martinson et al. [1987] for oxygen isotope event 3.1. A coral fragment from 385 cm depth with an age of 24.26 ka (Table 2) supports the association with 3.1. A much more pronounced minimum occurs in the planktonic δ^{18}O record at this level constraining late stage 3 isotope event 3.1 at 401.5 cm core depth.

An additional age control point was obtained by assigning oxygen isotope event 3.13 of Martinson et al. [1987] to the δ^{18}O minimum at 651.5 cm in the benthic isotopic record (Figure 5b). Beyond about 20 ka the Martinson et al. [1987] time scale is based on tuning to orbital parameters compared with U/Th dates. I.e., the age of 43.9 ka given by Martinson et al. [1987] for oxygen isotope event 3.13 must be considered calendar or calibrated ages. Laj et al. [1996] suggest a correction of 2000 yrs at 40 ka (^{14}C), rapidly decreasing to zero around 47 ka (^{14}C), to convert the ^{14}C time scale to calendar years. Thus a ^{14}C age of 42 ka is used here for oxygen isotope event 3.13 to ensure compatibility with the conventional ^{14}C time scale that has been established for core SO75-26KL.

For core SO75-6KL, eleven ^{14}C-AMS ages have been determined that span the last glacial-interglacial transition and reach back to the late stage of the Last

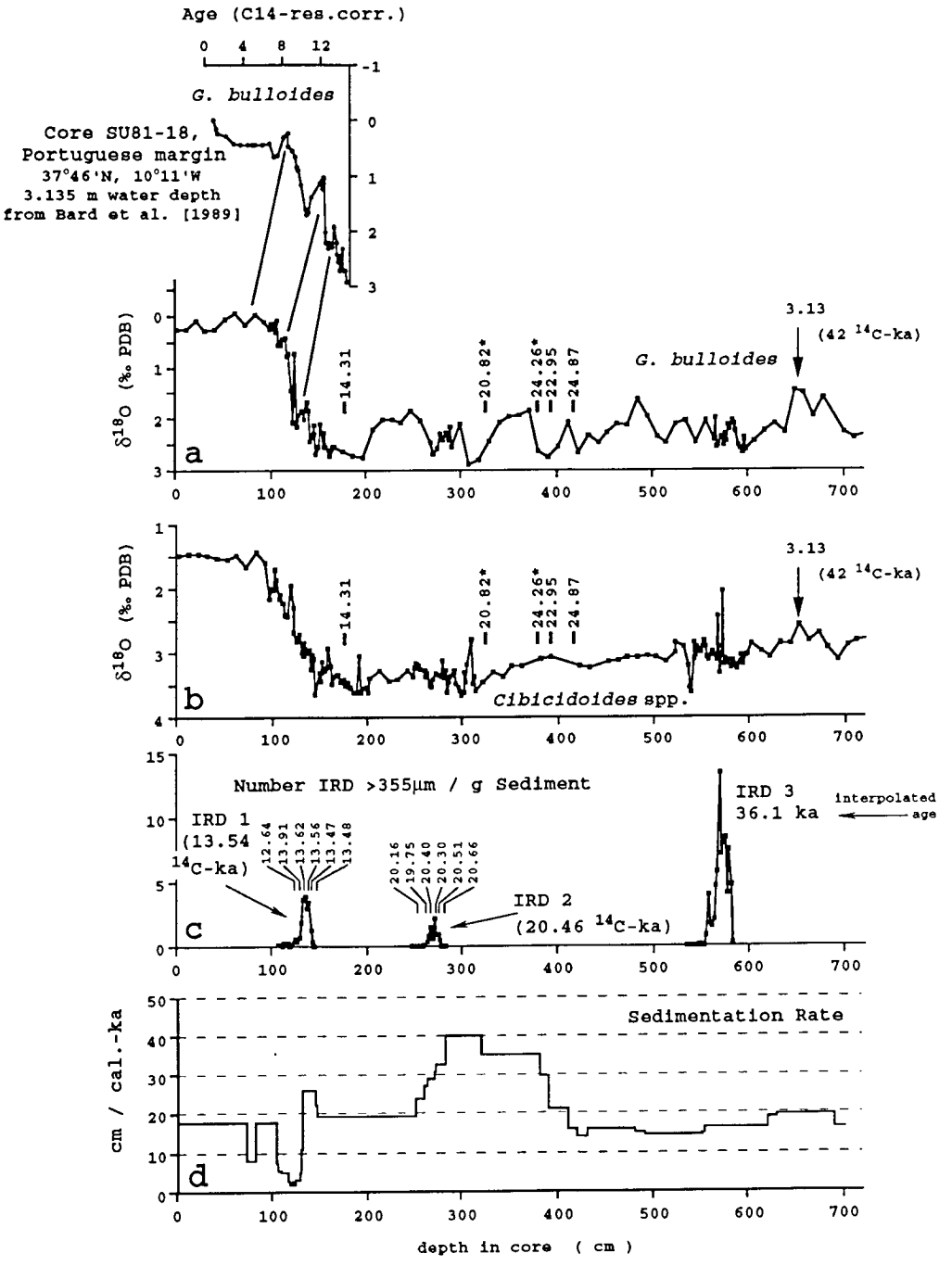

Figure 5. The stratigraphy for core SO75-26KL was established using planktonic and benthic oxygen isotope records (a, b) together with radiocarbon data. High-resolution dating of the two upper IRD layers (c) and the interpolated age for the third layer suggests they are coeval with 'Heinrich' events H1, H2, and H4. Sedimentation rates in (d) are calculated using a calibrated time scale.

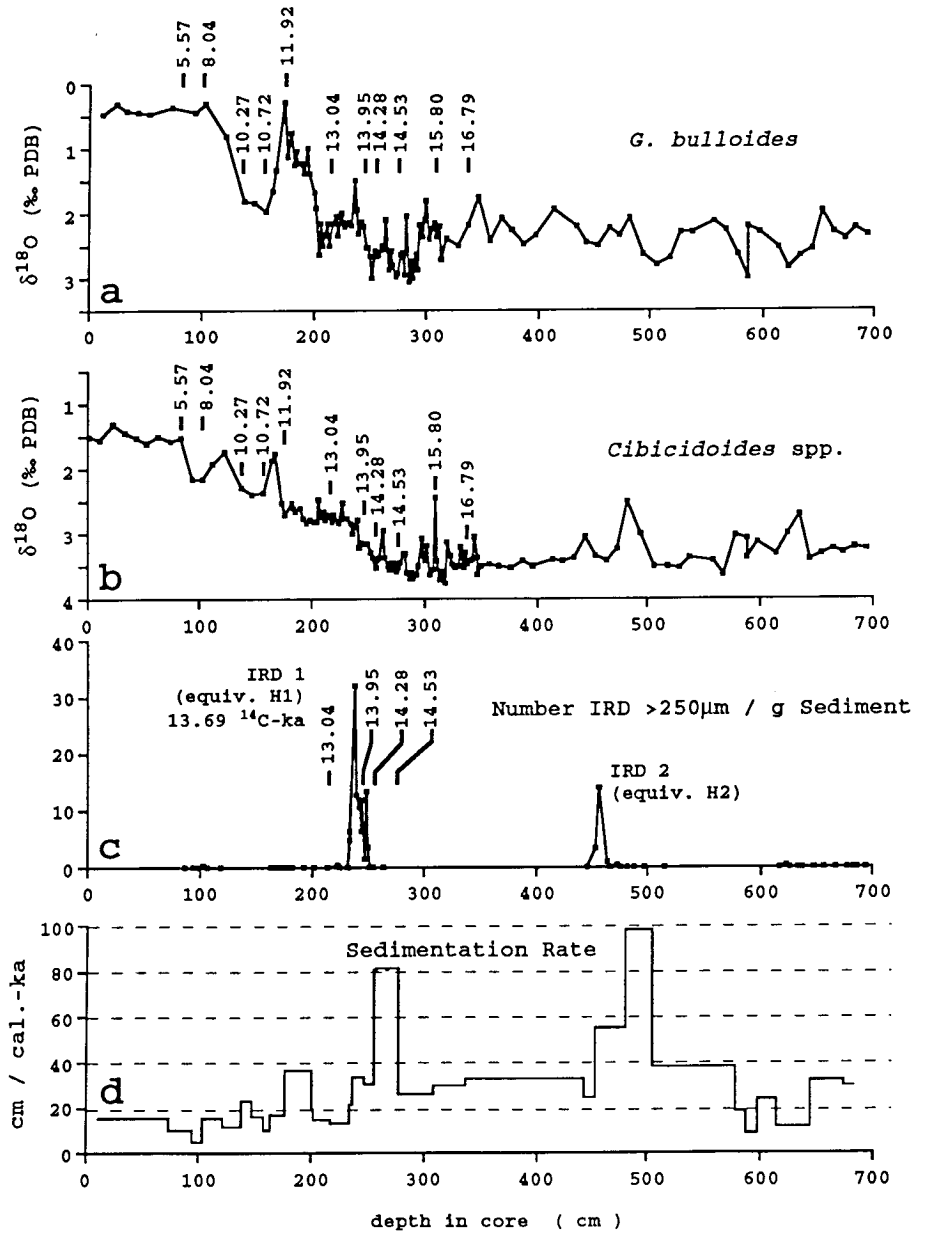

Figure 6. The stratigraphy for core SO75-6KL was established using planktonic and benthic oxygen isotope records (a, b) together with radiocarbon dating. The age of 13.7 ^{14}C-ka for the upper IRD layer (c) suggests it was coeval with 'Heinrich' event H1. Sedimentation rates in (d) are calculated using a calibrated time scale.

Table 2. ^{14}C-AMS ages for cores SO75-6KL and SO75-26KL

lab code	depth interval	mean depth	species [a]	individuals	^{14}C age [b]	error (ka)	^{14}C age [c]	calibrated age [d]
SO75-6KL								
GifA 94516	82-85 cm	83.50 cm	*G. bulloides*	1,549	5,970	±.07	5,570	5,570
GifA 94517	101-104	102.50	*G. bulloides*	1,400	8,440	±.08	8,040	8,740
GifA 94518	136-139	137.50	*G. bulloides*	1,810	10,670	±.09	10,270	11,340
GifA 94519	155-158	156.50	*G. bulloides*	632	11,120	±.08	10,720	12,432
GifA 94520	175-178	176.50	*G. bulloides*	1,330	12,320	±.09	11,920	14,033
GifA 94539	215-218	216.50	*G. bulloides*	1,044	13,440	±.10	13,040	15,700
GifA 94541	245-248	246.50	*G. bulloides*	631	14,350	±.10	13,950	17,625
GifA 94550	255-258	256.50	*G. bulloides*	287	14,680	±.13	14,280	17,966
GifA 94552	275-278	276.50	*G. bulloides*	353	14,930	±.12	14,530	18,126
GifA 94553	307-310	308.50	*G. bulloides*	380	16,200	±.13	15,800	19,028
GifA 94556	336-339	337.50	*G. bulloides*	400	17,190	±.14	16,790	20,082
SO75-26KL								
KIA 0002	122-126 cm	124 cm	*G. bulloides*	1,090	13,040	+.14 -.13	12,640	14,700
KIA 0003	128-132	130	*G. bulloides*	840	13,310	+.10 -.10	12,910	15,375
KIA 0004	132-136	134	*G. bulloides*	680	14,020	+.11 -.11	13,620	17,130
KIA 0005	136-140	138	*G. bulloides*	800	13,960	+16 -.16	13,560	17,000
KIA 0006	140-144	142	*G. bulloides*	680	13,870	+.90 -.90	13,470	16,775
KIA 0007	144-150	147	*G. bulloides*	640	13,880	+.23 -.20	13,480	16,800
KIA 0008	174-178	176	*G. bulloides*	690	14,710	+.13 -.13	14,310	17,985
KIA 0009	251-257	254	*G. bulloides*	590	20,560	+.22 -.21	20,160	23,673
KIA 0010	261-265	263	*G. bulloides*	1,080	20,150	+.22 -.22	19,750	23,234
KIA 0011	267-269	268	*G. bulloides*	890	20,800	+.24 -.23	20,400	23,933
KIA 0012	271-275	273	*G. bulloides*	900	20,700	+.38 -.36	20,300	23,825
KIA 0013	275-277	276	*G. bulloides*	930	20,910	+.15 -.14	20,510	24,052
KIA 0014	279-287	283	*G. bulloides*	760	21,060	+.23 -.23	20,660	24,214
KIA0015	320-322	321	gastropod shell		22,220	+.37 -.36	21,820	25,469
KIA0016	385	385	deep-water coral		24,660	+.34 -.33	24,260	27,875
KIA 0017	390-394	392	*G. bulloides*	725	23,350	+.52 -.49	22,950	26,652
KIA 0018	413.5-416.5	415	*G. bulloides*	930	25,270	+.66 -.61	24,870	28,445
MD952039								
KIA 779	38-39 cm	38.5 cm	*G. bulloides*	1,529	6,150	+.05 -.05	5,750	5,750
KIA 780	168-169	168.5	*G. bulloides*	1,053	12,620	+.11 -.11	12,220	14,283
KIA 781	208-209	208.5	*G. bulloides*	447	13,520	+.10 -.10	13,120	15,900
KIA 782	208-209	208.5	*N. pachyderma*	1,648	13,930	+.10 -.10	13,530	16,925
KIA 783	288-289	288.5	*G. bulloides*	396	14,250	+.11 -.11	13,850	17,475
KIA 784	288-289	288.5	*N. pachyderma*	1,464	14,650	+.11 -.11	14,250	17,946
KIA 785	542-543	542.5	*G. bulloides*	519	20,140	+.21 -.21	19,740	23,223
KIA 786	542-543	542.5	*N. pachyderma*	1,521	20,720	+.22 -.21	20,320	23,846
KIA 787	647.5-648.5	648.0	*G. bulloides*	1,000	22,810	+.28 -.27	22,410	26,108
KIA 788	818-819	818.5	*G. bulloides*	1,000	27,980	+.52 -.49	27,580	30,683
KIA 789	948.5-949.5	949.0	*G. bulloides*	578	29,000	+.59 -.55	28,600	31,775
KIA 790	1018.5-1019.5	1019.0	*G. bulloides*	275	30,130	+.69 -.64	29,730	32,764
KIA 791	1018.5-1019.5	1019.0	*N. pachyderma*	1,588	31,950	+.86 -.77	31,550	34,473

[a] *G.bulloides* was picked from the >250 µm size fraction; *N. pachyderma* (sin.) in core MD 952039 from the 150-250 µm fraction
[b] uncorrected
[c] corrected for reservoir age of 400 years
[d] calibration data are given in Table 4

Glacial Maximum (Figure 6, Table 2). The ages increase steadily with increasing core depth, age reversals similar to those observed in the ^{14}C-AMS record of Bard et al. [1989] are not observed. The ages fit well into the North Atlantic marine and climate stratigraphy. Interpolating linearly between the ^{14}C-AMS ages, the first marked minimum during the early stage of Termination Ia in the *G. bulloides* δ^{18}O record, at 210-250 cm core depth, occurs between 12.9 and 14.1 ka, in good agreement with the age range of 13.2-14.2 ka of an extreme minimum in planktonic (*N. pachyderma* sin.) δ^{18}O records from the Norwegian Sea [Sarnthein et al., 1995]. A second δ^{18}O minimum occurs between 173.5 and 195 cm depth in core SO75-6KL and is dated to 11.9-12.4 ka (by interpolation between the ^{14}C-AMS ages of 10.72, 11.92 and 13.04 ka at 156.5, 176.5 and 216.5 cm core depth; samples GifA 94520, 94539, 94541; Table 2), also in good agreement with a second meltwater event during the last deglaciation in the Norwegian Sea that has been dated to between 12.1 and 12.4 ka [Sarnthein et al., 1995].

The distinct planktonic δ^{18}O maximum between 137.5 and 156.5 cm in core SO75-6KL that marks the Younger Dryas cold event is dated by two ^{14}C-AMS ages to between 10.72 and 10.27 ka which correlates well with an age of 11-10 ^{14}C-kyr for the Younger Dryas chronozone as defined in continental Europe and dated in marine sequences [Mangerud et al., 1974; Jansen and Veum, 1990; Lehman and Keigwin, 1992; Lowe, 1992; Kaiser, 1993]. The abrupt termination of the Younger Dryas has been dated in the Greenland Dye-3 ice core to 10.72±.15 ka by annual layer counting [Hammer et al., 1986]. This age was later revised by Alley et al. [1993] to 11.64±.25 ka using annual layer countings in the Greenland GISP 2 ice core in conjunction with measurements of electrical conductivity, laser-light scattering and isotopic composition of the ice. The age undercount in the Dye-3 ice core by Hammer et al. [1986] probably resulted from flawed electrical conductivity measurements that had a decreased vertical resolution. Because of this, some annual layers were missed in the countings which finally led to an erroneously young age for the end of the Younger Dryas (see comments of Alley et al. [1993] in the caption to their Table 2). Converting the ice core calendar age of 11.64 ka to the conventional ^{14}C scale reveals an age of

10.0-10.2 ^{14}C-kyr, to which the ^{14}C-AMS age of 10.27 ka that has been measured in core SO75-6KL for the upper margin of the Younger Dryas planktonic $\delta^{18}O$ maximum fits perfectly well (Figure 6).

4.5.2 Detailed ^{14}C-AMS Dating of IRD Layers 1 and 2 (equivalent to 'Heinrich' Events 1 and 2)

In core SO75-26KL, six ^{14}C ages each were measured across IRD layers 1 (127-143 cm) and 2 (264- 278 cm) (Figure 7). Of the six ^{14}C ages across IRD 1 the first two show an increase with depth, while the lower four form a plateau in the age-depth function and even decrease with increasing depth by 140 years. This decrease is, however, similar to the standard deviations and therefore statistically not significant. The closely similar ages at different core depths indicate increased sedimentation rates for this part of the core, which contains the heart of the IRD layer 1, between 130 and 142 cm core depth (Figure 7a). The three AMS-dates for this interval give a mean age of 13.54±.07 ka (average depth 136 cm). The apparent age discontinuity between the IRD layer and overlying sediments is expected as a result of bioturbation whereby, after the rapid deposition of the IRD layer younger tests of *G. bulloides* are mixed down to and into the upper reaches of the IRD layer, but few older tests are mixed up. This leads to artificially young dates for the upper boundary of the IRD layer [Manighetti et al., 1995; Trauth, 1995]. The same reasoning predicts an artificially high age for the bottom of the IRD layer due to lack of young tests being mixed down once rapid deposition of the IRD layer started. This is not observed as sample KIA 0007 at 147 cm shows the same age as the IRD layer. For the age model for core SO75-26KL the average value of 13.54±.07 ka at 136 cm (samples KIA 0004-0006, Table 2) for IRD layer 1 is used together with the other three ages measured.

For the six AMS ^{14}C dates across IRD 2 the age differences are likewise small and, due to the larger statistical uncertainties at this age, generally not statistically significant (Table 2, Figure 7b). The three dates from the heart of the IRD layer (265-279 cm, Figure 7b) give an age of 20.46±0.12 ka at 272 cm depth for this episode of rapid accumulation. Again the two overlying dates are younger,

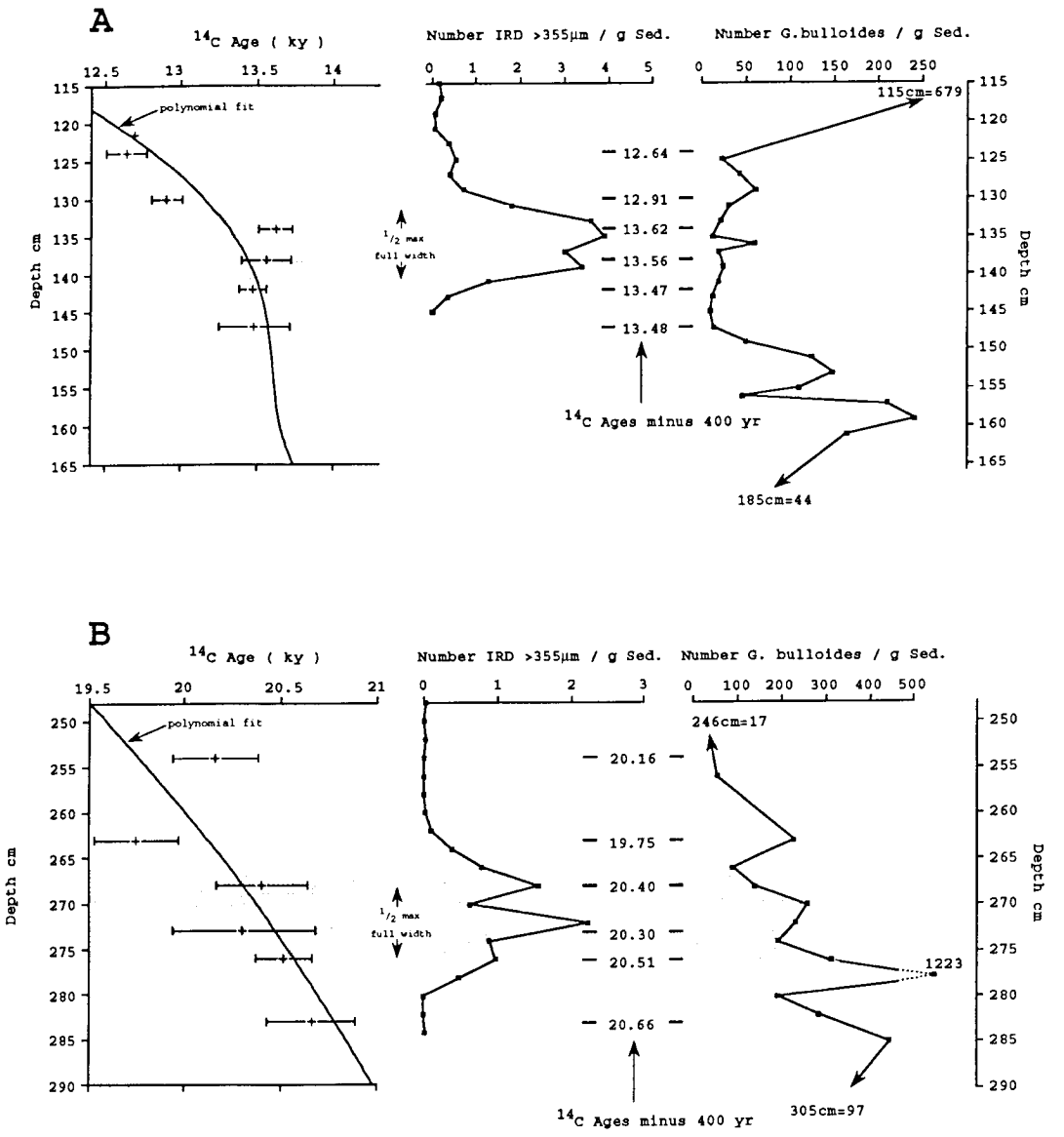

Figure 7. Age-depth function across (a) IRD layer 1 and (b) IRD layer 2. Within the range of error, ^{14}C-AMS ages do not change from below the IRD layers into the IRD maxima and imply rapid sedimentation during both events. Right-hand panel shows abundance distribution for *G. bulloides* that was used for ^{14}C-AMS dating.

though the age difference to sample KIA 0009 at 20.16±.2 ka is statistically significant. The average of 20.46±0.12 ka (KIA 0011-0013, Table 2) for IRD layer 2 together with the other three dates is used in the age model.

The age model for core SO75-26KL was derived using a polynomial fit through the ^{14}C-AMS data for H1 and H2, and through the ^{14}C-AMS data further down the core (Figure 7). The oldest ^{14}C-AMS age in the core of 24.87 ka at 415 cm core depth (sample KIA0018) was linked linearly with the Martinson [1987] age of 42 ^{14}C-ka for oxygen isotope event 3.13 at 651.5 cm core depth. According to this model, IRD layers 1 and 2 lasted from 13.1-13.4 ka and 20.2-20.6 ka. Mean sedimentation rates are 22 cm ka^{-1} at core SO75-26KL (Figure 5d). Sedimentation rates increase to 55 cm ka^{-1} and 32 cm ka^{-1} during IRD layers 1 and 2, respectively, suggesting rapid sedimentation during H1 and H2. Seven- to tenfold increases in sediment flux during 'Heinrich' events have been inferred using $^{230}Th_{ex}$ data from 'Heinrich' layers in the open North Atlantic [Francois and Bacon, 1994; Thomson et al., 1995]. Smaller increases at the site of core SO75-26KL support the contention that sediment flux from icebergs was reduced off Portugal because the site is outside the region of maximum iceberg flow.

Using the polynomially fitted age model, total duration of H1 and H2 in core SO75-26KL is 300 and 400 years, respectively. These estimates depend on how good the age estimates for top and bottom of the 'Heinrich' layers are. Rapid sedimentation in conjunction with differential bioturbation likely make the top age too young and the bottom age too old. As discussed above, the detailed ^{14}C-AMS datings show some evidence for the first, but not for the latter. Still, spacing of the ^{14}C data across both IRD layers is not sufficient to estimate ages of IRD boundaries unambiguously. Using ^{14}C-AMS data and age errors at face value, this would limit IRD 1 to 200-300 yrs, and IRD 2 to 300-600 yrs duration. These are still fairly wide ranges, but they fit to similar estimates derived from $^{230}Th_{ex}$ data [Francois and Bacon, 1994; Thomson et al., 1995]. They are at the low side of estimates (250-1250 yr) that have been derived from theoretical considerations of iceberg calving and sediment flux [MacAyeal, 1993; Dowdeswell et al., 1995].

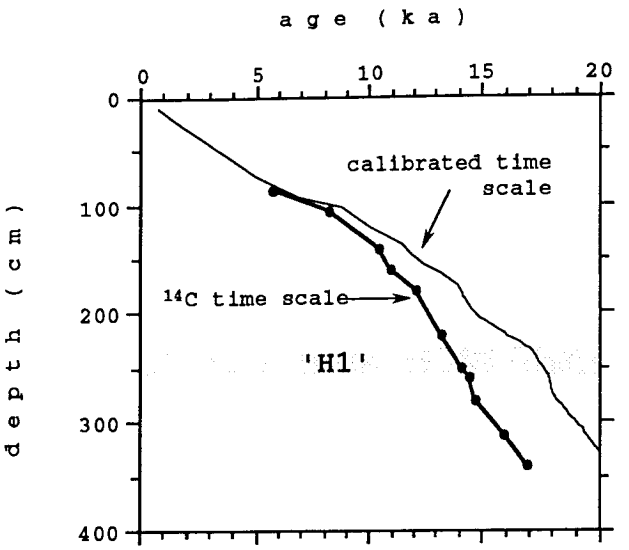

Figure 8a. Age-depth function for core SO75-6KL. The function shows a subtle kink below the IRD layer that is indicative of the deflection towards too old bottom ages of the IRD layer. This would be consistent with bioturbation models that use IRD layers as an effective barrier that suppresses bioturbational admixture of younger foraminiferal shells across the layer.

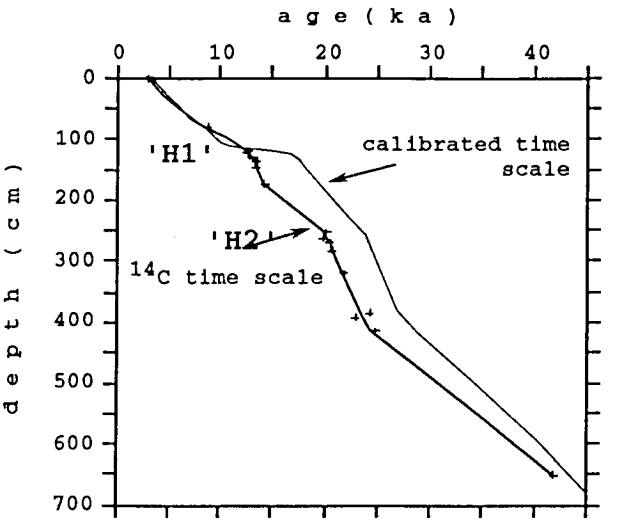

Figure 8b. Age-depth function for core SO75-26KL. Similar to the function for core SO75-6KL, the age-depth function shows subtle kinks at the IRD layers (H1, H2). Again, this would be consistent with bioturbation models that postulate differential bioturbational mixing around sedimentological barrier facies. See text for discussion.

For core SO75-6KL, three ^{14}C-AMS dates are within immediate reach of IRD layer 1 that occurs between 233.5 and 250 cm core depth (Figure 6, Table 2). Sample GifA 94539 at 216.5 cm lies 17 cm above the upper boundary of IRD 1, sample GifA 94541 at 246.5 is in the lower part of the layer, and sample GifA 94550 at 256.5 cm is 6.5 cm below the lower boundary of the IRD layer. Using these ages, IRD 1 in core SO75-6KL lasted 500 yrs, from 14.07 and 13.56 ka. The mean age of 13.7±.04 ka for H1 in this core is slightly older than that for the same event in core SO75-26KL (13.54±.07 ka), but within the range of error both ages are the same to within 50 years.

Mean sedimentation rates at the site of core SO75-6KL are 33.6 cm/ka with maximum rates of 96.6 and 80 cm/ka prior to H2 and H1 (Figure 6d). Increases in sedimentation rates before both 'Heinrich' events are also seen in core SO75-26KL and may be due to an early slow down of circulation in association with gradual decreases in convective overturn prior to the 'Heinrich' events.

The coverage with ^{14}C-AMS dates of H1 in core SO75-6KL is not as dense as in core SO75-26KL. But the age-depth functions of both cores show subtle kinks around the IRD layers (Figure 8a and b) that are indicative of deflections towards too old bottom ages of the IRD layers which suppress bioturbational admixture of younger foraminiferal shells from above, as postulated by bioturbation models (see discussion above). These kinks are reflected in the sedimentation rate profiles by distinctive increases in sedimentation rates just below the IRD layers (Figures 5d and 6d). The age models imply that sedimentation rates during the IRD events were 25-33 cm/cal-ka i.e., not much different from the long-term means (34 cm/cal-ka for core SO75-6KL; 22 cm/cal-ka for core SO75-26KL).

4.5.3 Lower Deep Water Reference Core MD95-2039

Core MD95-2039 was retrieved from the lower Portuguese margin during the third leg of the first IMAGES ("International Marine Global Change

Studies", a subprogram of PAGES-"Past Global Changes" in the International Geosphere Biosphere Program) cruise in July 1995. This was the maiden cruise of R/V *Marion Dufresne* and the intention was (i) to test the vessel's operational functions and (ii) to serve as a platform for an international research program on high-resolution paleoceanography of the North Atlantic [Bassinot et al., 1996].

Core MD95-2039 was retrieved at 3381 m water depth using the French long coring facility. The core is used here as a paleoceanographic reference section for the evolution of Northeast Atlantic lower deep waters off Portugal. The core is 35.7 m long and contains a continuous sedimentary sequence from the Holocene down to oxygen isotope stage 9.3 at 331 ka (Figure 9). The magnetic susceptibility record displays discrete maxima that correlate with enhanced IRD abundances as revealed by IRD countings across the upper 5 susceptibility maxima (J. Baas, unpublished data).

Paired ^{14}C-AMS data that were measured for the same sample consistently show higher ages for *N. pachyderma* (sin.) relative to ages determined for *G. bulloides* (samples KIA 781/782, KIA 783/784, KIA 785/786, KIA 790/791; Table 2). Since *N. pachyderma* (sin.) was picked from a smaller size fraction (150-250 µm compared to >250 µm for *G. bulloides*) contamination of the ages derived from this species with redeposited small shells cannot be excluded. Differential bioturbational in association with offsets in abundance peaks of both species may have further added to the apparent differences in age [e.g., Manighetti et al., 1995; Trauth, 1995]. Using the means of the paired measurements, the following ages were obtained for 'Heinrich' events H1 to H4 that are seen in the susceptibility record: H1 (214 cm core depth, c.d.) =13.38 ^{14}C-ka, H2 (544 cm c.d.) =20.06 ^{14}C-ka, H3 (768 cm c.d.) =26.05 ^{14}C-ka, and H4 (1019 cm c.d.) =30.64 ^{14}C-ka. Ages for H1 and H2 are reasonably close to those determined in core SO75-26KL. The ^{14}C-AMS age of 26.05 ka for H3 is between that of 27 ^{14}C-ka determined by Bond et al. [1992, 1993] in the northern North Atlantic and an interpolated age of 25.14 ^{14}C-ka for a planktonic foraminiferal faunal anomaly in core SO75-26KL that likely represents a cooling episode off Portugal coeval with H3 (see further below). The age of 30.64 ^{14}C-ka is much younger than that

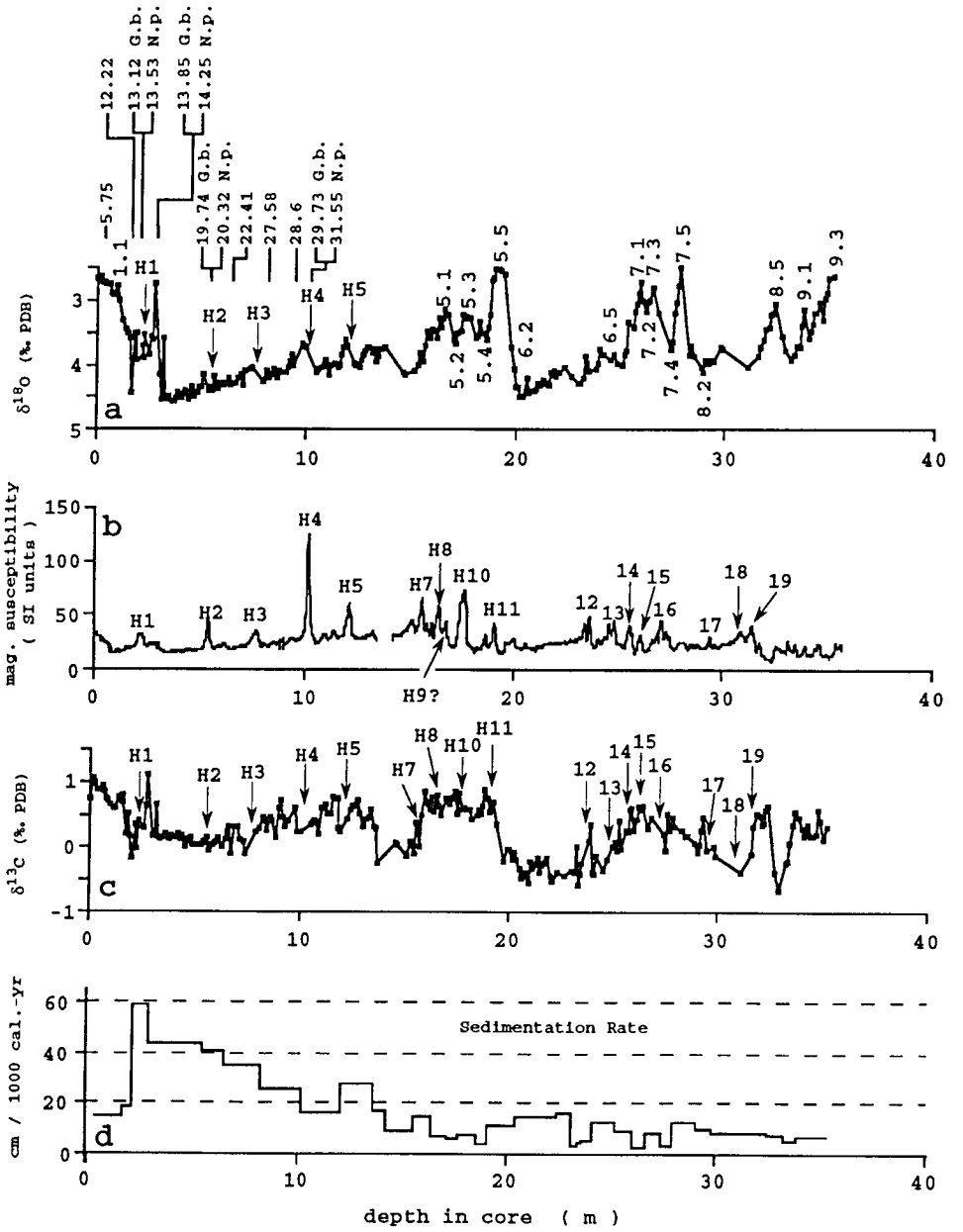

Figure 9. The stratigraphy for core MD95-2039 was established using the benthic oxygen isotope record together with radiocarbon datings and oxygen isotope event ages (a). The magnetic susceptibility record provides information on IRD layers (b). The benthic carbon isotope record (c) suggests only little response to the 'Heinrich' meltwater events at this water depth (3381 m). Sedimentation rates in (d) are calculated using a calibrated time scale.

of 36.1 ^{14}C-ka for H4 that has been determined by interpolation in core SO75-26KL, and also much younger than the ^{14}C-age of 35.5 ka from the northern North Atlantic [Bond et al., 1992, 1993]. The source for this apparent shift of more than 5 ka towards too young ages is hard to define: accidental contamination of the foraminiferal sample with carbonate dust or tap-water bicarbonate during sample preparation. To ensure stratigraphic comparability with the upper margin core SO75-26KL and other records from the northern North Atlantic, the ^{14}C-AMS ages of samples KIA 790 and KIA 791 are discarded, and an age of 36.1 ^{14}C-ka is used for H4.

The time scale for the upper 12 m of core MD95-2039 was derived using ^{14}C-AMS age data and chronostratigraphic events listed in Table 3. From oxygen isotope stage 4 down the base of the core, ages of oxygen isotope events listed in Imbrie et al. [1984] and Martinson et al. [1987] were used (Figures 9). According to the age model, the base of core MD95-2039 reaches oxygen isotope event 9.3 (331 ka; Imbrie et al. [1984]). Mean sedimentation rates at the site of core MD95-2039 are 17.9 cm/ka with maximum rates of 48.2 cm/ka between H1 and H2, and minimum rates of 2.9 cm/ka during stage 7.2. The decreased rates result from stretching the record so that the double δ^{18}O minimum prior to and after oxygen isotope event 7.2 match with isotope events 7.1 and 7.3.

During oxygen isotope stage 5, susceptibility maxima occur in core MD95-2039 in stages 5.5, 5.3, 5.1, and at the stage 5/4 boundary (Figure 9). These maxima correlate with 'Heinrich' events H11, H10, H8, and H8 as defined by Heinrich [1988] in sediment cores from the Dreizack seamount area in the Northeast Atlantic. H6 has been dated to 66 ka [Bond et al., 1992] and should occur in early stage 4 (between stages 4.22 and 4.23 of Martinson et al. [1987]). This event is not caught in the susceptibility record because of a gap in the data series. According to Heinrich's [1988] scheme, H9 occurs at the 5.3/5.2 transition, but the susceptibility record for core MD95-2039 does not show a peak in the corresponding core section. A secondary susceptibility peak occurs at 16.76 m, about 40 cm below the peak that correlates with H8, in the stage 5.2/5.1 transition. Whether or not this peak is associated with H9 is uncertain. The benthic (*Pyrgo murrhina*) and planktonic (*G. bulloides*) oxygen isotope records from

Table 3. Stratigraphic marker events used in this thesis for time scale development

Event	^{14}C-age, ka	Source
1.1	9.1	Martinson et al. [1987], Bard et al. [1989]
H1	13.7	SO75-6KL, ^{14}C-AMS
H2	20.46	SO75-26KL, ^{14}C-AMS
H3	27	Bond et al. [1993]
H4	36.1	SO75-26KL, interpolated
3.13	42	Martinson et al. [1987] (in ^{14}C-ka)
H5	50	Bond et al. [1993]
H6	66	Bond et al. [1993]
H7	70.41	MD950239, SPECMAP stratigraphy
H8	76.48	MD950239, SPECMAP stratigraphy
H9		missing
H10	96.18	MD950239, SPECMAP stratigraphy
H11	121.3	MD950239, SPECMAP stratigraphy

core Me69-17 that Heinrich [1988] used in his study do not resolve isotope stages 5.1 through 5.4 well enough to allow for a detailed comparison between the stratigraphic position of the stage 5 susceptibility peaks in core MD95-2039 and his IRD and foraminiferal faunal peaks. Thus, in this core section as well as further down in core MD95-2039 preference was given to ages of oxygen isotope events as chronostratigraphic fixpoints to establish the age model (Figure 9).

Further susceptibility peaks occur in early oxygen isotope stage 6 and in stages 7 and 8 and are numbered tentatively in Figure 9. Whether or not these peaks are associated with IRD maxima will be subject to future microscopic work.

4.5.4 Master Stratigraphy for the Portuguese Margin Cores: ^{14}C Ages and Calibrated Time Scale

^{14}C ages of 13.54±.07 ka and 13.7±.04 ka for IRD layer 1, 20.46±0.12 ka for IRD layer 2, and an interpolated age of 36.1 ka for IRD layer 3 fit well to ^{14}C-ages for 'Heinrich' layers 1 (13.64-14.99 ^{14}C-ka), 2 (19.86-21.77 ^{14}C-ka), and 4 (33.5-39.13 ^{14}C-ka) in sediment cores from the North Atlantic [Andrews and Tedesco, 1992; Bond et al., 1993; Cortijo, 1995; Manighetti et al., 1995]. The ages thus confirm that the IRD layers off Portugal are coeval with 'Heinrich' events in the open North Atlantic and represent the far eastern branches of iceberg drift across the northern North Atlantic during 'Heinrich' events 1, 2 and 4.

Time scales were derived for the benthic and planktonic isotope records of the Portuguese margin cores using these ages as chronostratigraphic fixpoints. For H1, preference was given to the mean ^{14}C-AMS age of 13.7 ka derived from core SO75-6KL that has higher sedimentation rates. Further fixpoints are isotope events 1.1 and 3.13 of Martinson et al. [1987] (see Table 3). For all cores, IRD countings were performed to determine the position of the 'Heinrich' events in the cores. Age scales of individual cores were then refined by graphical correlation of the isotope records to the records from cores SO75-26KL and SO75-6KL using the AnalySeries time series routine of Paillard et al. [1996]. The benthic

Table 4. Calibration data set for conversion of ^{14}C-time scale into a calibrated (calendar-year) time scale

^{14}C age ka	calibrated age ka	^{14}C age shift ka
7.0	7.7 [1]	0.7
9.1	9.8 [1]	0.7
10.0	10.8 [2]	0.8
10.4	11.6 [1,3]	1.2
10.9	12.9 [3]	2.0
11.4	13.6 [2]	2.2
12.6	14.6 [3]	2.0
13.6	17.1 [1]	3.5
14.1	17.85 [2]	3.75
14.8	18.3 [1]	3.5
15.68	18.9 [2]	3.22
20.0	23.5 [1]	3.5
22.68	26.4 [2]	3.72
26.0	29.5 [1]	3.5
30.0	33.0 [4]	3.0
35.0	37.75 [4]	2.75
40.0	42.0 [4]	2.0
45.0	45.5 [4]	0.5
49.0	49.0 [4]	0.0

[1] calibration according to age assignments in Table 1 of Winn, Sarnthein and Erlenkeuser [1991]

[2] turning point at ^{14}C-plateau

[3] age assignments were revised to take ^{14}C-plateaus at 10.0 ka and 12.7 ka into consideration (M. Sarnthein, pers. communication, Jan. '97)

[4] ^{14}C-time scale older than 26 ka was calibrated using the magnetic correction of Laj et al. [1996]

and planktonic oxygen isotope stratigraphies of the Portuguese margin cores are shown along their age scales in Figures 10 and 11.

The isotope records are discussed with reference to their ^{14}C age scales. To derive linear sedimentation rates and to compare the isotope records with paleo-records from ice cores that monitor the variability of North Atlantic and Antarctic climate, the conventional ^{14}C-time scale is converted into a calendar year or calibrated age scale (Figure 12, Tables 2, 4). The calibration of the past 26 ^{14}C-ka followed the unpublished calibration of Bard (International Conference of Paleoceanography, Kiel, 1992) using additional age assignments given in Table 1 of Winn et al. [1991]. Age assignments between 10.4 and 13.6 ^{14}C-ka were revised to take ^{14}C-plateaus near 10 and 12.7 ^{14}C-ka [Lotter et al., 1992; Becker and Kromer, 1993] into account (M. Sarnthein, personal communication, January 1997). For the period prior to 26.0 ^{14}C-ka, calibration followed the magnetic correction given in Laj et al. [1996] (Figure 12).

5.0 MINERALOGY OF IRD LAYERS OFF PORTUGAL AND ITS RELATION TO NORTH ATLANTIC 'HEINRICH' LAYERS

A distinct property of the 'Heinrich' deposits in the North Atlantic is the elevated concentration of detrital carbonate and the presence of dolomite grains in the IRD layers [Bond et al., 1992; Bond and Lotti, 1995]. This has been related to limestone bedrocks in the Hudson Strait area and in Arctic Canada which where eroded by ice, transported by floating icebergs into the North Atlantic and finally delivered to the sea floor during melting of the icebergs. Lead, strontium and neodymium isotope compositions of the IRD particles support this hypothesis in that these data point to the Canadian shield as the primary source for the lithic particles [Gwidazda et al., 1996; Revel et al., 1996].

To better constrain if the IRD layers that occur in sediment cores off Portugal are linked to the northern North Atlantic 'Heinrich' layers, the mineralogy of IRD layers 1, 2, and 3 in core SO75-26KL has been determined by X-ray diffractometry (XRD) [Park, 1994]. Ice-rafted particles in IRD layer 1 off Portugal and Morocco consist of a great variety of rock types with 17 % detrital carbonate

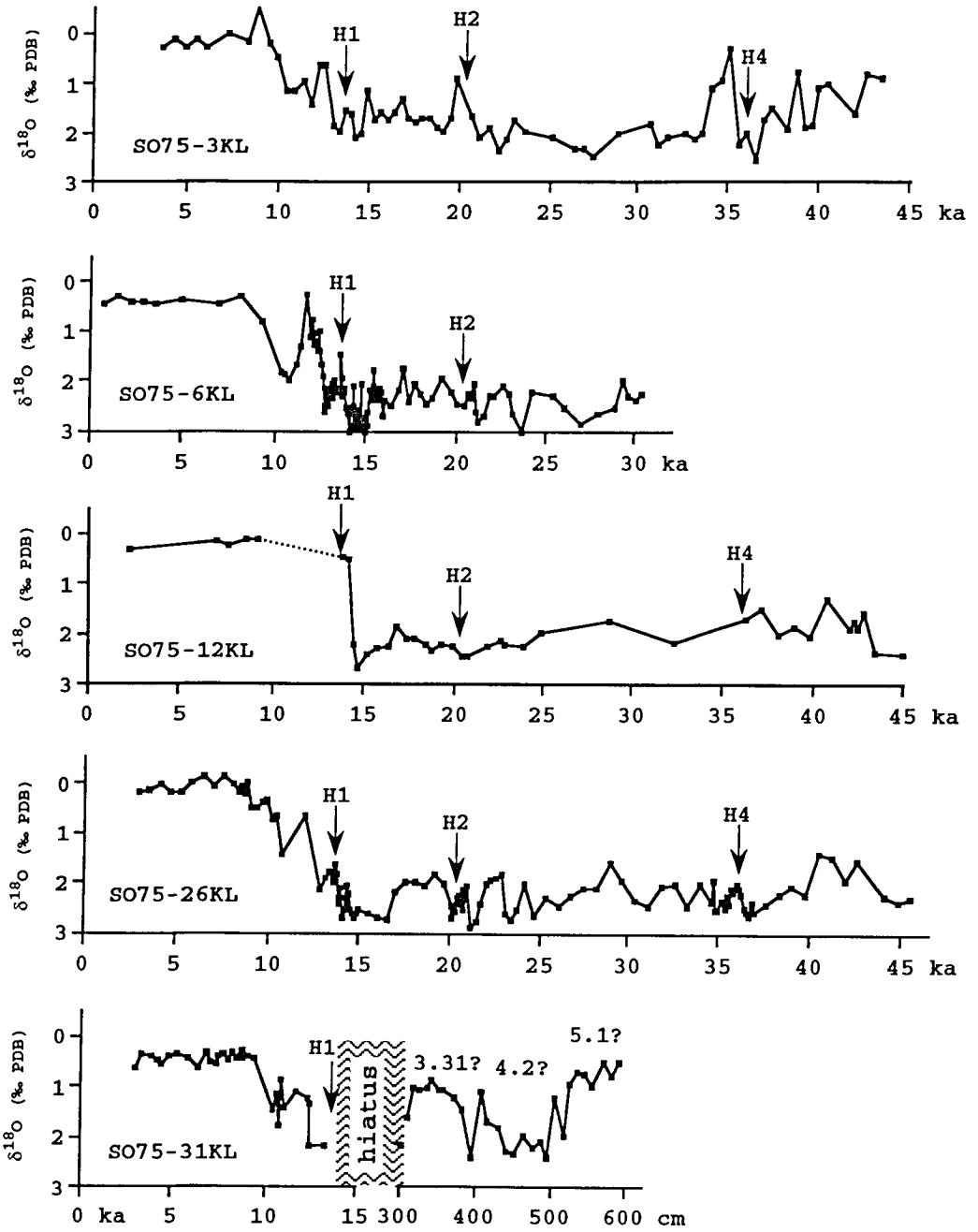

Figure 10. Planktonic (*G. bulloides*) oxygen isotope records from the southern Portuguese margin cores. Age scales are in 1000 radiocarbon years. The stratigraphic record of cores SO75-31KL and SO75-32KL is interrupted by a hiatus. The structure of the isotope record below the hiatus in both cores does not allow to determine a precise stratigraphy. Isotope events that are marked along these parts of the records are tentative. The depth positions of 'Heinrich' events have been determined by IRD counting.

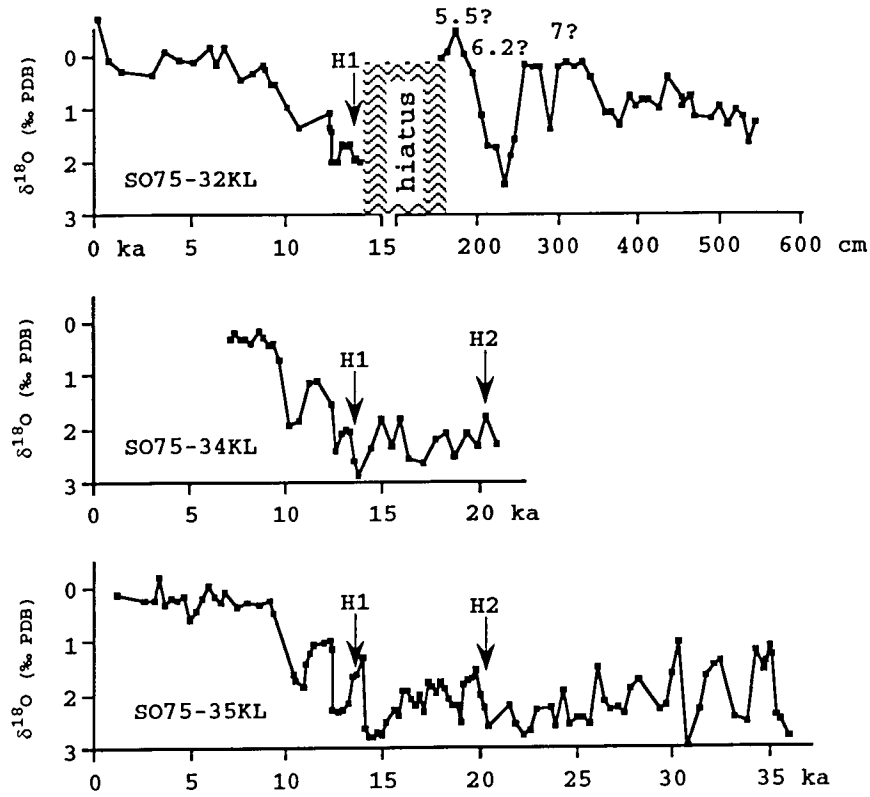

Figure 10, continued

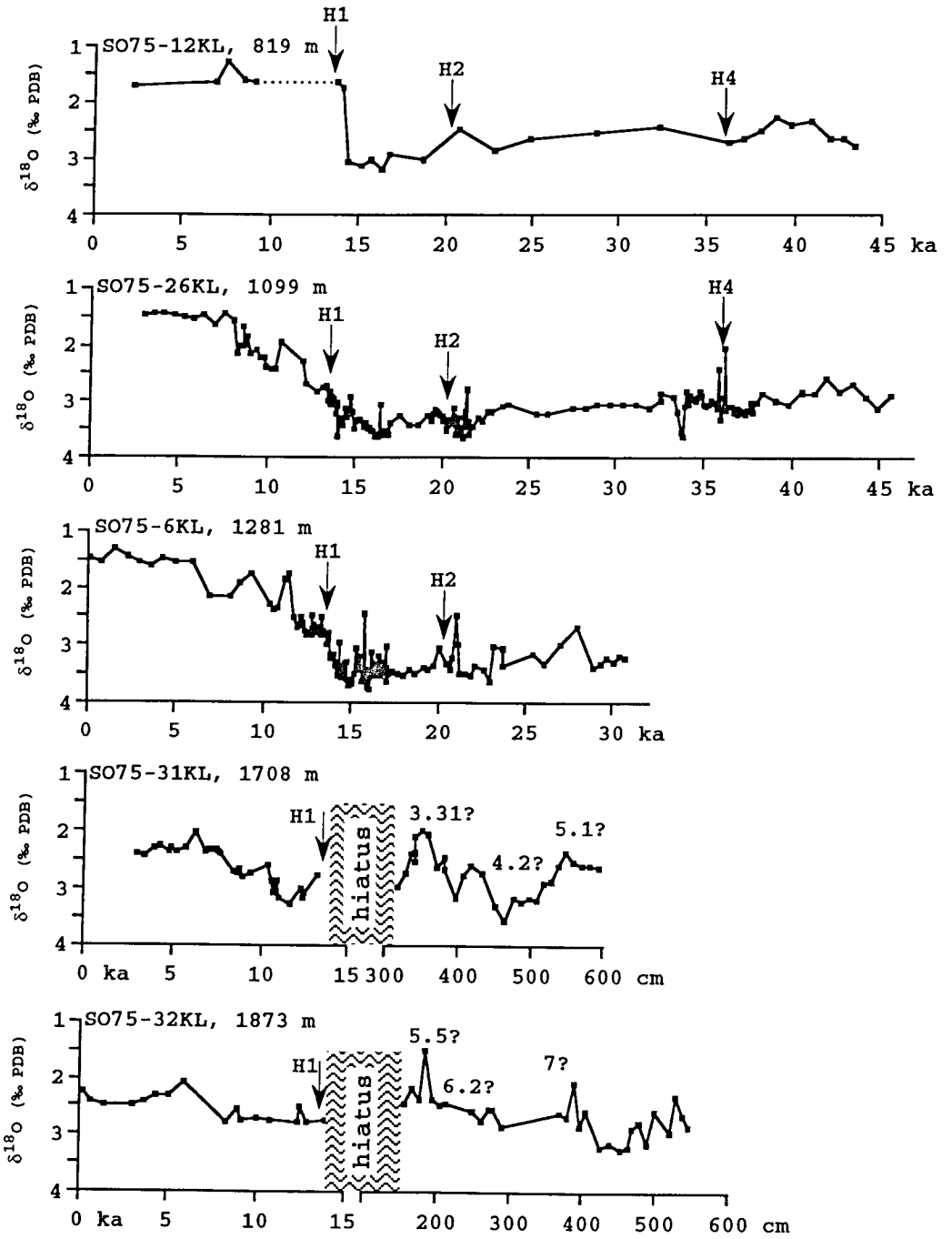

Figure 11. Benthic (*Cibicidoides* spp.) oxygen isotope records from the southern Portuguese margin cores. Age scales are in 1000 radiocarbon years. Numbering of isotope events below the hiatus in cores SO75-31KL and SO75-32KL is the same as in Figure 10. The isotope records are shown on the basis of increasing water depth of individual sediment cores. Position of 'Heinrich' events is derived from IRD countings.

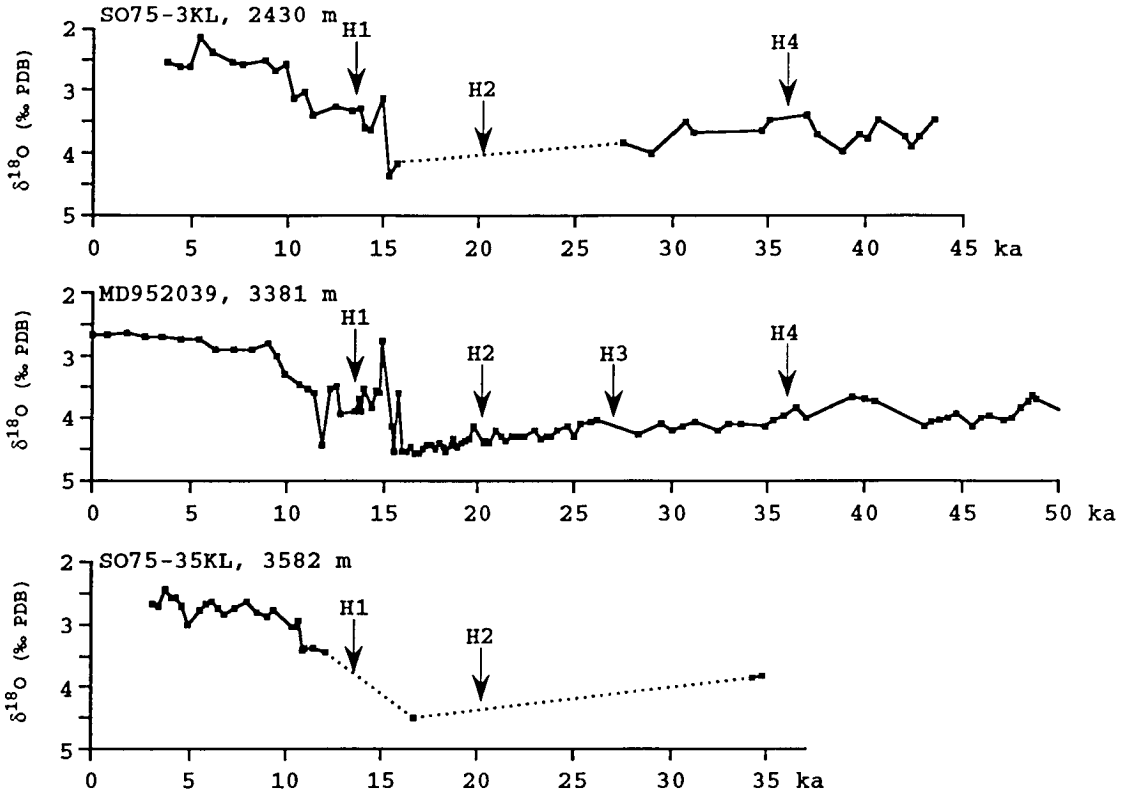

Figure 11, continued.

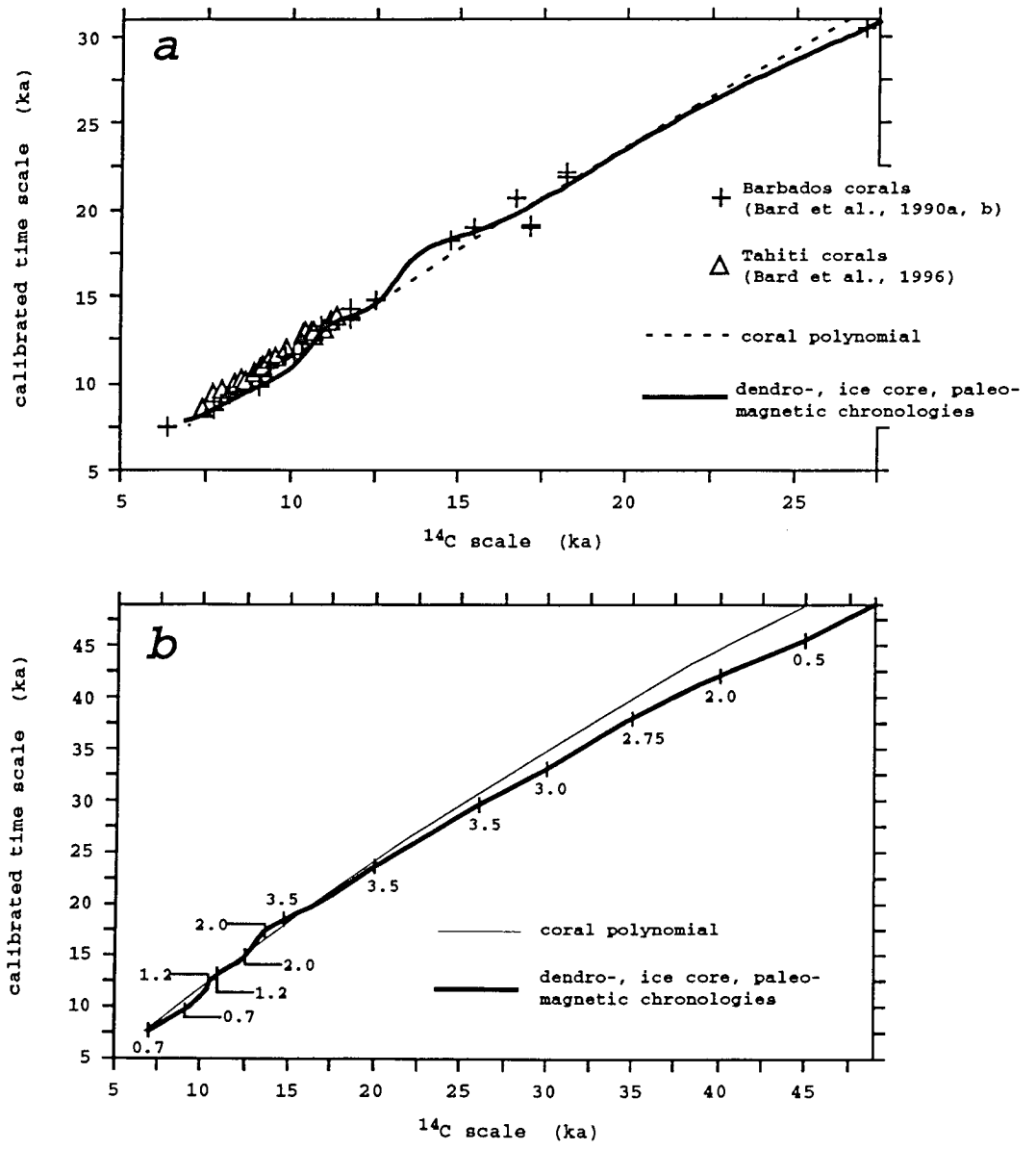

Figure 12. (a) ^{14}C versus calibrated (U/Th) time scale. Paired ^{14}C and U/Th datings show a non-linear offset between both scales that results from variable cosmogenic ^{14}C production during the past 50,000 years. (b) Calibration of ^{14}C ages in this thesis followed the relation indicated by the thick curve. Numbers give offsets between ^{14}C- and calibrated time scales. See also Tables 2 and 4.

and some striated specimens [Kudrass, 1973]. The XRD scans from core SO75-26KL show that primary IRD components are quartz, plagioclase, feldspar, and calcite [Park, 1994] (Figure 13). Since the XRD measurements were performed on bulk samples, most of the carbonate signal likely is of biogenic origin i.e., from calcareous foraminiferal tests and nannoplankton. Dolomite has been detected in minor quantities in samples from IRD layers 1 and 3 (equiv. H 1 and H4; Figure 13). After treatment with acetic acid the carbonate peaks disappeared from the diffractograms but the intensity peak of dolomite was still observed confirming the presence of dolomite in both IRD layers.

Dolomite-bearing carbonate bedrock is widespread in the Laurentide domain but small outcrops also exist on Ireland and Great Britain, and along the western shores of Norway and Svalbard (see Figure 1 in Bond et al. [1992]). Thus the presence of dolomite cannot uniquely document a Laurentide versus Scandinavian source for the icebergs. Yet, the XRD data show that the mineralogy of the IRD deposits off Portugal is not different from those of the open North Atlantic 'Heinrich' layers. In addition to the apparent close chronological correlation with the 'Heinrich' layers in the northern North Atlantic, this similarity in mineralogy is further evidence that the IRD layers on the Portuguese margin are derived from the same iceberg surges and ice sources that caused the North Atlantic 'Heinrich' events.

6.0 THE NORTH ATLANTIC EASTERN BOUNDARY CURRENT DURING 'HEINRICH' MELTWATER EVENTS: SURFACE CONDITIONS OFF PORTUGAL

6.1 Planktonic $\delta^{18}O$ Response to North Atlantic Climatic Anomalies

Marked negative planktonic $\delta^{18}O$ anomalies in conjunction with significantly decreased SST - inferred either from massive incursions of polar foraminifera *N. pachyderma* (sin.) or from planktonic foraminiferal census counts [Bond et al., 1992, 1993; Maslin et al., 1995] - at core sites in the northern North Atlantic document increased meltwater flux and cooling in the course of the 'Heinrich' events. Negative anomalies during or immediately after the

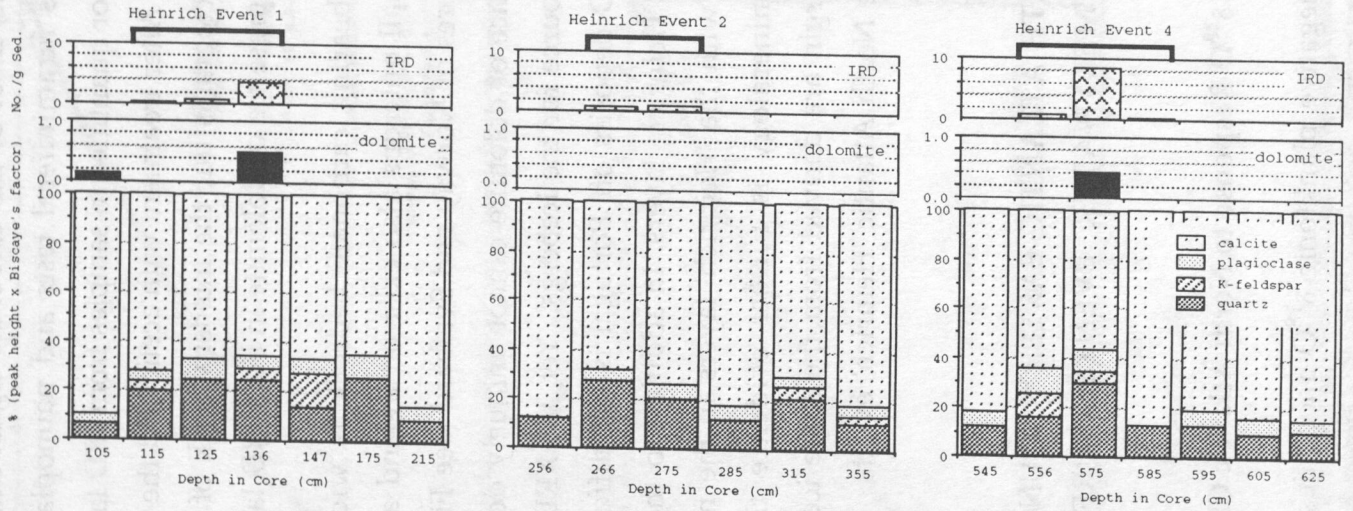

Figure 13. Mineral composition of IRD layers and sediments immediately above and below in core SO75-26KL. Dolomite is present in small quantities in IRD layers 1 and 3 (equiv. Heinrich events H1 and H4), calcite is most likely of biogenic origin (foraminifera and nannoplankton). These results imply that the mineral composition of the IRD layers at the Portuguese margin is not much different from that of the North Atlantic 'Heinrich' events. This similarity lends further support to the contention that the Portuguese IRD layers are derived from the same iceberg events that caused the 'Heinrich' layers in the open North Atlantic.

'Heinrich' events are also observed in the planktonic $\delta^{18}O$ records off Portugal (Figure 10). $\delta^{18}O$ depletion is strongest in cores SO75-3KL (H2, H4) and SO75-35KL (H1, H2, post-H4 at 35 ^{14}C-ka) that are farthest offshore. $\delta^{18}O$ amplitudes are between 0.6‰ (H1 in core SO75-3KL) and 2‰ (post-H4 in both cores). 'Central margin' sediment cores that are further inshore display similar anomalies, but the amplitudes are reduced to 0.7-1.0‰. Stratigraphic resolution in the deeper part of core SO75-12KL that is at the "inner" Portuguese margin, i.e. furthest nearshore, is lower due to larger sample spacing (20 cm), so that the potential post-H4 anomaly is not resolved. In the upper part of the core, however, stratigraphic resolution is comparable to that of the other cores, and the subdued $\delta^{18}O$ response during H2 suggests a less intense hydrographic change at this site. For H1, the isotope record of core SO75-12KL displays the largest $\delta^{18}O$ anomaly seen in all records, with an amplitude of 2.3‰. An inferred hiatus (see Chapter 4.5, *Stratigraphy*) immediately above this anomaly prohibits to evaluate the post-H1 surface response at this site.

The planktonic $\delta^{18}O$ records off Portugal show a further negative anomaly during mid-Termination I that occurs after H1 and immediately before the positive $\delta^{18}O$ excursion that marks the Younger Dryas cold event. The mid-Termination I negative $\delta^{18}O$ event is best resolved in core SO75-6KL with an amplitude of 2.3‰. The peak value of this anomaly of +0.3‰ PDB reaches the Holocene $\delta^{18}O$ level recorded at this site. This value is at the culmination of a negative trend that is covered by a sequence of 12 data points and is, therefore, considered reliable rather than a single-point excursion ("flyer"). Using ^{14}C-AMS ages of 10.7, 11.92, and 13.04 (samples GifA94519, 94520, 94539; Table 2) that were determined for samples immediately above, in the upper part of, and below the anomaly (Figure 6) yield an interpolated age range of 11.7-12.4 ^{14}C-kyr for the anomaly. A similar anomaly is documented between 11.0 and 12.4 ^{14}C-ka in nearby core SU81-18 that has been dated in detail with ^{14}C-AMS [Bard et al., 1987, 1989]. Mean ages of the anomaly are 12.1 ^{14}C-ka and 12.0 ^{14}C-ka in cores SO75-6KL and SU81-18, respectively, and fit well to the age of 12.0 ^{14}C-ka for meltwater pulse 1a (MWP 1a) that has been determined by Fairbanks [1989] using an "age-depth" growth function derived from ^{14}C-AMS dates along cores drilled into coral reefs offshore Barbados. Similar ^{14}C-AMS datings along coral

drill cores offshore Tahiti give an age of 11.79±.22 ^{14}C-ka for the end of MWP 1a [Bard et al., 1996], confirming the association of the negative planktonic $\delta^{18}O$ anomaly in core SO75-6KL with this event that partly overlaps with the first phase of deglaciation (Termination IA: 15.8-13.3 ^{14}C-kyr [Duplessy et al., 1986]). A mid-Termination I negative $\delta^{18}O$ excursion is observed at the other cores as well (Figure 10) and is used there for stratigraphic correlation among the records.

To synoptically map the response of planktonic $\delta^{18}O$ to North Atlantic climatic events, 13 stratigraphic reference levels were chosen for inter-core comparison (Figure 14):

- level 1 mean Holocene $\delta^{18}O$ is calculated using depleted interglacial values between 0 ^{14}C-ka and ≤ 9 ^{14}C-ka that generally form a plateau with only little $\delta^{18}O$ variation;

- level 2 represents the positive $\delta^{18}O$ anomaly of the Younger Dryas, between 10.2 and 10.9 ^{14}C-ka;

- level 3 documents the negative $\delta^{18}O$ anomaly during mid-Termination I that is associated with meltwater pulse (MWP-) 1a;

- levels 4, 5, 6 represent the periods immediately after, during and before 'Heinrich' event H1; to calculate the $\delta^{18}O$ signal during H1, only values of samples from the absolute IRD maximum were chosen (rather than values from across the entire section where IRD abundances are increased above background);

- levels 8, 9, 10 same as above, except for H2

- levels 11, 12, 13 same as above, except for H4

In Figure 15 the $\delta^{18}O$ signals are compared to signals that are documented in sediment cores from the northern North Atlantic (see also Figure 14). Core ENAM 93-21 from the Faeroe-Shetland Channel has been chosen for its high-resolution planktonic $\delta^{18}O$ record that allows in part a direct correlation with the Greenland ice core $\delta^{18}O$ record [Rasmussen et al., 1996a]. BOFS Core 5K

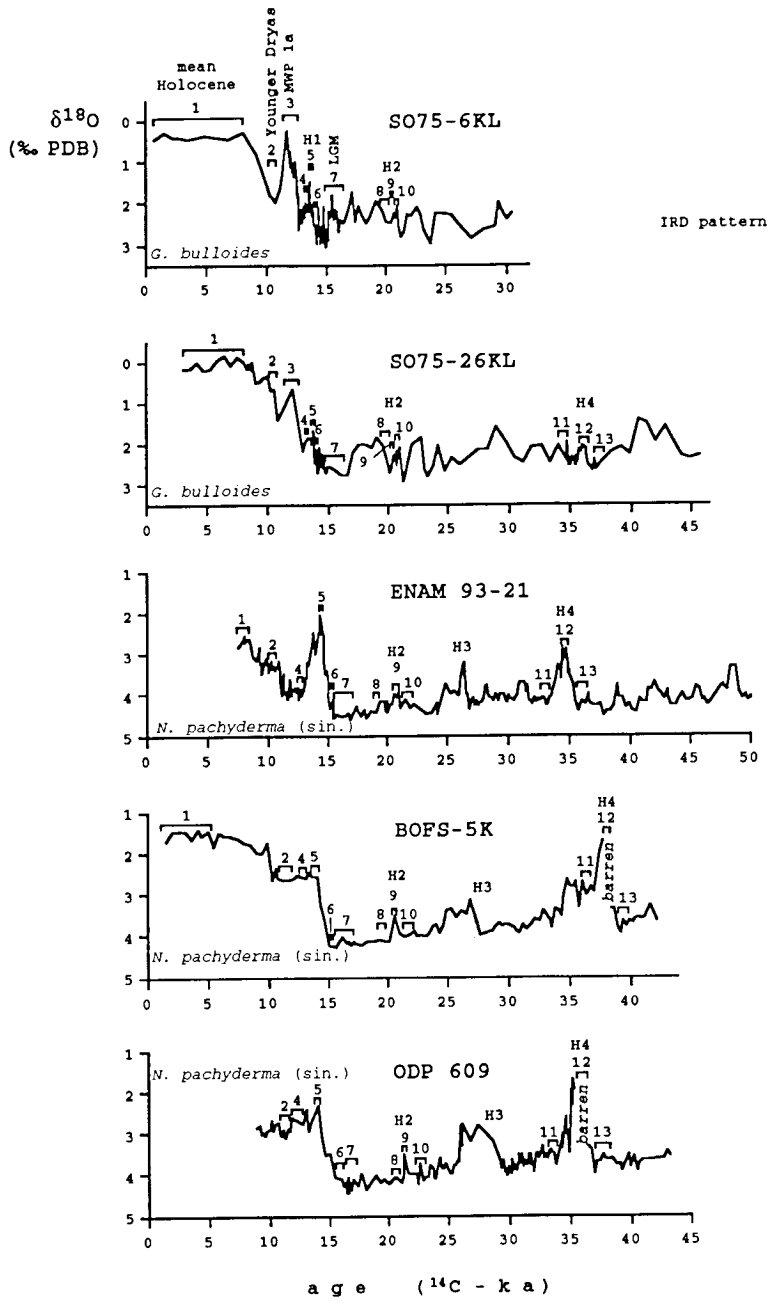

Figure 14. Planktonic oxygen isotope records from the Portuguese margin and the northern North Atlantic. Reference levels are chosen along the isotope records to compare oxygen isotope patterns that were associated with the 'Heinrich' events and deglacial climatic and hydrographic anomalies. The reference levels are described in the text. Time scales of the North Atlantic reference cores are used as published, no adjustments were made for optimal fitting to the Portuguese cores. The 'Heinrich' events are assumed to be synchronous stratigraphic markers, differences in timing are assumed to mirror differential influence of sedimentologic boundary conditions at the different core sites e.g., bioturbation. LGM is Last Glacial Maximum, MWP 1a is Meltwater Pulse 1a as defined in Fairbanks [1989].

from the Rockall Plateau has been chosen for its good documentation of the information (SST from planktonic foraminiferal census counts) is available from this core [Maslin et al., 1995]. DSDP Site 609 from the southern Rockall Plateau area has been chosen because it is located in the belt of maximum IRD abundance during the 'Heinrich' events [Bond et al., 1992, 1993]; as such, it is used here as a reference for maximum changes of North Atlantic surface conditions during 'Heinrich' events.

Planktonic $\delta^{18}O$ in the **Holocene** sections of the sediment cores offshore Portugal are similar, between 0.1‰ and 0.5‰ PDB with no systematic trend between the cores (Figure 15a). This uniform distribution goes along well with the only small temperature-salinity changes along the Portuguese margin. In the northern North Atlantic, a 1.2‰ increase in $\delta^{18}O$ from core BOFS-5K to core ENAM 93-21 documents the rapid decrease in temperature (and to a minor extent in salinity) upon approach of the Norwegian-Greenland Sea.

During the **Younger Dryas** (Figure 15b), core SO75-3KL displays the lightest values, 1.2‰ PDB compared to 1.4-1.9‰ PDB in the other Portuguese cores. The slightly depleted values in cores SO75-26KL, -31KL, and -32KL are either based on single data points or are calculated from sections that contain significant $\delta^{18}O$ variability (core SO75-31KL); these data may not be representative of Younger Dryas conditions offshore Portugal. The range of $\delta^{18}O$ variation of 0.7‰ between the core sites is similar to the $\delta^{18}O$ difference between the northern North Atlantic cores. There, core ENAM 93-21 again displays most increased $\delta^{18}O$, implying a marked oceanic front south of the core. This meridional pattern is similar to the one documented for the Holocene, in agreement with distribution patterns seen in the compilation of planktonic $\delta^{18}O$ from the northern North Atlantic and the Norwegian-Greenland Seas of Sarnthein et al. [1995] that shows north-south gradients similar to Holocene patterns.

Meltwater pulse IA is well documented in all cores from the Portuguese margin (Figure 15c). Most pronounced $\delta^{18}O$ depletion compared to post-H1 values is documented for cores SO75-3KL ($\Delta\delta^{18}O$=-1.3‰) and SO75-35KL ($\Delta\delta^{18}O$=-1.2‰) from the outer margin region. Over the central margin,

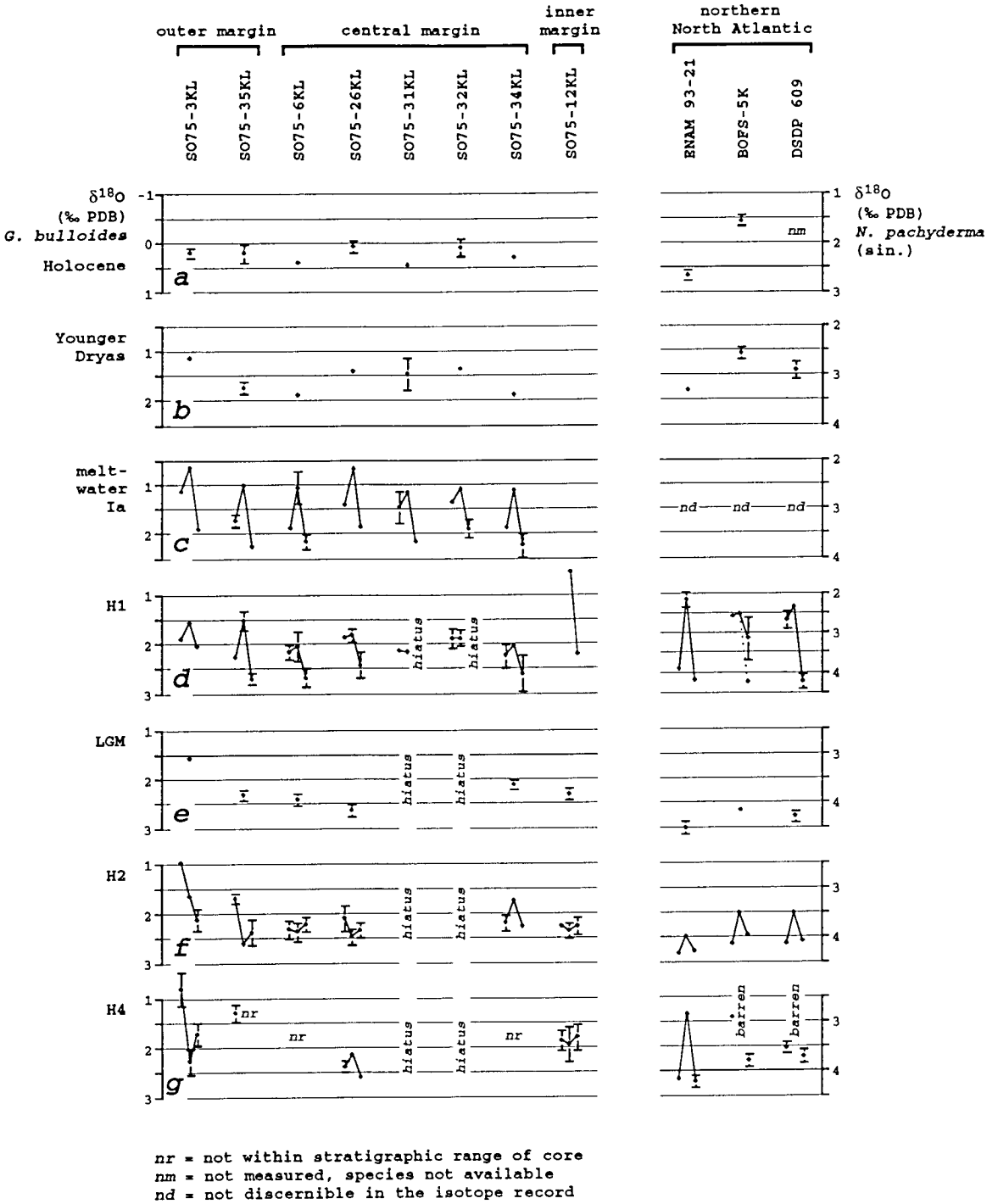

Figure 15. Planktonic O-isotope patterns for the different reference levels shown in Figure 14. Gradients between the different cores reflect the effects of variable meltwater flux, polar front movements, and surface circulation.

amplitudes are smaller, 0.8‰ -1.1‰, implying a slightly decreased influence of meltwaters closer to the Portuguese margin. Peak negative values reach similar $\delta^{18}O$ values, 1.0-1.1‰ PDB. Exceptions are cores SO75-3KL and SO75-26KL where the depletion reaches values of 0.65-0.7‰ PDB. As is seen in core SO75-6KL, the negative planktonic $\delta^{18}O$ anomaly during MWP 1a builds up gradually and reaches most negative values in the later part of the event (Figures 10 and 14). In cores SO75-3KL and SO75-26KL, MWP 1a is captured by two (-3KL) and one (-26KL) measurements only (Figure 10) which may not be representative of mean MWP 1a conditions.

At the northern North Atlantic core sites, no discrete $\delta^{18}O$ anomaly is documented during mid-Termination IA (Figure 14). Detailed evaluation of planktonic $\delta^{18}O$ from the northern North Atlantic and the Norwegian-Greenland Seas has shown that two meltwater phases existed during Termination IA, at 13.2-14.2 ^{14}C-kyr and 12.1-12.4 ^{14}C-kyr [Sarnthein et al., 1995]. The first event conceivably was coeval with 'Heinrich' event H1 (see below), the second event occurred in the same time interval as the culmination of MWP 1a. However, the event was not always discernible as a distinct negative excursion in the planktonic $\delta^{18}O$ records and was then picked on the basis of ^{14}C-AMS datings (see Figure 3 in Sarnthein et al. [1995]). Chronostratigraphic control on the northern North Atlantic sites ENAM93-21, BOFS 5K, and DSDP Site 609 that were chosen here for reference is not sufficient to allow for such selection and thus, faithful extraction of a MWP 1a $\delta^{18}O$ signal was not possible. Since a discrete $\delta^{18}O$ minimum is not seen in the records (Figure 14), however, it may be concluded that either the event was overprinted by the effects on planktonic $\delta^{18}O$ of deglacial temperature increases or it was masked by the generally increased flux of ^{18}O-depleted meltwaters during Termination IA. These effects were less pronounced off Portugal and thus, the influence of MWP 1a on the surface hydrography and planktonic $\delta^{18}O$ was much stronger there (see also Bard et al. [1987, 1989]).

During **'Heinrich' event H1**, planktonic $\delta^{18}O$ depletion decreases from north to south along the Portuguese margin (Figure 15d). The largest $\delta^{18}O$ depletion of $\Delta\delta^{18}O$=-1.7‰ is documented for core SO75- 12KL from the inner Portuguese margin. At the outer margin, amplitudes are 0.6-1.2‰, amplitudes

at the central margin sites are consistently around 0.6‰ towards more negative values. No amplitudes could be determined for cores SO75-31Kl and -32KL where the stratigraphic record is interrupted by a hiatus immediately below the H1 IRD layer. Far larger $\delta^{18}O$ depletion is observed at the northern North Atlantic sites ENAM 93-21 ($\Delta\delta^{18}O$=--2.0‰) and DSDP Site 609 ($\Delta\delta^{18}O$=--1.9‰). For core BOFS-5K, an amplitude of 0.6‰ was determined using an early Termination-IA level as reference for the pre-H1 conditions, during which planktonic $\delta^{18}O$ was already depleted. If LGM values of +4.2‰ PDB are chosen for reference, the amplitude of $\delta^{18}O$ depletion during H1 is 1.2‰, i.e. still smaller than those observed for core ENAM 93-21 and DSDP Site 609.

Regional mapping of the early-Termination-IA meltwater event in the northern North Atlantic (13.2-14.2 ^{14}C-kyr) reveals a gradient towards stronger $\delta^{18}O$ depletion in the central northern North Atlantic (Figure 9a in Sarnthein et al. [1995]). This regional gradient is mirrored in the apparent $\Delta\delta^{18}O$ offset between BOFS-5K and the two other North Atlantic reference cores that are further to the west (DSDP Site 609) and north (ENAM 93-21). The regional distribution pattern of planktonic $\delta^{18}O$ in the Norwegian-Greenland Seas was used to infer melting of the Barents ice shelf that was independent from the Laurentide surge which resulted in enhanced IRD deposition of 'Heinrich' event H1 in the northern North Atlantic [Sarnthein et al, 1995]. The enhanced meltwater flux from the Barents shelf supposedly promoted the development of an anticyclonic surface circulation in the Norwegian-Greenland Seas which brought cold and less saline waters along the Norwegian cost to the northern North Atlantic [Sarnthein et al., 1995] resulting in the observed $\delta^{18}O$/meltwater gradient there. The strong planktonic $\delta^{18}O$ depletion that is documented for core SO75-12KL at the inner Portuguese margin may point to a coastal current that carried cold low-salinity waters from the northern North Atlantic to the south.

During the **Last Glacial Maximum** (LGM) distribution of planktonic $\delta^{18}O$ along the Portuguese margin and at the northern North Atlantic reference sites is more uniform (Figure 15e). This pattern is consistent with a southerly position of the North Atlantic polar front at approximately 40°N during this period, that was bent towards the south upon approaching the Portuguese margin

[CLIMAP, 1981]. Planktonic $\delta^{13}C$ that apparently was near equilibrium with the atmosphere [Spielhagen and Erlenkeuser, 1994], occurrence of sub-polar planktonic foraminiferal species in the northern Norwegian Sea [Hebbeln et al., 1994], as well as planktonic foraminiferal census counts that imply remarkably warm summer-time SST estimates of 2.8°-5.1°C in the northern North Atlantic and Norwegian-Greenland Seas [Sarnthein et al., 1995; Weinelt et al., 1996] all provide circumstantial evidence of partly ice-free conditions at the LGM in the area. These findings are to some extent reproduced in numerical simulations of surface conditions in the northern North Atlantic and Norwegian-Greenland Seas [Seidov and Maslin, 1996; Seidov et al., 1996] and are in direct contrast to the early assumptions e.g., of CLIMAP [1981]. The rather uniform distribution of planktonic $\delta^{18}O$ seen in Figure 15e (and in Figure 6a of Sarnthein et al. [1995]) is nevertheless consistent with a southward shift of the polar front and strongly reduced temperature and salinity gradients north of the front. Increased $\delta^{18}O$ values at the central and inner margin cores relative to values in core SO75-3KL from the outer margin likely document colder nearshore waters in response to increased upwelling during the LGM [Abrantes, 1991].

Planktonic $\delta^{18}O$ patterns during **'Heinrich' events H2 and H4** off Portugal are different from those observed during MWP 1a and H1, and also different from the patterns observed at the northern North Atlantic core sites (Figure 15f, g). $\delta^{18}O$ values during both events are increased compared to conditions prior to and after the events. This pattern is most evident in cores SO75-3KL and -35KL from the outer continental margin area. Whereas core SO75-35KL does not reach the IRD layer of 'Heinrich' event H4 (apparently, penetration of the core into the sediments was stopped by the H4 IRD layer) it shows a negative $\delta^{18}O$ anomaly at the base of the core which is comparable to that seen after H4 in core SO75-3KL (Figure 10). Planktonic $\delta^{18}O$ depletion after H2 and H4 fits into conceptual models and evidence from Greenland ice core data that imply rapid warming after the meltwater events as thermohaline convection started up again after the meltwater events [Dansgaard et al., 1993; Bond et al., 1993]. Exceptions from this pattern are cores SO75-26KL and -34KL that show a slight $\delta^{18}O$ depletion during H4 (-26KL) and H2 (-34KL). The post-H2 $\delta^{18}O$ decrease is small at the coring sites from the central and inner margin cores. The lack of a

post-H2 decrease in $\delta^{18}O$ in core SO75-34KL suggests that the influence on surface conditions of the meltwater events - both in terms of surface temperature and salinity changes - was weakest at this site which is furthest south along the Portuguese margin. Likewise, the negative $\delta^{18}O$ anomaly that is documented in core SO75-26KL during H4 results from the lack of a post-H4 negative $\delta^{18}O$ excursion that is best developed in cores SO75-3KL and -35KL (assuming the penetration of core SO75-35KL into the sediments was stopped by the H4 IRD layer and the pronounced negative $\delta^{18}O$ anomaly at the base of core SO75-35KL represents the post-H4 anomaly). Thus, the larger amplitudes in $\delta^{18}O$ change during H2 and H4 in cores SO75-3KL and -35KL suggest that surface conditions changed strongest at these sites that are farthest offshore, implying the existence of distinct onshore gradients of surface temperature and salinity during the events.

During the H2 and H4 events, planktonic $\delta^{18}O$ at the northern North Atlantic reference sites is depleted, contrary to the positive anomalies seen off Portugal. This offset in planktonic $\delta^{18}O$ patterns during both events suggests that meltwater flux to - and thus planktonic $\delta^{18}O$ depletion at - the Portuguese margin was reduced during H2 and H4 compared to the northern North Atlantic, thus enhancing the effects of cooling during the events on planktonic $\delta^{18}O$ off Portugal. In the northern North Atlantic, meltwater advection was strong enough to partly compensate for the effects of surface cooling that would have increased planktonic $\delta^{18}O$.

The observed planktonic $\delta^{18}O$ patterns suggests that surface conditions off Portugal were highly variable during the past 50 ^{14}C-kyr. Distinct gradients of surface ocean conditions existed across the Portuguese margin during the climatic events listed above. Negative $\delta^{18}O$ signals, during MWP 1a as well as post-H4 and post-H2, are strongest developed at the outer margin core sites. During the LGM and the Younger Dryas cold event, core SO75-3KL at the northernmost position over the outer Portuguese margin consistently shows depleted values compared to the other cores from the Portuguese margin. This points to colder surface temperatures over the central and inner Portuguese margin probably in association with enhanced glacial-maximum upwelling [Abrantes, 1991].

During the last glacial maximum, the polar front was shifted to the south and was in immediate reach of the Portuguese margin, as implied by steep surface temperature and salinity gradients in the area [CLIMAP, 1981; Thiede, 1977; Duprat, 1983; Duplessy et al., 1991]. Planktonic foraminiferal census counts imply a southward penetration of cold subpolar waters further offshore, and the presence of warmer waters over the central margin and further nearshore [Thiede, 1977; Molina-Cruz and Thiede, 1978; Pflaumann, 1980; Duprat, 1983] (Figure 16). This nearshore incursion of warmer surface waters is reminiscent of today's northward advection of warm saline surface waters along the western Iberian margin that develops during periods of weakened trade wind strength [Haynes and Barton, 1990]. However, during the last glacial, the warm water incursion more likely reflects a northward branch of warm saline surface waters that were derived from the North Atlantic Drift Current (Figure 16).

Distinct negative planktonic $\delta^{18}O$ anomalies suggest that low-salinity surface waters reached the Portuguese margin during meltwater pulse 1a and 'Heinrich' event 1 (Figure 15). During H2 and to a minor extent during H4, planktonic $\delta^{18}O$ off Portugal remains increased and negative anomalies occur after the events. This suggests that cooling as indicated from planktonic census counts (see below) partly compensated for the effects of low-salinity surface waters on planktonic $\delta^{18}O$, and caused $\delta^{18}O$ values to remain increased. It was only after the 'Heinrich' meltwater events when surface temperatures rose that the last spurs of meltwater, combined with the temperature increase, resulted in marked negative planktonic $\delta^{18}O$ decreases. The negative $\delta^{18}O$ anomaly during H1 implies that the flow of low-salinity water which contained glacial meltwater was stronger compared to the previous 'Heinrich' events. H1 occurred early in the last glacial-interglacial transition during the onset of ice sheet disintegration around the North Atlantic. Therefore, meltwater flow to the North Atlantic and its southward export in the North Atlantic eastern

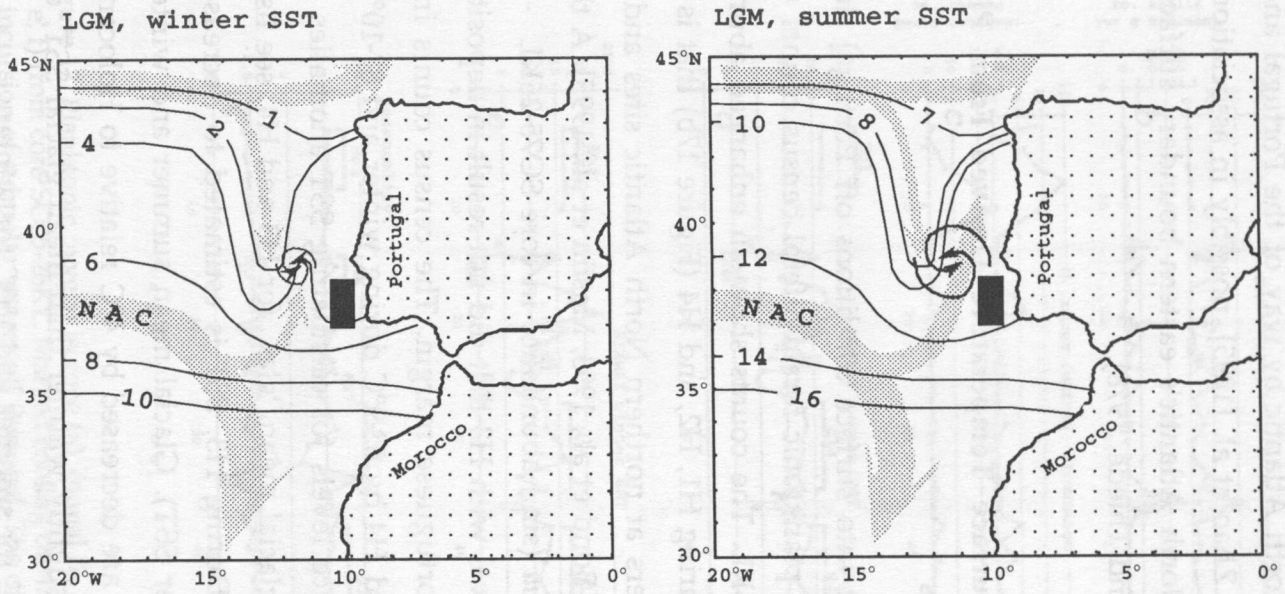

Figure 16. Sea surface temperature at the western Iberian margin during the Last Glacial Maximum (LGM) after Duprat [1983]. The North Atlantic polar front was deflected to the south upon approaching the Portuguese margin (see also CLIMAP [1981]). The incursion of warmer waters at the central and inner margin off Portugal likely documents a northward branching of the North Atlantic Drift Current (NAC) that carried warm surface waters across the North Atlantic. Hypothetic surface currents are indicated. The black box marks the location of the Portuguese margin cores used in this thesis. Schematic after Duprat [1983].

boundary current was strong enough that surface cooling could not suppress the negative planktonic $\delta^{18}O$ anomaly.

Meltwater and SST anomalies coeval with 'Heinrich' events are also recorded at subtropical Northeastern Atlantic sites as far south as Cape Blanc (21°N, Northwest Africa) and presumably document export of cold low-salinity waters from the northern North Atlantic by way of the Portugal and Canary Currents [Wang et al., 1995; Zhao et al. [1995], possibly in association with an enhanced strength of the North Atlantic's eastern boundary surface current [Thiede, 1977; Molina-Cruz and Thiede, 1978].

6.2 Variability of Sea Surface Temperature Derived From Planktonic Foraminiferal Census Counts

To gain further insight into surface conditions off Portugal during the 'Heinrich' meltwater events, planktonic foraminiferal census counts were carried out along core SO75-26KL. The counts show an enhanced abundance of polar *N. pachyderma* (sin.) during H1, H2, and H4 (Figure 17b) that is also characteristic for 'Heinrich' layers at northern North Atlantic sites and signifies marked SST decreases there [Bond et al., 1993; Maslin et al., 1995]. A third marked increase in *N. pachyderma* (sin.) abundance in core SO75-26KL - centered at 25.1 ^{14}C-ka - likely is coeval with H3 that did not result in deposition of an IRD layer on the central Portuguese margin. The census counts imply SST decreases during H1, H2, and H4 by 8°-9°C during winter and 8°-10°C during summer (Figure 17) (reference levels for calculating SST anomalies are LGM for H1, pre-H2 for H2, and glacial mean, 'gla', for H3 and H4; see lists of SST statistics along Figure 17). During H3, SST is estimated to decrease by 7°C (winter SST) to 8°C (summer SST). Glacial mean summer and winter SST of 17°C and 12°C, respectively, are decreased by 4°C relative to Holocene values. Conditions prior to H2 are slightly warmer than mean glacial SST, estimated temperatures are around 20°C for summer and 15°C for winter.

The warm mean glacial and glacial-maximum temperatures that were estimated from the planktonic census counts clearly demonstrate that subtropi-

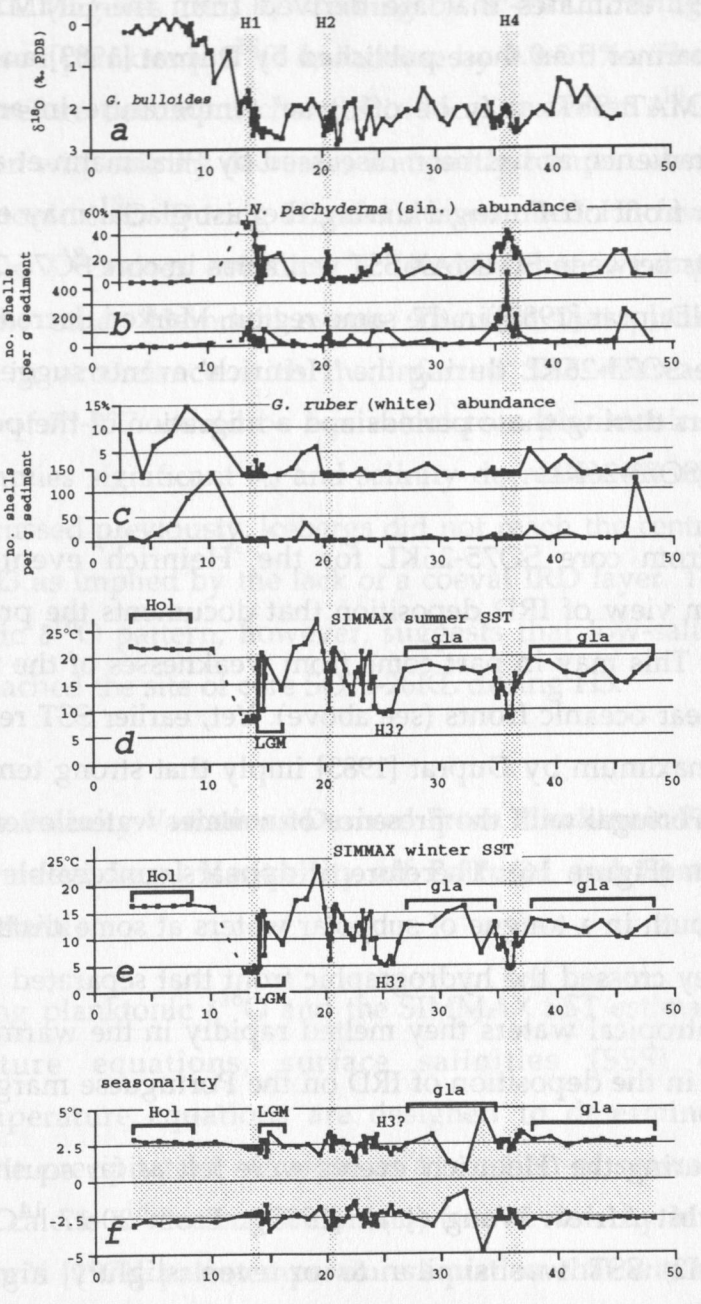

summer SST		
Hol	21.9	±0.3
H1	8.3	±0.4
LGM	16.8	±3.8
LGM min	10.1	
H2	15.1	±4.3
H2 min	10.2	
H3(?)	9.9	±0.6
H4	12.7	±2.9
H4 min	8.7	±0.2
gla	17.4	±1.3

winter SST		
Hol	16.4	±0.1
H1	3.8	±0.4
LGM	11.7	±3.0
LGM min	6.8	
H2	10.5	±3.0
H2 min	6.0	
H3(?)	5.6	±0.7
H4	7.4	±2.2
H4 min	4.3	±0.2
gla	12.2	±2.2

seasonal ΔT		
Hol	5.5	±0.3
H1	4.6	±0.1
LGM	5.1	±1.1
LGM min	3.3	
H2	5.3	±1.0
H2 min	4.2	
H3(?)	4.3	±0.5
H4	5.3	±0.8
H4 min	4.4	±0.2
gla	5.2	±1.7

Figure 17. Planktonic oxygen isotope (a), faunal (b, c), and inferred SST records (d, e, f) from core SO75-26KL. Marked cooling during H1, H2, and H4 suggests an incursion of subpolar waters off Portugal. The distinct faunal and SST anomaly at 25 ^{14}C-ka likely represents cooling during H3. H3 did not result in an IRD layer off Portugal. In the absence of direct radiocarbon dating, the association of the faunal and SST anomaly with H3 remains speculative. SST statistics for the 'Heinrich' events and other reference levels are given along panels d, e, and f.

cal waters reached the site of core SO75-26KL during the last glacial and that the site was south of the glacial polar front (see also Figure 16). It must be noted, however, that the SST estimates that are derived from the SIMMAX MAT technique are 2-5°C warmer than those published by Duprat [1983] and Bard et al. [1989]. SIMMAX MAT SSTs may be off 'true' temperature in areas with strong temperature gradients, as has been discussed by Pflaumann et al. [1996]. The existence of such front off Portugal during the last glacial may explain at least in part the offsets between SIMMAX SST estimates in core SO75-26KL and previous estimates by Duprat [1983] in the same region. Marked decreases of the SST estimates in core SO75-26KL during the 'Heinrich' events suggest advection of subpolar waters during these periods and a migration of the polar front across the site of core SO75-26KL.

SST estimates from core SO75-26KL for the 'Heinrich' events appear unexpectedly warm in view of IRD deposition that documents the presence of icebergs off Portugal. This may in part come from weaknesses of the SIMMAX analogue technique near oceanic fronts (see above). Yet, earlier SST reconstructions for the glacial maximum by Duprat [1983] imply that strong temperature gradients existed off Portugal with the presence of warmer waters over the central and inner margin (Figure 16). Therefore, it appears conceivable that icebergs drifted to the south in a tongue of subpolar waters at some distance from the margin. When they crossed the hydrographic front that separated cold subpolar from warm subtropical waters they melted rapidly in the warmer nearshore waters resulting in the deposition of IRD on the Portuguese margin.

SST decreases during the 'Heinrich' events were felt as far south as Cape Blanc (21°N, Northwest Africa; Wang et al. [1995]). From 20-17 ^{14}C-kyr i.e., immediately after H2, SST was similar to or even slightly higher than Holocene values. For this interval, enhanced occurrences of "warm" planktonic foraminiferal species *Globigerina ruber* (white variety) are documented in core SO75-26KL that are not seen in the post-H3 and -H4 periods (Figure 17c). The marked increase in *G. ruber* (white) abundance and the inferred SST increase imply stronger advection of subtropical waters, possibly in conjunction with an enhanced surface circulation in the North Atlantic subtropical gyre that brings warm subtropical waters to the Portuguese margin.

Despite the significant cooling of surface waters during the 'Heinrich' events, planktonic $\delta^{18}O$ displays negative anomalies during H1 and H4 in core SO75-26KL (Figures 15d, h). Cooling by 8°-10°C during these events should have caused planktonic $\delta^{18}O$ to increase by 2.0-2.5‰. The negative $\delta^{18}O$ excursions therefore document changes in local seawater $\delta^{18}O$ composition (δ_w) in association with salinity decreases that partly compensated the effects of cooling on planktonic $\delta^{18}O$. During H2 and the assumed H3 faunal and SST anomaly planktonic $\delta^{18}O$ does not show a decrease that is comparable to those seen during the other 'Heinrich' events. The fact that planktonic $\delta^{18}O$ does not increase in accordance with the inferred SST decrease (the inferred SST decrease of 7°-8°C would be equivalent to a planktonic $\delta^{18}O$ increase by 1.8-2.0‰) implies significant δ_w and salinity decreases during both events. As has been discussed previously, icebergs did not reach the central Portuguese margin during H3 as implied by the lack of a coeval IRD layer. The combined SST and planktonic $\delta^{18}O$ pattern, however, suggests that low-salinity subpolar surface waters reached the site of core SO75-26KL during H3.

6.3 Paleo-Salinity Variations Derived From Planktonic Foraminiferal $\delta^{18}O$ and SST Estimates: Local Variability off Portugal and Comparison to the Open North Atlantic

Using planktonic $\delta^{18}O$ and the SIMMAX SST estimates as input to paleotemperature equations, surface salinities (SSS) can be calculated. Paleotemperature equations are designed to determine water temperature during the precipitation of calcite as a function of seawater $\delta^{18}O$ composition (δ_w) and calcite $\delta^{18}O$ composition (δ_c) (see review by Mix [1987]). Here I use Shackleton's [1974] paleotemperature equation that was empirically calibrated to low temperatures (<16.9°C) by comparing benthic foraminiferal $\delta^{18}O$ from deep Pacific sediment cores to ambient water temperatures:

$$T = 16.9 - 4 * (\delta_c - \delta_w) \qquad \text{equation 1}$$

Glacial-interglacial variation of seawater δ_w that is driven by ice volume changes is derived from the mean ocean δ_w record of Vogelsang [1991] (Figure

18a). The mean ocean δ_w record has been constructed by using benthic foraminiferal $\delta^{18}O$ data from Norwegian Sea sediment cores and assuming that bottom water salinity (and temperature) there remained constant during glacial-interglacial times; data gaps in some glacial sections (stages 6, 8, 10) of the record were filled in by using benthic foraminiferal $\delta^{18}O$ data from deep Pacific core V19-30 [Labeyrie et al., 1987; Vogelsang, 1990]. A mean-ocean δ_w increase by 1.1‰ during the Last Glacial Maximum that is implied by these data has recently been confirmed by pore-water $\delta^{18}O$ measurements in sediment cores from the equatorial Atlantic [Schrag et al., 1996].

I have normalised the mean ocean δ_w record to local δ_w at the site of core SO75-26KL that was calculated from equation 1 by using the late Holocene *G. bulloides* $\delta^{18}O$ value of 0.2‰ PDB from core SO75-26KL as input for δ_c. Summer SST as inferred from the planktonic foraminiferal census counts was used for T in equation 1, after correcting by -1°C to account for an apparent offset from equilibrium fractionation as revealed by statistical analysis of *G. bulloides* $\delta^{18}O$ from core-top samples [Duplessy et al., 1992]. I.e., "isotopic" temperature recorded by *G. bulloides* $\delta^{18}O$ is lower by 1°C than "true" summer SST [Duplessy et al., 1992]. The pattern of $\delta^{18}O$ values from modern *G. bulloides* and of surface temperature shows that $\delta^{18}O$ of *G. bulloides* is highly correlated with summer SST at 7°-22°C, at a constant offset of 1°C, but is only poorly correlated to winter SST [Duplessy et al., 1991, 1992]. Therefore, "isotopic" summer SST is the more reliable input to equation 1. Late Holocene "isotopic" summer SST at the site of core SO75-26KL is 20.9°C, local δ_w is calculated to be 1.4‰ PDB (1.67‰ SMOW, using an offset of 0.27‰ between PDB and SMOW scales [Hut, 1987]).

Using the records of local δ_w and "isotopic" summer SST shown in Figure 18a, equilibrium δ_c was predicted and compared to the measured $\delta^{18}O$ record from core SO75-26KL (Figure 18b). The offset between measured $\delta^{18}O$ and

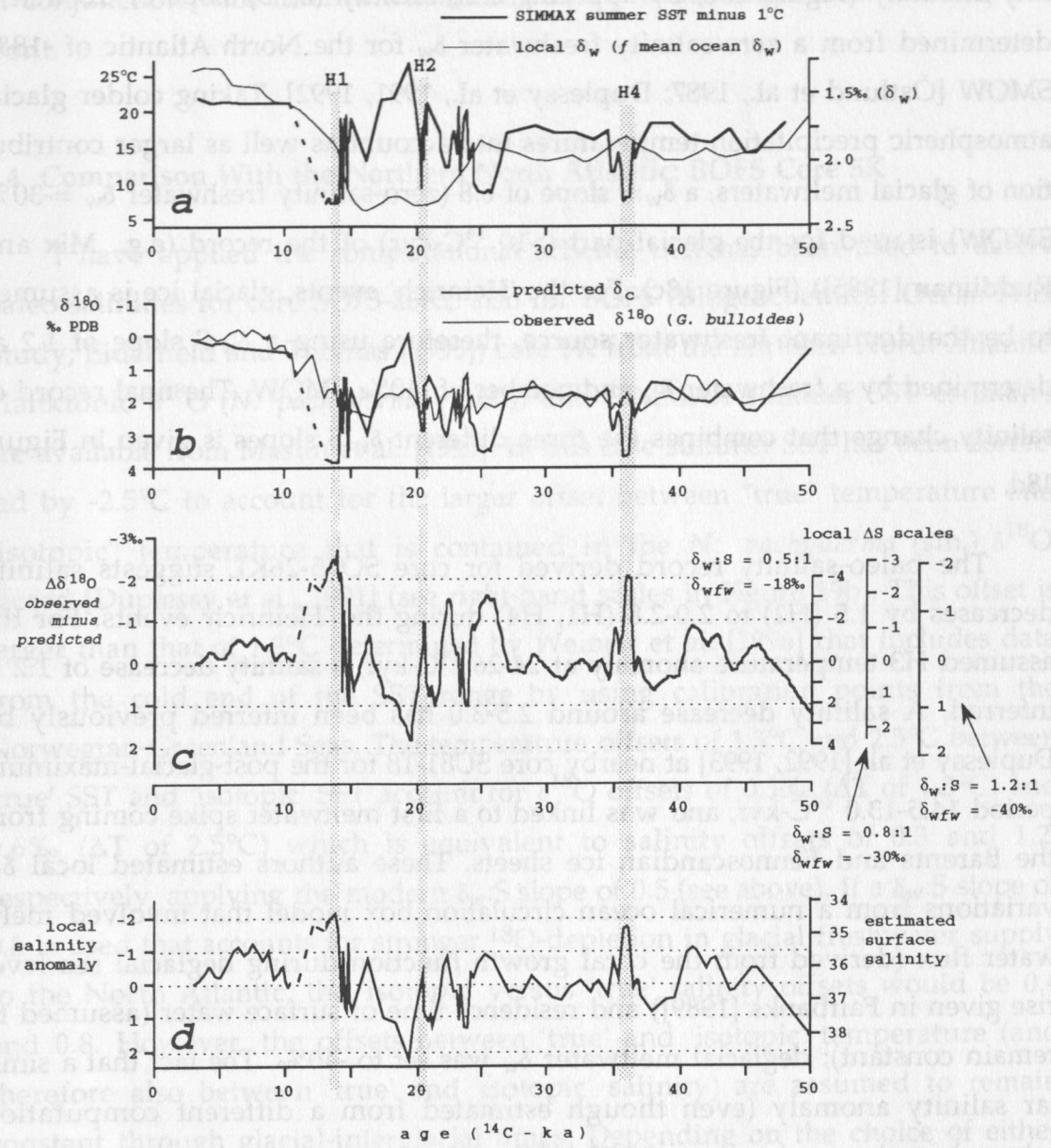

Figure 18. Estimated SST from core SO75-26KL in combination with a seawater oxygen isotope record (a) has been used to predict equilibrium oxygen isotope variations at the core site (b). The deviation of observed planktonic from predicted oxygen isotope levels monitors local salinity variations that are calculated using different isotope signals for glacial freshwater endmembers (c). An estimated surface salinity record is shown in (d). Inferred SST has been corrected to account for offsets between 'isotopic' and 'true' temperature [Duplessy et al., 1991].

predicted δ_c is the local seawater δ_w anomaly and is converted into a local salinity anomaly (Figure 18c) by applying a δ_w:salinity (δ_w:S) slope of 0.5 that is determined from a zero-salinity freshwater δ_w for the North Atlantic of -18‰ SMOW [Östlund et al., 1987; Duplessy et al., 1991, 1992]. Taking colder glacial atmospheric precipitation temperatures into account as well as larger contribution of glacial meltwaters, a δ_w:S slope of 0.8 (zero-salinity freshwater δ_w =-30‰ SMOW) is used for the glacial part (>10 ^{14}C-kyr) of the record (e.g., Mix and Ruddiman [1985]) (Figure 18c). For the 'Heinrich' events, glacial ice is assumed to be the dominant freshwater source, therefore using a δ_w:S slope of 1.2 as determined by a freshwater δ_w endmember of -40‰ SMOW. The final record of salinity change that combines the three different δ_w:S slopes is given in Figure 18d.

The paleo-salinity record derived for core SO75-26KL suggests salinity decreases by 1.5 (H2) to 2.0-2.8 (H1, H4) during the 'Heinrich' events. For the assumed H3 temperature anomaly at 24-26 ^{14}C-kyr, a salinity decrease of 1.2 is inferred. A salinity decrease around 2.5-3.0 has been inferred previously by Duplessy et al. [1992, 1993] at nearby core SU81-18 for the post-glacial-maximum period 14.5-13.0 ^{14}C-kyr, and was linked to a first meltwater spike coming from the Barents and Fennoscandian ice sheets. These authors estimated local δ_w variations from a numerical ocean circulation box model that involved meltwater flux (derived from the coral growth function during deglacial sea-level rise given in Fairbanks [1989]) and residence time of surface water (assumed to remain constant); deglacial meltwater δ_w was set to -40‰. The fact that a similar salinity anomaly (even though estimated from a different computation scheme) is observed at core SO75-26KL and that the anomaly in this core is associated with H1 suggests that the low-salinity waters were derived from the northern North Atlantic and presumably also contained major meltwater components from the Laurentide ice sheet.

The paleo-salinity estimates from core SO75-26KL also show that mean-glacial salinities were similar to Holocene salinities supporting the earlier suggestion based on inferred warm SST that the site of core SO75-26KL was in the advection path of subtropical surface waters during glacial-interglacial times and that it was only during the North Atlantic 'Heinrich' meltwater events

that low-salinity subpolar waters reached the Portuguese margin, conceivably in conjunction with intermittent southward/onshore migrations of the polar front.

6.4 Comparison With the Northern North Atlantic: BOFS Core 5K

I have applied the computational scheme that has been used to derive paleo-salinities for core SO75-26KL also for BOFS (Biogeochemical Ocean Flux Study; Elderfield and Thomas [1995]) core 5K from the northern North Atlantic. Planktonic $\delta^{18}O$ (*N. pachyderma* (sin.)) and SIMMAX summer SST estimates are available from Maslin et al. [1995]. In this case summer SST has been corrected by -2.5°C to account for the larger offset between "true" temperature and "isotopic" temperature that is contained in the *N. pachyderma* (sin.) $\delta^{18}O$ record [Duplessy et al., 1991] (see right-hand scales in Figure 19b). This offset is larger than that of 1.3°C determined by Weinelt et al. [1996] that includes data from the cold end of the SST range by using calibration points from the Norwegian-Greenland Seas. The temperature offsets of 1.3°C and 2.5°C between 'true' SST and 'isotopic' SST account for $\delta^{18}O$ offsets of 0.3‰ (ΔT of 1.3°C) and 0.6‰ (ΔT of 2.5°C) which is equivalent to salinity offsets of 0.3 and 1.2, respectively, applying the modern δ_w:S slope of 0.5 (see above). If a δ_w:S slope of 0.8 is used that accounts for stronger ^{18}O-depletion in glacial freshwater supply to the North Atlantic, the 'isotopic' versus 'true' salinity offsets would be 0.4 and 0.8. However, the offsets between 'true' and 'isotopic' temperature (and therefore also between 'true' and 'isotopic' salinity) are assumed to remain constant through glacial-interglacial times. Depending on the choice of either correction value, the paleo-salinity estimates would shift on an absolute salinity scale but amplitudes of variation would remain the same. To circumvent the problem of selecting the most appropriate correction value, I have normalized the paleo-salinity estimates to modern salinities, thus documenting absolute salinity variations relative to the modern that are independent from the choice of an 'isotopic' correction value.

The data from BOFS-5K suggest that summer SST in the open North

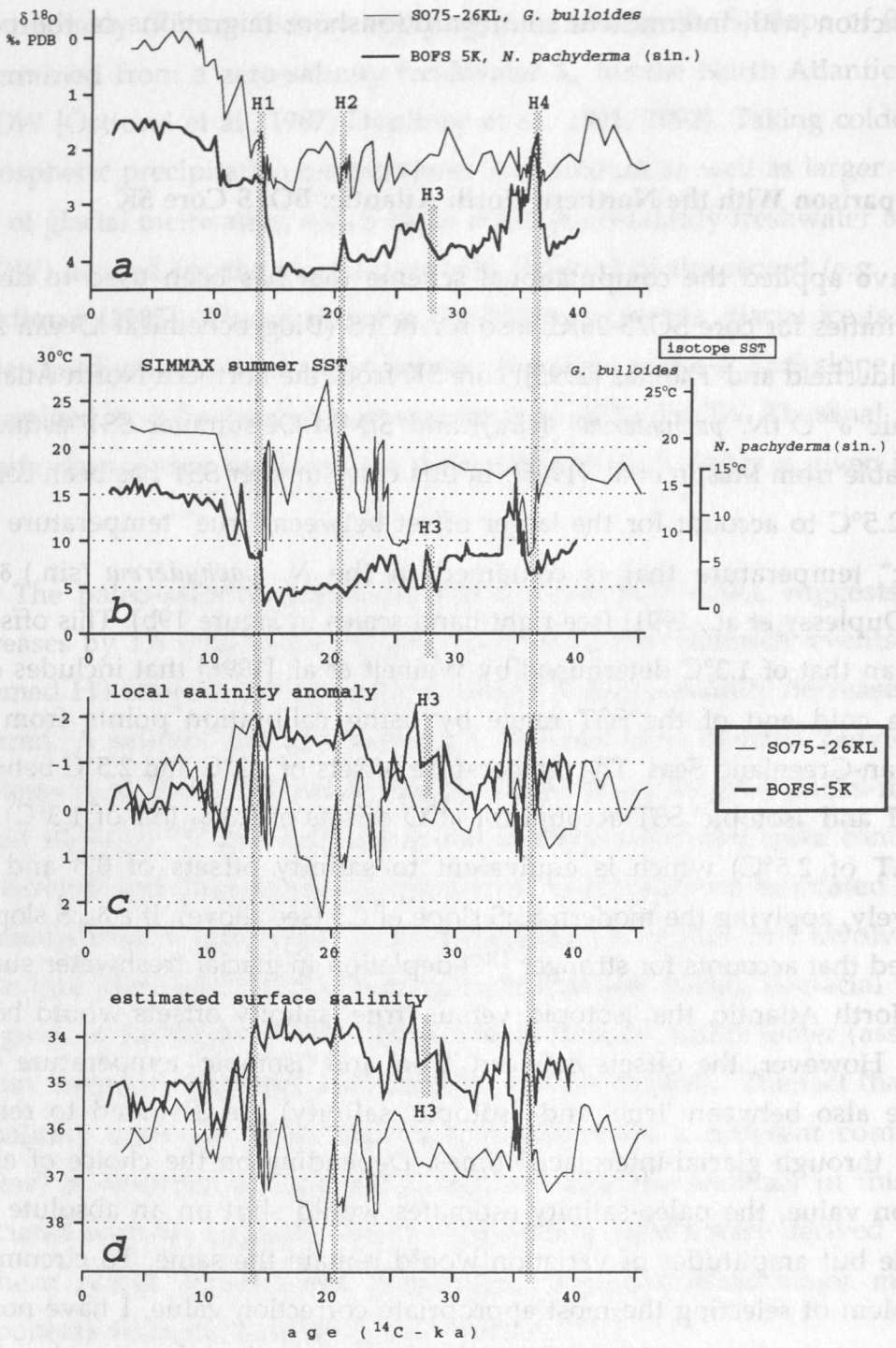

Figure 19. Paleosalinity estimates for core BOFS-5k from the northern North Atlantic followed the same scheme as shown in Figure 18. Comparison of estimated salinity variation along cores SO75-26KL and BOFS-5K suggests that salinity gradients were reduced between both cores during the 'Heinrich' events. This implies an expansion of subpolar conditions to the southern Portuguese margin, as has also been inferred from estimated SST decreases there.

Atlantic was continuously lower and glacial salinities depleted compared to core SO75-26KL (Figure 19), as is expected from the hydrographic gradient between subpolar and subtropical waters that separates both core sites [CLIMAP, 1981]. The SST gradient between both sites was increased by 3°C during the last glacial, i.e. 10° for the mean-glacial period as compared to 7°C during the Holocene. Inferred salinity decreases of 0.5 for H1 and H2, and 1.5 for H4 at core BOFS-5K are distinctly smaller than those of 1.5-3.0 that are estimated for SO75-26KL. Coverage with planktonic $\delta^{18}O$ and SST estimates during H3 is insufficient in core BOFS-5K due to low abundances of planktonic foraminifera in this interval. For the post-H2 warm period at SO75-26KL a temperature gradient of nearly 20°C is indicated, which appears unrealistic at first glance but cannot be ruled out as the occurrence of 'warm' planktonic foraminiferal species *G. ruber* (white) indeed suggests warmer than mean-glacial conditions off Portugal (see above) for this period.

There are few instances when SST and paleo-salinity estimates indicate a reduced (or even reversed) hydrographic gradient between cores BOFS-5K and SO75-26KL. During H1 and H4, values converge and reach similar levels. The SST convergence during H1 is caused by deglacial warming by 5°C at BOFS-5K and cooling by 8°C at SO75-26KL. The salinity decrease at BOFS 5K during H1, however, is only 0.5 i.e., one fifth of the coeval decrease estimated for SO75-26KL (ΔS=2.5) further south. During H4, cooling at core SO75-26KL is 10°C whereas at core BOFS-5K SST barely decreases by 2°C. SST and paleo-salinity values remain on a similar level for a brief period after H4 when SST and paleo-salinity increases at both sites, before SST and paleo-salinity decreases at core BOFS-5K but remain high at core SO75-26KL. A reversed gradient is indicated for a brief period at 13.0 ^{14}C-ka when paleo-salinity at the northern core BOFS-5K increases over that inferred for core SO75-26KL. This may well be an artefact of inadequate stratigraphical resolution in core SO75-26KL for which the age model suggests decreased sedimentation rates during this interval (see Figure 5d; note that a similar minimum in the sedimentation rate curve is indicated if ^{14}C-ages are used for computation instead of calibrated ages as in Figure 5d).

If the SST anomaly between 27-24 ^{14}C-kyr in core SO75-26KL is indeed coeval with H3, then would the SST and paleo-salinity anomalies have to be

lined up (i.e., shifted to older ages) with the occurrence of H3 in BOFS-5K. In this case the SST estimates at BOFS-5K and SO75-26KL would converge whereas the paleo-salinity gradient would have remained similar to what is indicated for the periods before and after H3. It must be noted that no SST estimates were possible from the peak maximum of the H3 IRD layer in core BOFS-5k because of low planktonic foraminiferal abundances in this section [Maslin et al., 1995].

Maslin et al. [1995] used the occurrence of distinct salinity decreases during the 'Heinrich' events as circumstantial evidence for significantly decreased surface density that potentially led to a strong reduction (H1) if not a complete halt (H4, H3) of thermohaline overturn in the northern North Atlantic. This inference is supported by benthic foraminiferal $\delta^{13}C$ data and numerical circulation experiments which suggest strongly reduced ventilation of the deep North Atlantic during the 'Heinrich' events and deglacial meltwater events [Jansen and Veum, 1990; Keigwin et al., 1991; Lehman and Keigwin, 1992; Sarnthein et al., 1994; Jung, 1996; Seidov et al., 1996]. The salinity anomalies that Maslin et al. [1995] estimated for core BOFS-5K, however, are larger (ΔS=1.0-2.5) - and therefore potentially more effective in reducing water mass sinking - than those estimated here (ΔS=0.5-1.5) for the same core (Figure 19). The difference is due to a more positive meltwater δ_w value of -35‰ SMOW (compared to -40‰ SMOW used here) that these authors used for their estimation of salinity drawdown.

The amplitude of inferred salinity anomalies during the 'Heinrich' events decreases along with the δ_w value that has been used to estimate the salinity decrease. The fact that SIMMAX MAT and concurrent transfer function SST estimates deviate from each other adds further uncertainty to the determination of salinity change through time. But paleoceanographic time series that are available from the northern and subtropical North Atlantic and new data from shallow sediment cores at the upper Portuguese margin consistently demonstrate that the meltwater incursions that went along with the 'Heinrich' events and the deglacial of ice sheets around the North Atlantic affected the North Atlantic's thermohaline circulation and caused distinct reductions in ventilation from mid-depth water masses around 1100 m off Portugal (shown further below in this thesis) to water depths around 4000 m in the northern North

Atlantic [Veum et al., 1992; Keigwin and Jones, 1994; Sarnthein et al., 1994; Jung, 1996]. From this it must be inferred that the salinity reductions - whatever their true magnitude was - were large enough to slow down thermohaline overturn in the northern North Atlantic, or bring it to a complete halt.

Bond et al. [1993] argued that 'Heinrich' events mark the final stages of longer-term cooling cycles which drove the glacial North Atlantic from subpolar to polar conditions. Cooling cycles are not seen in the SST record from core SO75-26KL (Figure 17). If the cycles indeed existed, it appears they were not transmitted southwards across the southern border of the 'Heinrich' belt (appr. 40°N). Surface water cooling off Portugal occurred only during the 'Heinrich' events. Cooling (inferred from the $U^{k}_{37'}$ temperature index) that was coeval with 'Heinrich' events is also observed as far south as Cape Blanc (21°N) off Northwest Africa [Zhao et al., 1995]. Apparently, the temperature signals "leaked" through the glacial polar front to the south by way of the Portugal and Canary Currents. The incursion of polar and subpolar foraminiferal taxa off Portugal and evidence of surface cooling and salinity decreases off Cape Blanc [Wang et al., 1995; Zhao et al., 1995] indicate an increased southward transportation of surface water in the North Atlantic's eastern boundary current, in general agreement with earlier micropaleontological evidence [Thiede, 1977; Molina-Cruz and Thiede, 1978]. Such scenario also concurs with results from numerical circulation models that simulate changes in North Atlantic circulation in response to freshwater anomalies and indicate a southward penetration of low-salinity waters along the northeast Atlantic margin to 30°-20°N (see Figure 2 in Manabe and Stouffer [1995], Figure 8 in Seidov et al. [1996]).

7.0 GLACIAL-INTERGLACIAL EVOLUTION OF MID-DEPTH CIRCULATION OFF PORTUGAL: MEDITERRANEAN OUTFLOW VERSUS MID-DEPTH WATERS FROM NORTH ATLANTIC SOURCES

Benthic isotope studies have revealed distinct changes of deep water patterns in the North Atlantic during late-glacial and deglacial meltwater surges [Keigwin et al., 1991; Veum et al., 1992; Sarnthein et al., 1994; Seidov et al., 1996]. 'Heinrich' events and associated meltwater surges also affected deep water properties that reflect re-organisations in mid-depth and deep circulation [Jung, 1996; Rasmussen, 1996]. The close correlation between marked benthic $\delta^{13}C$ decreases and the occurrence of 'Heinrich' layers in cores SO75-6KL and -26KL from the upper Portuguese margin are suggestive of mid-depth circulation changes that were related to changing surface ocean conditions in the northern North Atlantic during the 'Heinrich' meltwater and IRD events. However, ambient bottom waters at both core locations today receive a significant contribution of saline Mediterranean Outflow Water (MOW). Variations either in the relative amount of MOW received at the core sites or in depth of MOW core layer may have contributed to the observed negative benthic $\delta^{13}C$ anomalies. Glacial-interglacial variability of MOW advection and hydrography needs therefore to be evaluated to better constrain the interpretation of benthic $\delta^{13}C$ from the upper Portuguese margin in view of the North Atlantic's thermohaline circulation.

7.1 Mediterranean Paleoceanography: Glacial-Interglacial Evolution and Conceptual Models

Advection of MOW to the North Atlantic is driven by the Mediterranean's water budget and limited by the internal hydraulics of the Gibraltar Straits [Madelain, 1970; Bethoux, 1979; Bryden and Stommel, 1984; Armi and Farmer, 1985; Bryden and Kinder, 1991]. Today, Atlantic surface waters enter the Mediterranean with a salinity of 36.5. By the time they reach the Levantine Basin in the easternmost Mediterranean, salinity of these waters is increased by more than 2.5 due to continued evaporation that is in excess to precipitation thus causing a net freshwater loss to the atmosphere. Haline overturn in the

Levantine Basin leads to the formation of saline Levantine Intermediate Water and Eastern Mediterranean Deep Water [Malanotte-Rizzoli and Robinson, 1988].

Intermediate and deep water formation is very limited in the western Mediterranean. It occurs regionally in the Ligurian Sea when dense surface waters sink to greater depth in response to winter cooling and enhanced evaporation due to dry "Mistral" winds, producing Western Mediterranean Deep Water (WMDW) [MEDOC Group, 1970; Schott and Leaman, 1991; Leaman, 1995]. These waters contribute only very little - if at all - to the body of MOW as the shallow sill of the Strait of Gibraltar (280 m) inhibits an outflow of WMDW into the Atlantic. Only if winter-time buoyancy loss due to cooling results in a small enough density contrast between intermediate and deep water can the deep waters be drawn up into the outflow layer and flow over the sill [Bryden and Stommel, 1983; Bryden and Kinder 1991].

Numerous paleoceanographic studies have focused on the history of the Atlantic-Mediterranean water exchange in the course of late Quaternary glacial-interglacial sea-level changes in conjunction with changes of the Mediterranean's hydrography [e.g., Faugeres et al., 1984; Vergnaud-Grazzini et al., 1986; Thunell et al., 1987; Thunell and Williams, 1989; and references therein]. Early work on sedimentary patterns east and west of the Strait of Gibraltar suggested that current reversals towards an estuarine flow pattern (i.e., deep inflow, surface outflow) as opposed to today's anti-estuarine flow pattern (i.e., surface inflow, deep outflow) occurred during post-glacial sea-level rises [Olauson, 1961; Huang and Stanley, 1972]. The current reversal would have been caused by enhanced fresh water fluxes from melting alpine glaciers and re-establishment of the marine connection between the eastern Mediterranean and the Black Sea at the end of the last glacial [Kullenberg, 1952; Olausson, 1961]. The net effect of this re-organisation would have led the Mediterranean towards a positive water balance forcing surface waters to flow to the west and out into the Atlantic.

The sedimentological evidence used in support of this hypothesis was discussed controversially, however, in part because of inadequate stratigraphic

resolution but in part also because of different concepts in interpreting grain size distributions [Huang and Stanley, 1972; Diester-Haass, 1973; Huang and Stanley, 1974; Sonnenfeld, 1974]. Foraminiferal faunal, stable isotope and trace element patterns on both sides of the Gibraltar Strait suggested that the modern current pattern was maintained during the last glacial and during the post-glacial sea level rise [Faugeres et al., 1984; Stow et al., 1986; Zahn et al., 1987; Grousset et al., 1988; Vergnaud-Grazzini et al., 1989]. According to these studies, MOW continued to flow into the North Atlantic during the last glacial even though sea level was about 80-120 m below its present level thus reducing the dimensions of the Strait of Gibraltar [Bethoux, 1984; Bryden and Stommel, 1984; Thunell et al., 1987].

Mediterranean climate change and associated hydrographic variations do not strictly follow a glacial-interglacial pattern but are strongly influenced by insolation changes in the course of Earth's orbital precession variations, at a period of 21,000 years. During periods of minimum precession, enhanced northern hemisphere insolation leads to increased precipitation and larger volumes of river discharge to the Mediterranean [Rossignol-Strick, 1983 and 1985; Hilgen, 1991; Lourens et al., 1994; Mommersteg et al., 1995]. Coeval variations in intensity of the North Atlantic Oscillation [Hurrell, 1995] in response to varying meridional pressure gradients likely drove North Atlantic depression tracks further to the east enhancing moisture transport to the Mediterranean [Rohling and Hilgen, 1991]. The combined effects of these orbitally driven changes would reduce Mediterranean salinity every 21 ka, leading to distinctive changes in the Mediterranean's physical circulation [Hilgen, 1991; Rohling, 1994]. Most recent precession-related wet climate conditions occurred in the Mediterranean during the early Holocene and are marked by the deposition of Sapropel 1, 5.0-8.3 ^{14}C-ka ago [see discussion in Rohling, 1994].

During the Last Glacial Maximum, Mediterranean climates conceivably were more arid than today. Compiling planktonic foraminiferal $\delta^{18}O$ records from sediment cores at similar latitudes in the Mediterranean and the open North Atlantic, Thunell and Williams [1989] estimated glacial-interglacial hydrographic changes in the Mediterranean. Changes in glacial-interglacial $\delta^{18}O$ amplitudes from 1.8‰ in the open North Atlantic over 2.9‰ in the

western Mediterranean to 3.1‰ at core sites in the eastern Mediterranean were used to infer salinity increases of 1.2 and 2.7 for the western and eastern basins in response to a more negative water balance due to higher evaporation rates [Thunell and Williams, 1989]. Glacially increased aridity is also implied by climate modelling that predicts about 10% decreases of rainfall over the eastern Mediterranean region [Clemens and Prell, 1991; Prell and Kutzbach, 1992; deMenocal and Rind, 1993], and by increased abundances of pollen assemblages in the Mediterranean borderlands that today are associated with dry climates [Rossignol-Strick, 1983; Gasse et al., 1990; Gasse and van Campo, 1994; Mommersteg et al., 1995].

7.2 Hydraulic Constraints on MOW Flow to the North Atlantic: the Overmixing Model

I use the overmixing model of Bryden and Stommel [1984] to estimate the limiting effects of glacial-interglacial sea-level change and varying Atlantic-Mediterranean salinity contrasts on the advection of MOW (Figure 20). The model is designed to predict salinity difference and inflow and outflow through the Strait of Gibraltar by way of the mass and salt conservation equation

$$Q_M = -\frac{S_A}{S_M - S_A} \cdot E = -\frac{S_A}{S_A \cdot \sqrt[3]{2F}} \qquad \text{equation 2}$$

with

$$F = \frac{\rho_M}{\beta \cdot S_A} \cdot \frac{\left[\frac{E}{(W \cdot \frac{H}{2})}\right]^2}{g \cdot \frac{H}{2}} \qquad \text{equation 3}$$

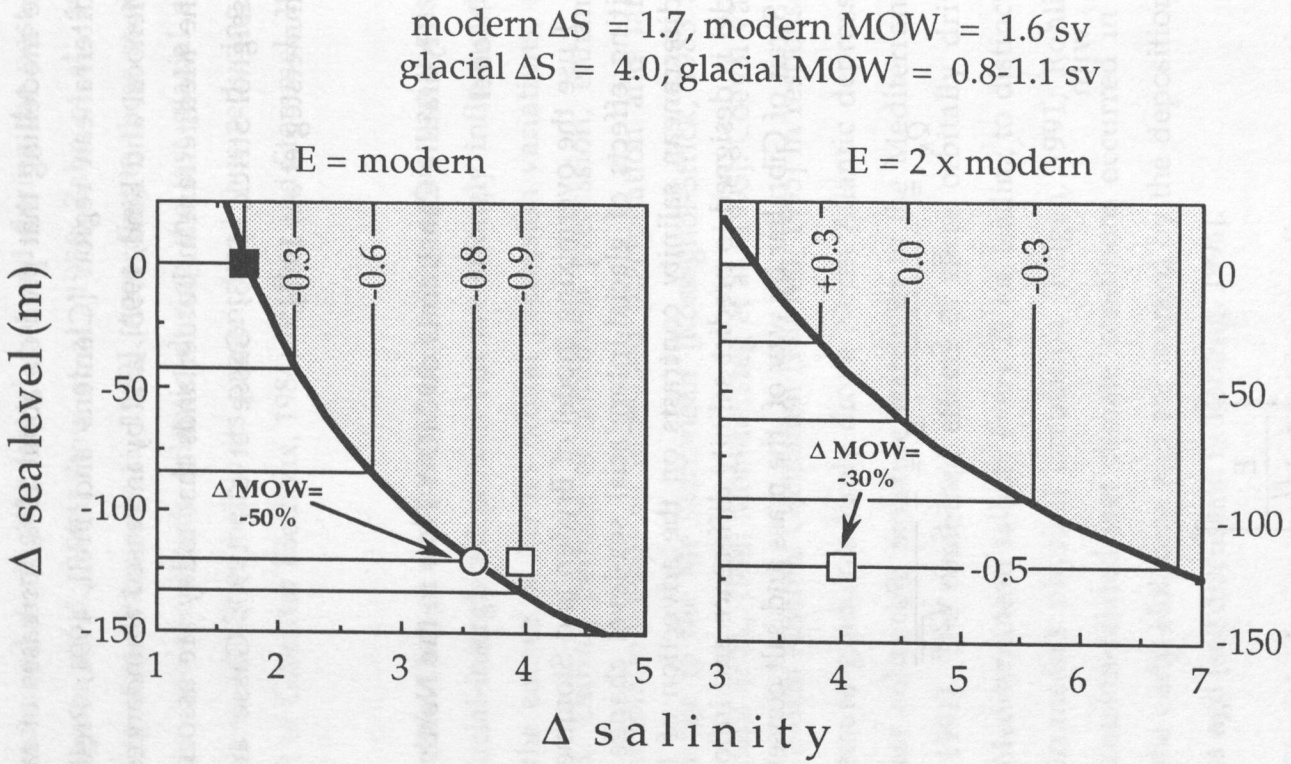

Figure 20. Advection of Mediterranean Outflow Water (MOW) through the Strait of Gibraltar depends on the Atlantic-Mediterranean salinity gradient (a function of evaporation over the Mediterranean) and the geometry of the Gibraltar Strait (a function of sea level). Using the 'overmixing' model of Bryden and Stommel [1984], reductions in MOW flow can be estimated as a function of glacial-interglacial sea level variation and varying Atlantic-Mediterranean salinity gradient. The calculations indicate that MOW advection during the last glacial should have been reduced to 30-50% of its present rate.

where Q_M is the rate of MOW in 10^{12} cm^3 s^{-1}, S_A and S_M are salinity of inflowing Atlantic and outflowing MOW, E is the evaporation in 10^{11} cm^3 s^{-1}, F describes flow velocity as a function of evaporation and the seastrait's geometry (non-dimensional, comparable to the Froude number), ρ_M is the density of MOW, β relates density to salinity (0.77×10^{-3} g cm^{-3} ‰$^{-1}$; permil is used here to indicate salinity which otherwise is non-dimensional), W and H are width and depth of the Strait of Gibraltar, and g is the gravitational acceleration.

Independent parameters for equations 2 and 3 are [Bryden and Stommel, 1984]:

- width (W) and depth (H) of the Gibraltar sill: 12 km and 284 m;
- salinity of incoming Atlantic surface water (S_A): 36.5;
- evaporation (E) over the Mediterranean: 0.76×10^{11} cm^3 s^{-1}

Using the modern control parameterization, the model predicts a mean salinity difference between inflowing Atlantic surface waters and outflowing Mediterranean intermediate waters of 1.7 and an flow rate of MOW of 1.59 $\times 10^{12}$ cm^3 s^{-1}, in reasonable agreement with oceanographic observations [Bryden and Stommel, 1984].

Prescribing Atlantic-Mediterranean salinity difference as a function of global climate in conjunction with lowered glacial sea level and varying Mediterranean hydrography, the model may be used to estimate rates of advection (Figure 20). Assuming a hyperbolic geometry of the Strait of Gibraltar, the width of the strait is linked to its depth (which, in turn, is a function of sea level) by the square function

$$W = \sqrt{\frac{H}{0.0079}} \cdot 2 \qquad \text{equation 4}$$

where W and H are width and depth at a given sea-level low or high stand. Substituting equation 4 in equation 3 allows to predict reductions in MOW

advection through the Strait of Gibraltar into the Atlantic as a function of sea-level change and varying Atlantic-Mediterranean salinity offsets.

Thunell and Williams [1989] estimated Mediterranean salinity to be higher than today, by 1.2 in the western Mediterranean and 2.7 in the eastern Mediterranean (see above). These salinity increases are in addition to the mean ocean salinity increase of 1 that accounts for a sea-level drop of 120 m. Assuming that the salinity increase due to the ice volume effect was the same for the Atlantic and Mediterranean and using a mean Mediterranean salinity increase of 2.0, the Atlantic-Mediterranean salinity offset was increased at the glacial maximum to 3.7 (i.e., 1.7 today plus 2.0).

As Figure 20 shows, a glacial maximum sea-level lowering by 120 m and an increase in the Atlantic-Mediterranean salinity offset to 3.7 [Thunell and Williams, 1989] would reduce MOW by some 50 %, from 1.6 Sv today to 0.8 Sv at the glacial maximum. If one allows for a two-fold increase in evaporation over the Mediterranean, MOW would be reduced to 1.1 Sv, equivalent to 63 % of its modern advection. Hence, the contribution of MOW to the North Atlantic conceivably was reduced, giving way to a stronger influence of North Atlantic mid-depth water masses on the hydrography of the upper Portuguese margin.

7.3 Benthic Foraminiferal $\delta^{18}O$ at the Upper Portuguese Margin: T-S Fields and MOW Mixing with North Atlantic Mid-Depth Waters

The concept of combining T-S diagrams with equilibrium $\delta^{18}O$ (δ_c) fractionation estimates (Figure 21; Zahn and Mix [1991]) is a valuable tool to estimate water mass properties on the basis of foraminiferal $\delta^{18}O$. T-S-δ_c diagrams provide the constraint of vertical density stratification to the T-S related interpretation of foraminiferal $\delta^{18}O$ that helps to narrow down paleo T-S estimates to physically plausible solutions [Zahn and Mix, 1991; Labeyrie et al., 1992; Sarnthein et al., 1995; Weinelt et al., 1996]. I use this concept here to estimate the contribution of MOW and Atlantic type water masses to the upper Portuguese margin during the last glacial.

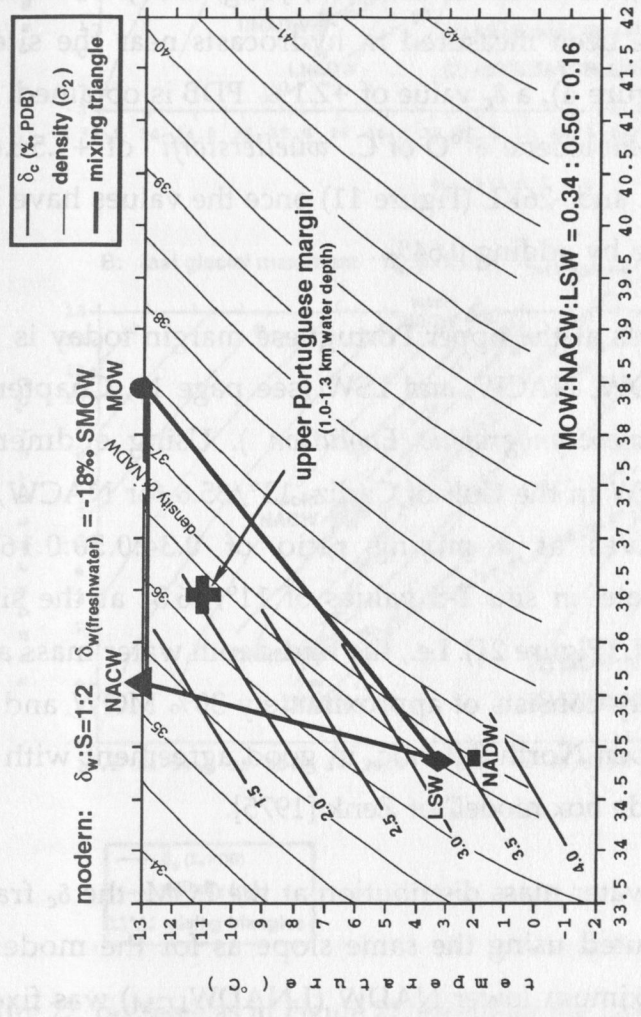

Figure 21. T-S diagram showing water mass endmembers that contribute today to the site of core SO75-26KL. Density lines are for the 200 dbar surface (approx. 2000 m water depth). Isolines of δ_c equilibrium fractionation are computed using the paleotemperature equation of Shackleton [1974] and a δ_w:salinity slope of 0.5 for the modern North Atlantic; freshwater δ_w is -18‰ (SMOW). NACW (triangle) is North Atlantic Central Water, MOW (full dot) is Mediterranean Outflow Water, NADW (rectangle) is North Atlantic Deep Water, LSW (diamond) is Labrador Sea Water. Cross shows T-S values at the upper Portuguese margin. Dotted lines give mixing triangle between water mass endmembers. Today, a mixing ratio of 34% MOW, 50% NACW, and 16% LSW contributes to the hydrography at the upper Portuguese margin.

The modern δ_c fractionation lines shown in Figure 21 have been computed using the paleotemperature equation of Shackleton [1974] (equation 1, page 59) and a δ_w:salinity slope of 0.5 (δ_w=oxygen isotope composition of seawater) which results from a North Atlantic freshwater endmember around -18‰ in δ_w (SMOW). This slope represents the δ_w:salinity relationship for modern North Atlantic deep and mid-depth waters (see also discussion in Duplessy et al. [1991]). NADW is fixed in the diagram at a benthic δ_c of +3.6‰ PDB and T-S values of 2°C/34.9 that are commonly measured at coring sites in the North Atlantic [Labeyrie et al., 1992; Sarnthein et al., 1994; Jung, 1996]. For the T-S values of 11°C/36.3 that have been measured in hydrocasts near the sites of SO75-6KL and SO75-26KL (Figure 4), a δ_c value of +2.1‰ PDB is obtained. This value is consistent with late-Holocene $\delta^{18}O$ of *C. wuellerstorfi* of +1.5±.08‰ PDB (n=18) in cores SO75-6KL and -26KL (Figure 11) once the values have been corrected to the *Uvigerina*-scale by adding 0.64‰.

The mid-depth water mass at the upper Portuguese margin today is derived from mixing between MOW, NACW, and LSW (see page 11, Chapter 3.0, *Oceanographic Setting and Paleoceanographic Evolution*). Using endmember T-S values of 13°/38.4 for MOW in the Gulf of Cadiz, 13°/35.6 for NACW, and 3°/34.9 for LSW, one arrives at a mixing ratio of 0.34:0.50:0.16 for MOW:NACW:LSW to generate *in situ* T-S values of 11°/36.3 at the site of cores SO75-6KL and SO75-26KL (Figure 21). I.e., the mid-depth water mass at the upper Portuguese margin today consists of approximately 30% MOW and 70% mid-depth waters from the open North Atlantic, in good agreement with estimates derived from the "cascade box model" of Zenk [1975].

For a first evaluation of water mass distribution at the LGM, the δ_c fractionation lines have been computed using the same slope as for the modern δ_c lines (Figure 22a). Glacial maximum lower NADW ($LNADW_{LGM}$) was fixed to T-S values of 0°C/35.8 and a δ_c value of +5.3‰ PDB [Labeyrie et al., 1992; Sarnthein et al., 1995; Jung, 1996]. From glacial-interglacial variations of planktonic foraminiferal $\delta^{18}O$ and from planktonic foraminiferal census counts along sediment cores from the Mediterranean it was concluded that salinities of glacial-maximum Mediterranean waters were higher by 1.2-2.7 and tempera-

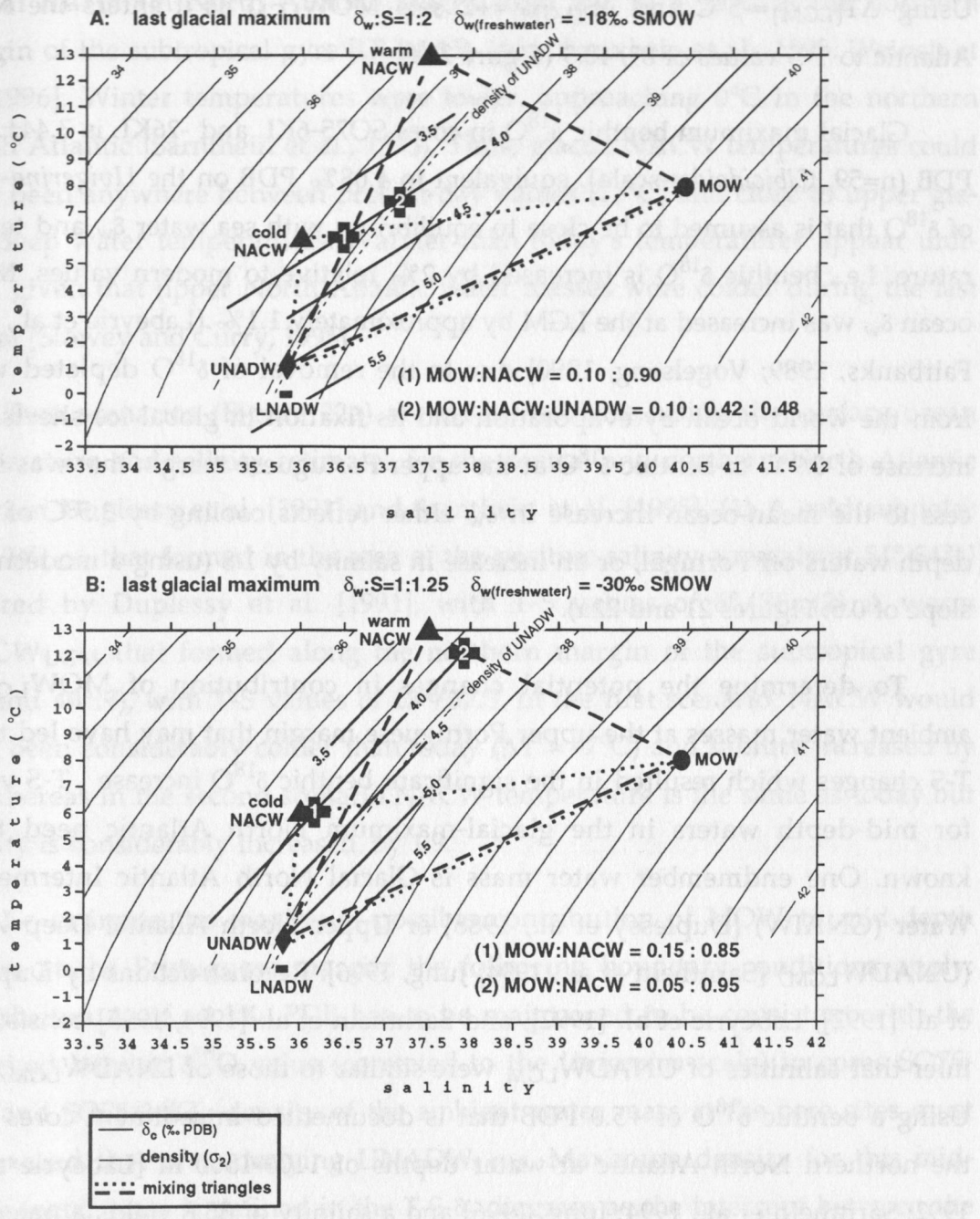

Figure 22. (a) Same as in Figure 21, except for the Last Glacial Maximum. T-S values for mixing endmembers have been changed to estimated LGM values (see text). UNADW (diamond) is Upper North Atlantic Deep Water. Crosses indicate T-S values at a benthic oxygen isotope value of +4.1‰ (PDB) that is documented in cores SO75-6KL and -26KL. Estimates are made for largest possible MOW contribution, if MOW mixes with cold (cross 1) or warm (cross 2) NACW. Mixing ratios for crosses 1 and 2 are indicated. δ_c fractionation is computed by using the same parameterization as in Figure 21 and correcting for a mean glacial δ_w increase of 1.2‰. (b) Same as in (a), except that δ_w:salinity slope is set to 0.8, freshwater δ_w is -30‰ (SMOW). This configuration accommodates glacially lowered precipitation temperatures and the contribution of meltwaters.

tures lower by 4°-6°C [Thiede, 1978; Thunell, 1979; Thunell and Williams, 1989]. Using $\Delta T_{(LGM)}$=-5°C and $\Delta S_{(LGM)}$=+2 sets MOW_{LGM} as it enters the North Atlantic to T-S values of 8°/40.3 (Figure 22a).

Glacial maximum benthic $\delta^{18}O$ in cores SO75-6KL and -26KL is 3.44±.21‰ PDB (n=59, *Cibicidoides*-scale), equivalent to 4.08‰ PDB on the *Uvigerina*-scale of $\delta^{18}O$ that is assumed to be close to equilibrium with sea water δ_w and temperature. I.e., benthic $\delta^{18}O$ is increased by 2‰ relative to modern values. Mean-ocean δ_w was increased at the LGM by approximately 1.1‰ [Labeyrie et al., 1987; Fairbanks, 1989; Vogelsang, 1990] due to the removal of $\delta^{18}O$ depleted water from the world ocean by evaporation and its fixation in global ice sheets. The increase of 0.9‰ of benthic $\delta^{18}O$ at the upper Portuguese margin that was in excess to the mean-ocean increase in δ_w either reflects cooling by 3.5°C of mid-depth waters off Portugal, or an increase in salinity by 1.8 (using a modern δ_w:S slope of 0.5; Figures 21 and 22a).

To determine the potential changes in contribution of MOW_{LGM} to ambient water masses at the upper Portuguese margin that may have led to the T-S changes which resulted in the significant benthic $\delta^{18}O$ increase , T-S values for mid-depth waters in the glacial-maximum North Atlantic need to be known. One endmember water mass is Glacial North Atlantic Intermediate Water (GNAIW) [Duplessy et al., 1988] or Upper North Atlantic Deep Water ($UNADW_{LGM}$) [Sarnthein et al., 1994; Jung, 1996]. Reconstructions by Duplessy et al. [1992], Labeyrie et al. [1992], and Sarnthein et al. [1994, 1995] consistently infer that salinities of $UNADW_{LGM}$ were similar to those of $LNADW_{LGM}$, 35.8. Using a benthic $\delta^{18}O$ of +5.0 PDB that is documented in sediment cores from the northern North Atlantic at water depths of 1100-1500 m [Labeyrie et al., 1992; Sarnthein et al., 1994; Jung, 1996] and a salinity of 35.8 yields a paleotemperature of +1°C for $UNADW_{LGM}$ (Figure 22a). The T-S values for $UNADW_{LGM}$ thus are 1°/35.8.

Not much paleodata are available to trace the glacial-interglacial evolution of NACW as the second endmember for mixing with MOW_{LGM}. Slowey and Curry [1995] infer a cooling of 2°C at mid-depths (1-2 km) around the Bahamas, pointing to similar cooling of surface waters in the North Atlantic

subtropical gyre, the potential source region for NACW. Summer SST in the glacial maximum North Atlantic ranges from 5°C to > 13°C at the northern margin of the subtropical gyre [CLIMAP, 1981; Sarnthein et al., 1995; Weinelt et al., 1996]. Winter temperatures were lower, approaching 0°C in the northern North Atlantic [Sarnthein et al., 1995]. Thus, glacial NACW temperatures could have been anywhere between present-day values (13°C) and close to upper glacial deep water temperatures. Warmer than today's temperatures appear unlikely, given that upper North Atlantic water masses were colder during the last glacial [Slowey and Curry, 1995].

Two scenarios (Figure 22a) are discussed here, using the surface ocean temperature and salinity estimates for the central and northern North Atlantic given in Duplessy et al. [1991] and Sarnthein et al. [1995]. (1) A cold subpolar $NACW_{LGM}$ that formed in the area of the positive salinity anomaly at 51°-54°N inferred by Duplessy et al. [1991], with T-S values of 6°/36. (2) A warm $NACW_{LGM}$ that formed along the northern margin of the subtropical gyre (around 40°N), with T-S values of 13°/37.5. In the first scenario, NACW would have been considerably colder than today (ΔT = -7°C) and salinity increased by 0.4 whereas in the second scenario NACW temperature is the same as today but salinity is considerably increased, by 1.9.

To estimate the maximum possible contribution of MOW to mid-depth waters at the Portuguese margin, the following boundary conditions apply: equilibrium δ_c of +4.1‰ PDB has to be maintained to be consistent with the observed benthic $\delta^{18}O$ value (corrected to the *Uvigerina*-scale) in cores SO75-6KL and SO75-26KL; density of the ambient water mass at the core sites must not exceed that of underlying $UNADW_{LGM}$. Maximum density for this mid-depth water mass is defined in the T-S-δ_c diagram as the intercept between the +4.1‰ δ_c isoline and the 37.6 (s_2) isopycnal of $UNADW_{LGM}$ at a T-S value of 7.2°/37.1 (Figure 22a). This point also defines the maximum contribution of MOW as it is closest along the +4.1‰ δ_c isoline to the T-S coordinate of glacial MOW (Figure 22a).

As is shown in Figure 22a, the cold and warm NACW scenarios both indicate a maximum possible contribution of 10% to the mid-depth water mass at

the Portuguese margin. In the case of the cold NACW, maximum MOW contribution is entirely defined by mixing between MOW and NACW, T-S values of the mixing product are 6°/36.4. In the case of a warm NACW, MOW mixes with a water mass that consists of roughly equal parts of UNADW and NACW. T-S values are 7.2°/37.1 as defined by the intercept between the +4.1‰ δ_c isoline and the 37.6 (s_2) isopycnal of $UNADW_{LGM}$ (Figure 22a).

Both scenarios imply that the contribution of MOW to mid-depth waters at the upper Portuguese margin was only 10% compared to 30% today. These numbers change slightly if a more negative freshwater δ_w value of -30‰ (SMOW) is used to account for lower glacial precipitation temperatures in the North Atlantic region, and a stronger contribution of glacial meltwater (Figure 22b). Using a δ_w value of -30‰ (SMOW), the slope of the δ_c lines in the T-S field is steeper and the +4.1‰ δ_c fractionation line does not intersect the density isoline of UNADW. Thus, the maximum possible MOW contribution is defined by the intercepts of the +4.1‰ δ_c fractionation line with the mixing lines between MOW and warm or cold NACW. Maximum MOW contribution is 5% if it mixes with cold NACW, and 15% if it mixes with warm NACW (Figure 22b). I.e., the contribution of glacial MOW to the mid-depth North Atlantic would have been reduced by 50% to more than 80% of its present contribution.

Sea-level lowering by as much as 120 m during the last glacial reduced the geometry of the Strait of Gibraltar and must have reduced the through-flow of MOW to the North Atlantic [Bryden and Stommel, 1984]. Using Bryden's and Stommel's [1984] overmixing model implies reductions of MOW by 30-50%, depending on the rates of evaporation over the Mediterranean (see page 71, Chapter 7.2, *Hydraulic Constraints on MOW Flow to the North Atlantic:*). The T-S considerations shown in this chapter, in association with potential mixing scenarios, also imply a reduced MOW flow to the upper Portuguese margin. Both contentions are further supported by physical considerations, that T-S values of 8°/40.3 estimated for MOW_{LGM} yield a density of 40 (s_2) which is considerably higher than that of 37.6 for $UNADW_{LGM}$. The density contrast between MOW and underlying deep waters is thus increased from 0.7 today (Figure 21) to 2.4 at the LGM (Figure 22). If MOW still contributed to the hydro-

graphy of the shallow North Atlantic, significant mixing with less saline North Atlantic waters was required to lower MOW density and to allow it to flow at shallow depths. Enhanced MOW density that requires intensive mixing with less saline Atlantic waters to increase its buoyancy together with a reduced mass flow of MOW therefore supports the conclusion that MOW must have played a less significant role in the glacial-maximum mid-depth North Atlantic.

Based on elevated benthic $\delta^{13}C$ levels during the last glacial at core sites immediately west and south of the Gulf of Cadiz, Zahn et al. [1987] postulated a stronger influence of MOW on the North Atlantic's hydrography during the LGM. This hypothesis was subsequently supported by Oppo and Fairbanks [1987] using similar isotope evidence from Caribbean sediment cores. Even though it was recognized that the advection of MOW must have been reduced at the LGM due to lower sea level it was hypothesized that MOW left a stronger imprint on the North Atlantic than today because convection rates and water mass renewal was thought to be significantly reduced in the glacial-maximum northern North Atlantic [Zahn et al., 1987].

With new data from the northern North Atlantic and the Nordic Seas [Duplessy et al., 1991; Labeyrie et al., 1992; Oppo and Lehman, 1993; Sarnthein et al., 1994, 1995; Weinelt et al., 1996; Yu et al., 1996] it seems today more plausible to assume that the subpolar North Atlantic remained an important source of mid-depth and deep ventilation also during the last glacial. Therefore, the influence of MOW on the upper water masses of the North Atlantic must have been reduced at the LGM, as is also inferred from the T-S-δ_c discussion above. The reduction was probably less severe during early stage 2 and stage 3 when sea level was higher, but from the above considerations it must be concluded that the glacial sections of the benthic isotope records from upper Portuguese margin cores SO75-6KL and -26KL primarily document the variability of North Atlantic mid-depth ventilation and, as such, monitor thermohaline overturn in the glacial North Atlantic.

7.4 Regional Differences in Benthic $\delta^{18}O$ and $\delta^{13}C$ at Subtropical and Northern North Atlantic Core Sites - Implications for Mid-Depth Hydrographic Gradients

Comparing the benthic isotope record of core SO75-26KL with similar records from other North Atlantic mid-depth sediment cores [Zahn et al., 1987; Slowey and Curry, 1995; Jung, 1996; Rasmussen et al., 1996; Lackschewitz et al., 1997] shows that benthic $\delta^{18}O$ at the upper Portuguese margin is depleted relative to $\delta^{18}O$ data from the subtropical and northern North Atlantic (Figure 23). Most positive values - conceivably indicating lowest mid-depth water temperatures - are documented for northern North Atlantic cores SO82-05 (Reykjanes Ridge; Lackschewitz et al. [1997]) and ENAM93-21 (Faeroe-Shetland Channel; Rasmussen et al. [1996]). Core ENAM93-21 today is in the advection path of 'young' overflow waters from the Norwegian-Greenland Seas to the northern Northeast Atlantic [Hopkins, 1991], and conceivably also during the latest Quaternary as is indicated by a tongue of extremely positive benthic $\delta^{13}C$ immediately south of the Iceland-Faeroe Rise [Sarnthein et al., 1994]. This regional benthic $\delta^{13}C$ maximum is best developed during the late Holocene, the Younger Dryas cold episode, and the LGM, but it is also seen during the pre-LGM period early in oxygen isotope stage 2 (see benthic $\delta^{13}C$ map series in Sarnthein et al. [1994]) and documents the presence of a chemically 'young' water mass in the area.

Core SO82-05 from the Reykjanes Ridge southwest of Iceland is influenced by Norwegian-Greenland Sea overflow waters that flow through the Denmark Strait, and by re-circulating mid-depth waters that form locally in the northwestern North Atlantic e.g., the Labrador Sea [Talley and McCartney, 1982; McCartney, 1992; Schott et al., 1993; Visbeck et al., 1995]. The extremely positive Holocene and glacial benthic $\delta^{13}C$ values in this core support the contention of a continuous flow, but at different rates, of young mid-depth waters - upper NADW - through the northern North Atlantic (Figure 23) [Zahn et al., 1987; Duplessy et al., 1988; Labeyrie et al., 1992; Oppo and Lehman, 1993; Sarnthein et al., 1994]. Paleoceanographically reliable benthic $\delta^{13}C$ data are not available for core ENAM93-21 because epibenthic foraminifera are rare in this core. The benthic isotope curve from this core, shown in Figure 23, was measured using

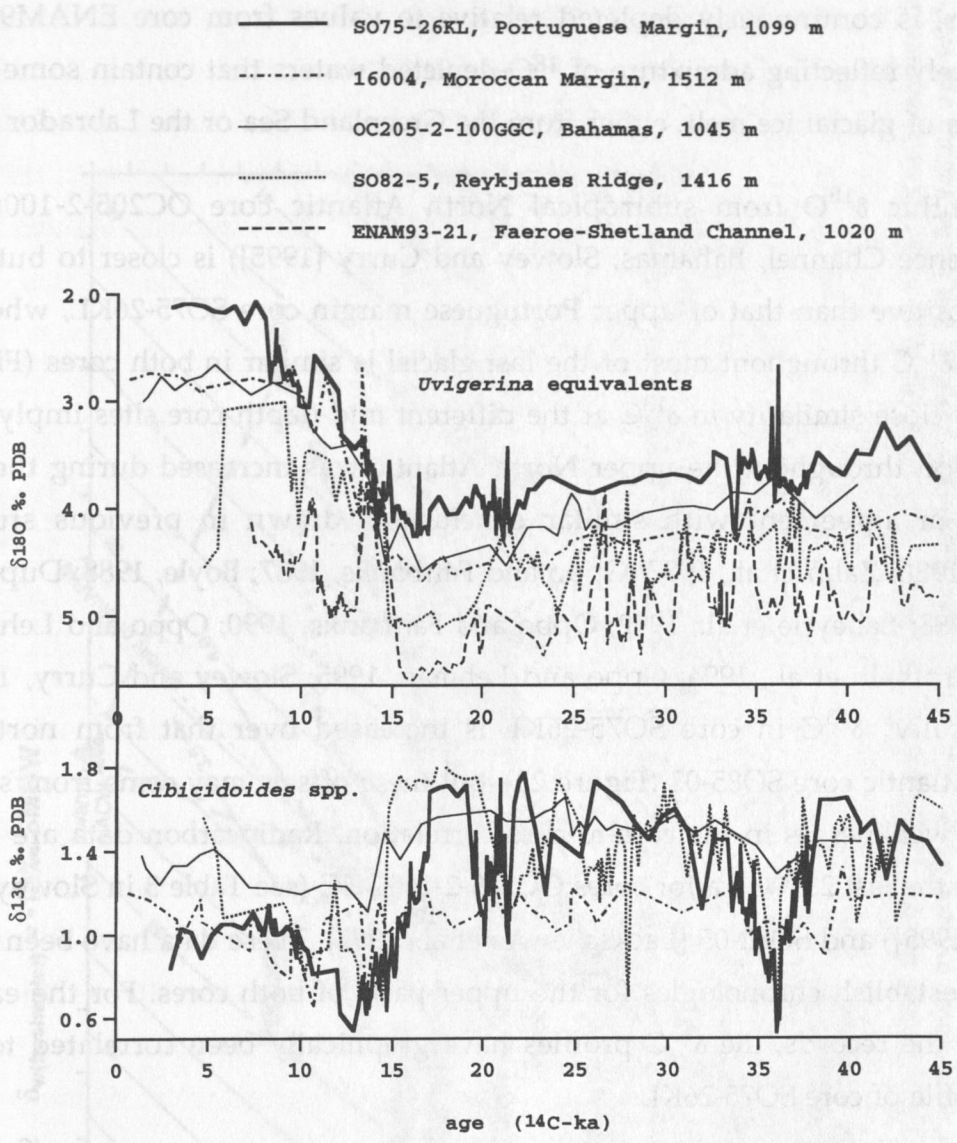

Figure 23. Benthic isotope records from mid-depth core sites in the subtropical and northern North Atlantic. Comparison with the isotope records from core SO75-26KL reveals gradients that monitor distinct circulation changes during the last glacial. See text for discussion.

Nonion zaandamae [Rasmussen et al., 1996b], an infaunal benthic foraminiferal species that documents pore-water $\delta^{13}C$ signals rather than $\delta^{13}C$ signals from overlying bottom waters [Corliss and Chen, 1988]. Benthic $\delta^{18}O$ in core SO82-05, however, is continuously depleted relative to values from core ENAM93-21, most likely reflecting admixture of ^{18}O-depleted waters that contain some contribution of glacial ice melt, either from the Greenland Sea or the Labrador Sea.

Benthic $\delta^{18}O$ from subtropical North Atlantic core OC205-2-100GGC (Providence Channel, Bahamas; Slowey and Curry [1995]) is closer to but still more positive than that of upper Portuguese margin core SO75-26KL, whereas benthic $\delta^{13}C$ throughout most of the last glacial is similar in both cores (Figure 23). The close similarity in $\delta^{13}C$ at the different mid-depth core sites imply that ventilation throughout the upper North Atlantic was increased during the last glacial, in agreement with similar conclusions drawn in previous studies [Boyle, 1986; Zahn et al., 1987; Oppo and Fairbanks, 1987; Boyle, 1988; Duplessy et al., 1988; Labeyrie et al., 1992; Oppo and Fairbanks, 1990; Oppo and Lehman, 1993; Sarnthein et al., 1994; Oppo and Lehman, 1995; Slowey and Curry, 1995]. Periodically, $\delta^{13}C$ in core SO75-26KL is increased over that from northern North Atlantic core SO85-02 (Figure 23), but these offsets may come from stratigraphic weaknesses in the core-to-core correlation. Radiocarbon data are available for the last 23 ^{14}C-ka for cores OC205-2-100GGC (see Table 3 in Slowey and Curry [1995]) and SO82-05 [Lackschewitz et al., 1997]. These data have been used here to establish chronologies for the upper parts of both cores. For the earlier parts of the records, the $\delta^{13}C$ profiles have graphically been correlated to the $\delta^{13}C$ profile of core SO75-26KL.

The differences in benthic $\delta^{18}O$ between the North Atlantic coring sites point to basin-wide T-S gradients that most likely document regionally different mixing ratios between type-water masses that contribute to the glacial mid-depth and deep North Atlantic. Assuming that densities of ambient water masses were similar at the subtropical and northern North Atlantic coring sites, one can estimate T-S values by plotting glacial-maximum benthic $\delta^{18}O$ values from each core into a T-S-δ_c diagram, following the track of a narrow density

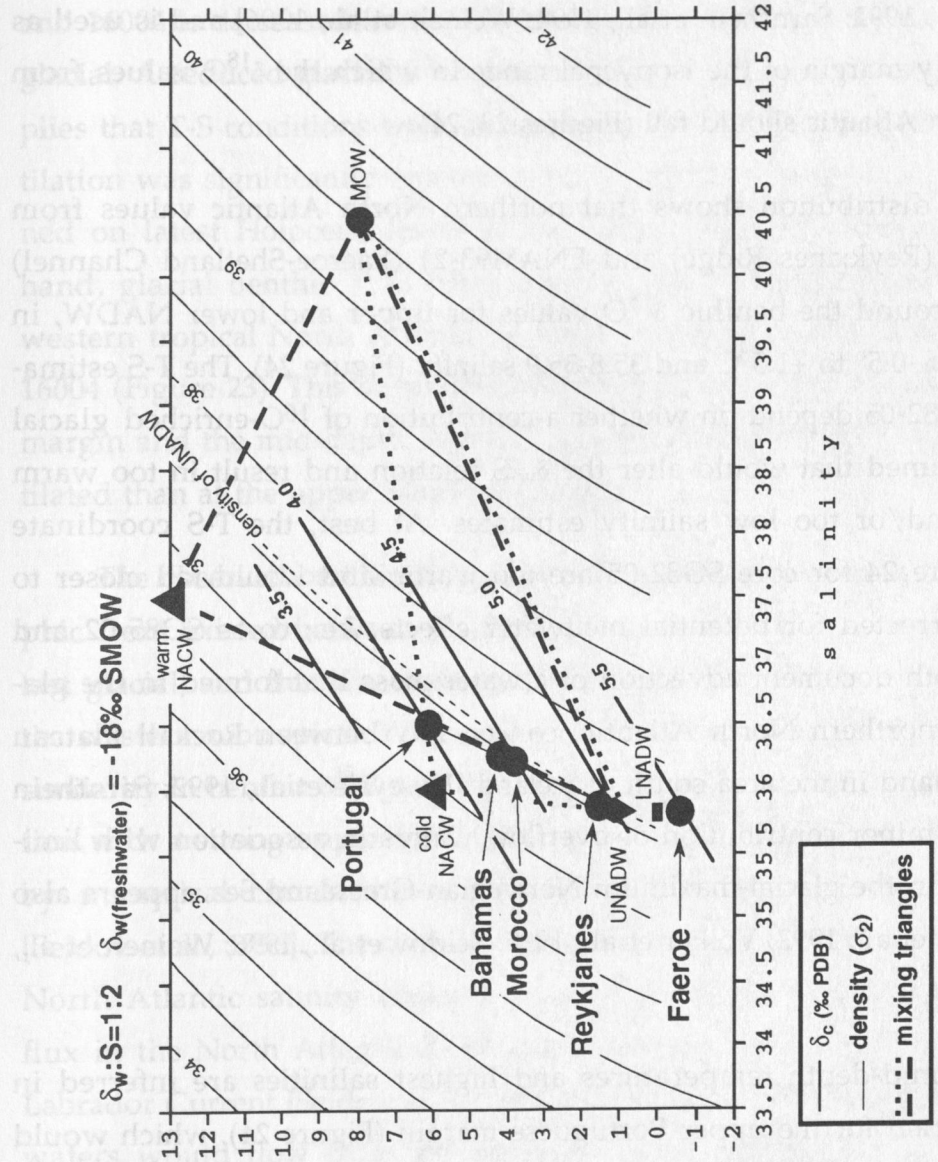

Figure 24. Benthic oxygen isotope values for the Last Glacial Maximum from mid-depth isotope records shown in Figure 23. Assuming that densities of ambient water masses at the individual core sites were similar, the LGM values are within a narrow isopycnal range in the T-S diagram that is defined by Upper/Lower North Atlantic Deep Water and mid-depth waters off Portugal which display most negative oxygen isotope values. The pattern suggests systematic increases in NACW contribution as one moves away from the northern North Atlantic.

range that is defined by the lowest and highest plausible density. In Figure 24, glacial-maximum benthic $\delta^{18}O$ is plotted in such a way that the upper Portuguese margin value of +4.1 (±0.21)‰ is fixed at the same T-S coordinate as in Figure 22a, using scenario 1 i.e., the cold NACW case. The most positive glacial-maximum $\delta^{18}O$ of +5.5 (±0.09)‰ that is documented for core ENAM93-21 falls close to the $\delta^{18}O$ value of +5.3 for glacial-maximum lower NADW [Labeyrie et al., 1992; Sarnthein et al., 1994; Weinelt et al., 1996] and is used as the high-density margin of the isopycnal range in which the $\delta^{18}O$ values from the other North Atlantic should fall (Figures 23, 24).

The data distribution shows that northern North Atlantic values from cores SO82-05 (Reykjanes Ridge) and ENAM93-21 (Faeroe-Shetland Channel) are grouped around the benthic $\delta^{18}O$ values for upper and lower NADW, in the T-S range of -0.5° to +1.5°C and 35.8-35.9 salinity (Figure 24). The T-S estimates for core SO82-05 depend on whether a contribution of ^{16}O-enriched glacial ice melt is assumed that would alter the δ_w:S relation and result in too warm temperature and/or too low salinity estimates. At best, the T-S coordinate shown in Figure 24 for core SO82-05 are too warm, and would fall closer to UNADW if corrected for potential meltwater effects. I.e., cores SO85-02 and ENAM93-21 both document advection of a water mass that formed in the glacial-maximum northern North Atlantic, conceivably between Rockall Plateau and Greenland and in the area south of Iceland [Labeyrie et al., 1992; Sarnthein et al., 1994]. A minor contribution of overflow waters in association with limited convection in the glacial-maximum Norwegian-Greenland Sea appears also possible [Veum et al., 1992; Völker et al., 1995; Seidov et al., 1996; Weinelt et al., 1996].

Warmest mid-depth temperatures and highest salinities are inferred in the T-S-δ_c diagram for the upper Portuguese margin (Figure 24), which would be consistent with an admixture (of smaller amounts than today) of MOW, or (stronger than today) contribution of NACW (see page 74, Chapter 7.3, *Benthic Foraminiferal $\delta^{18}O$ at the Upper Portuguese Margin*). A critical test here is to compare benthic isotope data from core SO75-26KL with similar data from upper Moroccan margin core 16004 (Figure 23).

Core 16004 today lies in the southern extension of MOW, and its benthic

$\delta^{13}C$ record was used by Zahn et al. [1987] to infer a stronger imprint of MOW on the glacial mid-depth North Atlantic. During the Holocene, benthic $\delta^{13}C$ in core 16004 is similar to that in core SO75-26KL indicating that both cores are influenced by the same water mass i.e., MOW. During the last glacial, values of both cores diverge with benthic $\delta^{13}C$ in core SO75-26KL being increased by up to 0.6‰ over that in core 16004. The benthic $\delta^{18}O$ offset between cores SO75-26KL and 16004 is decreased from 0.7‰ during the Holocene to 0.5‰ during the last glacial. A reduced glacial $\delta^{18}O$ offset together with an increased $\delta^{13}C$ offset implies that T-S conditions were more similar during the last glacial whereas ventilation was significantly enhanced at the upper Portuguese margin but remained on latest Holocene levels at the upper Moroccan margin. On the other hand, glacial benthic $\delta^{13}C$ from core OC205-2-100GGC from the mid-depth western tropical North Atlantic is closer to values from SO75-26KL than from 16004 (Figure 23). This suggests that mid-depth waters at the upper Portuguese margin and the mid-depth subtropical western North Atlantic were better ventilated than at the upper Moroccan margin.

The observed benthic $\delta^{13}C$ pattern suggests that an upper ocean hydrographic front existed between the Portuguese and Moroccan margins during the last glacial, and that the degree of ventilation was similar off Portugal and in the western subtropical North Atlantic. Such mid-depth front and an east-west similarity in benthic $\delta^{13}C$ may have developed during the last glacial in association with a strong upper ocean reverse (i.e., anticyclonic) gyre that is indicated by numerical circulation experiments using glacial boundary conditions [Seidov et al., 1996]. The mid-depth reverse gyre circulation is entirely driven by North Atlantic salinity changes in conjunction with decreased heat and salt flux in the North Atlantic Drift Current and a more pronounced low-salinity Labrador Current [Seidov et al., 1996]. Newly formed well-ventilated mid-depth waters would flow from the northern North Atlantic along the Portuguese margin in southwesterly direction and pass the Moroccan margin at great distance before they turn directly west at about 30°N and flow into the western sector of the North Atlantic (see Figure 7c in Seidov et al. [1996]). The observed benthic $\delta^{13}C$ gradients between cores SO75-26KL, 16004, and OC205-2-100GGC (representing the western subtropical North Atlantic) may serve as paleoceano-

graphic evidence for the existence of such mid-depth anticyclonic gyre circulation during the last glacial. Such circulation pattern would also support the conclusion drawn above from benthic $\delta^{18}O$ in conjunction with δ_c fractionation and water mass mixing that Mediterranean Outflow Waters played a minor role in defining the hydrography of glacial mid-depth waters in the North Atlantic, and that the upper Portuguese margin was mainly under the influence of mid-depth waters that formed in the glacial North Atlantic.

7.5 Benthic $\delta^{13}C$ Anomalies in Cores SO75-6KL and -26KL: Thermohaline Instabilities in the North Atlantic During 'Heinrich' Meltwater Events

Benthic $\delta^{13}C$ in mid-depth cores SO75-26KL and -6KL (1099 m and 1281 m water depth) is increased during the last glacial by 0.5-0.7‰ compared to Holocene values (Figure 25). Increased benthic $\delta^{13}C$ has been observed in glacial sediments at mid-depth sites from various ocean basins and has been used to infer an enhanced partitioning of carbon between the upper and deep ocean [Boyle, 1986; Zahn et al., 1987; Oppo and Fairbanks, 1987; Boyle, 1988; Duplessy et al., 1988; Oppo and Fairbanks, 1990; Mix et al., 1991; Zahn et al., 1991; de Menocal et al., 1992; Oppo and Lehman, 1993, 1995]. For the North Atlantic it was speculated that a shift of convection cells from the Nordic Seas to the northern North Atlantic was accompanied by cooling of surface waters and decreased evaporation rates that resulted in decreased salinities and enhanced buoyancy of the surface waters north of the glacial polar front [Boyle and Keigwin, 1987; Oppo and Lehman, 1993]. As a result, surface densities in the northern North Atlantic were just high enough to allow for convection to mid-depths or upper deep water levels, thus enhancing ventilation there over that of lower deep waters and bottom waters [Duplessy et al., 1988; Sarnthein et al., 1994; Sarnthein and Altenbach, 1995].

Increased benthic $\delta^{13}C$ levels in cores SO75-26KL at 1099 m water depth and SO75-6KL at 1281 m water depth support this conceptual model in that they document enhanced ventilation of glacial mid-depth levels at the upper Portuguese margin. Benthic $\delta^{13}C$ in both cores is significantly decreased during

the 'Heinrich' events documenting strongly reduced water mass ventilation at the upper Portuguese margin during 'Heinrich' events H1, H2, and H4 (Figure 25). In core SO75-26KL, benthic $\delta^{13}C$ decreases by 1.1‰ during H4, by 0.7‰ during H2, and 0.25‰ during H1. In core SO75-6KL, decreases are 0.5‰ during H2 and 0.4 during H1. A further $\delta^{13}C$ anomaly occurs at interpolated ages of 25.4-23.4 ^{14}C-ka in core SO75-26KL and 29.0-26.1 ^{14}C-ka in core SO75-6KL (Figure 25). This anomaly is not associated with an IRD layer. In core SO75-26KL, a 'cold' planktonic foraminiferal faunal anomaly occurs in the same core section that likely documents an influx of subpolar surface waters during H3 (see page 56, Chapter 6.2, *Variability of Sea Surface Temperature*). Two planktonic ^{14}C-AMS datings (samples KIA0017 and 0018, Table 2) of 24.87 ^{14}C-ka (415 cm core depth, c.d.) and 22.95 ^{14}C-ka (392 cm c.d.) constrain the timing of the planktonic faunal and benthic $\delta^{13}C$ anomalies in core SO75-26KL. There is no independent chronostratigraphic control on the third benthic $\delta^{13}C$ anomaly in core SO75-6KL, but it cannot be excluded that it documents the ventilation slow-down during H3.

'Heinrich' event H3 has been considered exceptional in that its IRD and trace element composition point to a more northerly (Scandinavian?) origin, and its IRD layer contains little or no carbonate minerals and is not well represented in the North Atlantic's 'Heinrich' belt [Grousset et al., 1993]. None of the sediment cores from the upper and central Portuguese margin presented here contain an H3 IRD layer. However, the magnetic susceptibility record of deep water reference core MD95-2039 that was taken at the lower continental slope - i.e., farthest offshore - displays a positive anomaly that represents the H3 IRD layer. Also, an IRD layer coeval with H3 was found in core D11975P on Tore Seamount (39°N, 12.5°W), about 50 nmi to the northwest of the site of core SO75-26KL [Lebreiro et al., 1996]. I.e., the icebergs reached Tore Seamount and the outer Portuguese margin during H3 but they did not reach the central and upper continental slope coring sites, likely because of regional surface circulation patterns prevented the icebergs to reach the site of core SO75-26KL.

At the deeper core sites along the Portuguese slope, the benthic $\delta^{13}C$

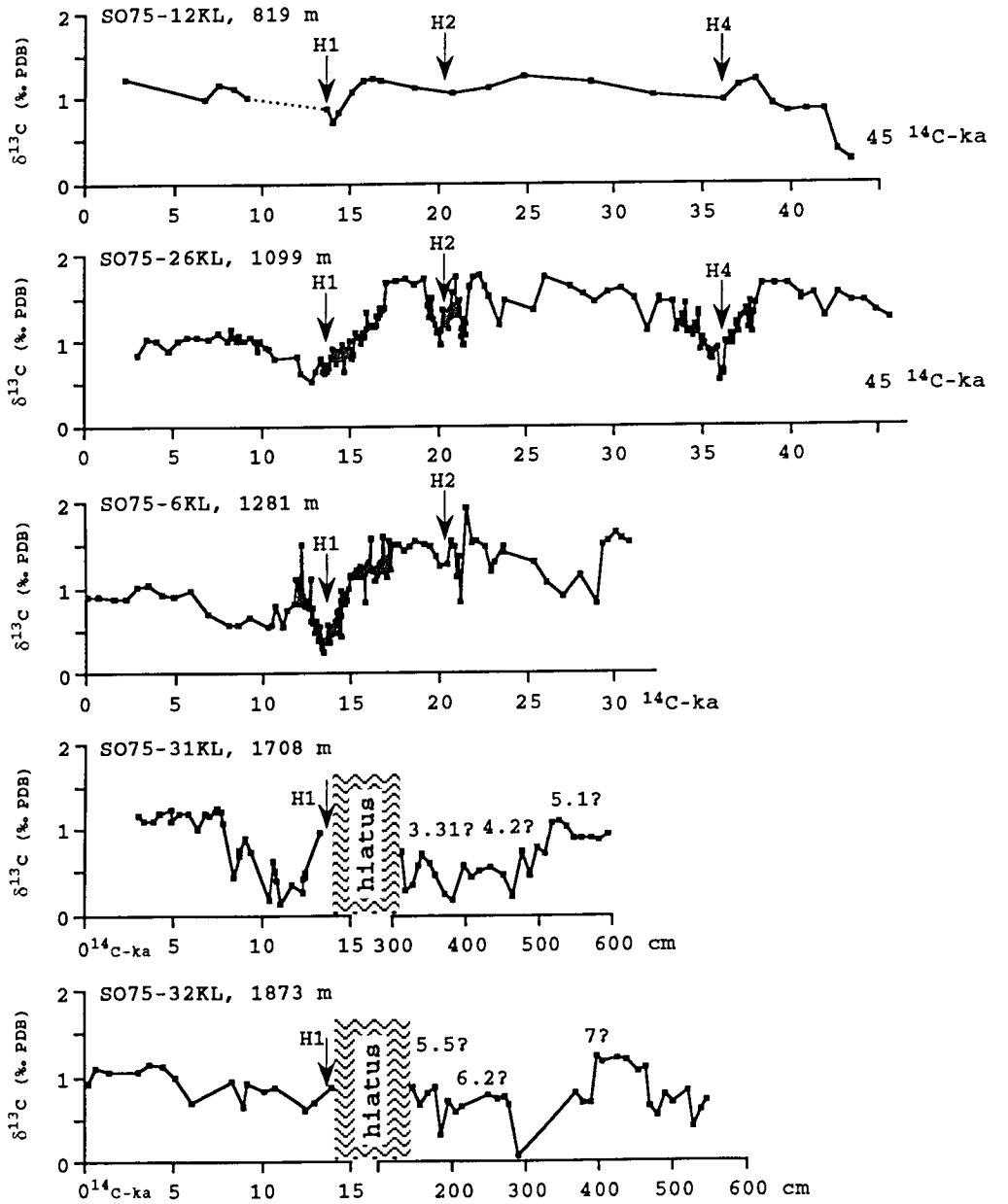

Figure 25. Benthic (*Cibicidoides* spp.) carbon isotope records from the southern Portuguese margin cores. Numbering of isotope events below the hiatus in cores SO75-31KL and SO75-32KL is the same as in Figures 10 and 11. The isotope records are shown on the basis of increasing water depth of individual sediment cores. Position of 'Heinrich' events is derived from IRD countings. The isotope records are used to monitor the North Atlantic's ventilation response to the 'Heinrich' meltwater events.

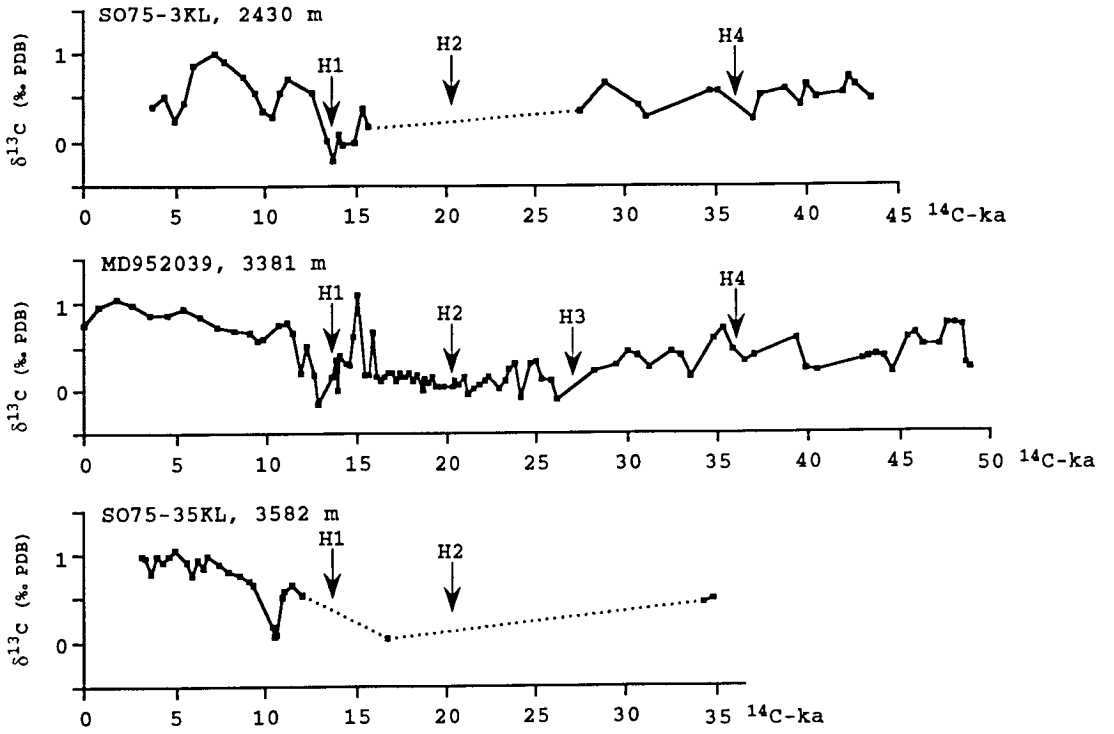

Figure 25, continued

response to the 'Heinrich' events is not adequately resolved, either because discontinuous occurrence of epibenthic *Cibicidoides* species makes establishment of continuous epibenthic isotope records impossible or because of sedimentation gaps (cores SO75-31KL, -32KL). Disappearance of epibenthic foraminiferal species in conjunction with the Heinrich layers is indicative of ventilation changes and decreases in oxygenation that is a limiting factor in benthic ecology (see next chapter below; Baass, Schönfeld, Zahn, manuscript submitted [December 1996]). It is only for H1 in cores SO75-3KL and MD95-2039 that few benthic $\delta^{13}C$ data are available which indicate decreases by 0.3‰ (SO75-3KL) and 0.1‰ (MD95-2039). I.e., the ventilation response to H1 at the site of core SO75-3KL is similar to that indicated by benthic $\delta^{13}C$ in the shallower cores SO75-6KL and -26KL. It is, however, strongly subdued at the lower deep water reference site MD95-2039 at 3381 m water depth. Modelling studies and synoptic benthic $\delta^{13}C$ mapping in the glacial Northeast Atlantic indicate the presence of a $\delta^{13}C$-depleted water mass of possibly Southern Ocean origin at this depth [Sarnthein et al., 1994; Seidov et al., 1996]. Thus, ventilation of lower deep waters was already decreased, and the ventilation slow-down during H1 did not result in a further benthic $\delta^{13}C$ depletion in core MD95-2039.

7.6 Thermohaline Links Between Mid-Depth Ventilation off Portugal and Northern North Atlantic Surface Conditions

The pattern of reduced mid-depth ventilation during the 'Heinrich' events that is implied by the negative benthic $\delta^{13}C$ anomalies in cores SO75-6KL and -26KL during IRD deposition confirms considerations of planktonic $\delta^{18}O$ and SST anomalies that have been used to infer significant density decreases of surface waters in the northern North Atlantic during 'Heinrich' events which should have resulted in reductions of water mass convection [Maslin et al., 1995]. Similar evidence has been found for meltwater pulses during the last deglaciation [e.g., Keigwin et al., 1991] and the evidence found in the upper Portuguese margin cores supports the hypothesis of a close linkage between surface ocean conditions in the North Atlantic and convective overturn [Paillard and Labeyrie, 1994; Weaver and Hughes, 1994; Rahmstorf, 1994,

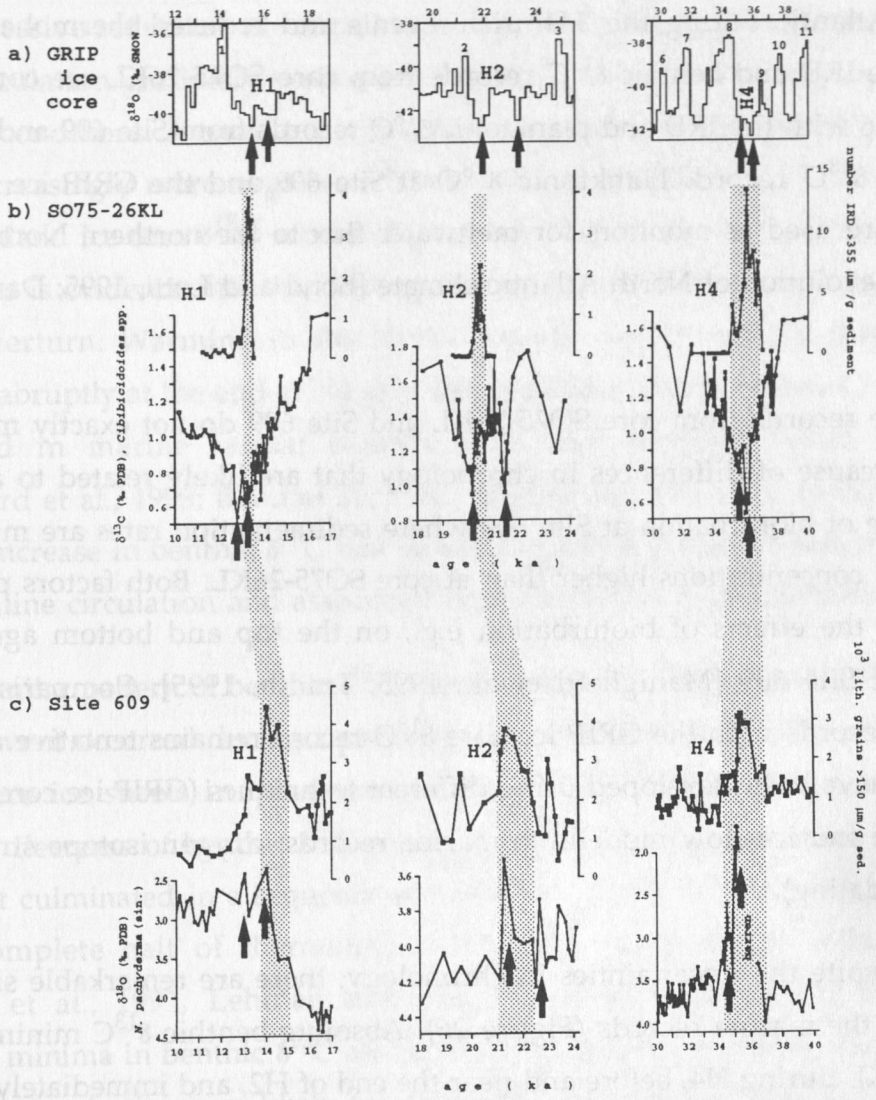

Figure 26. (a) Greenland ice core (GRIP) oxygen isotope variabiliy surrounding 'Heinrich' events 1 (left), 2 (center), and 4 (right). (b) Benthic carbon isotope and IRD patterns in core SO75-26KL during these events. (c) Planktonic oxygen isotope and IRD patterns at Site 609. Arrows mark episodes with minimum planktonic oxygen isotope values at Site 609, minimum benthic carbon isotope values at core SO75-26KL, and minimum ice core oxygen isotope values. The similarity of the foraminiferal isotope and IRD patterns at both sites, and the apparent correlation of the marine and GRIP data suggest a close coupling between surface forcing and thermohaline overturn during peak meltwater flow. Early decreases and late resumption of fully increased values around H1 and H4 indicate that thermohaline reduction started well before the events and lasted much longer than the events. Inferred gradual spin-up of thermohaline circulation over periods of 1-3 ka after all 3 Heinrich events is in direct contrast to sudden warmings seen in the GRIP data.

1995].

To evaluate the relation between changing surface forcing in the northern North Atlantic during the 'Heinrich' events and reduced thermohaline overturn, the IRD and benthic $\delta^{13}C$ records from core SO75-26KL are compared in Figure 26 with the IRD and planktonic $\delta^{18}O$ records from Site 609 and the GRIP ice core $\delta^{18}O$ record. Planktonic $\delta^{18}O$ at Site 609 and the GRIP ice core $\delta^{18}O$ record are used as monitors for meltwater flux to the northern North Atlantic and the evolution of North Atlantic climate [Bond and Lotti, 1995; Dansgaard et al., 1993].

The records from core SO75-26KL and Site 609 do not exactly match each other because of differences in chronology that are likely related to a stronger influence of bioturbation at Site 609 where sedimentation rates are much lower and IRD concentrations higher than at core SO75-26KL. Both factors potentially enhance the effects of bioturbation e.g., on the top and bottom ages of IRD layers at Site 609 [Manighetti et al., 1995; Trauth, 1995]. Comparison of the marine records with the GRIP ice core $\delta^{18}O$ record remains tentative as the age models have been developed using different techniques (GRIP ice core: ice layer counting and ice flow modelling; marine records: oxygen isotope stratigraphy and ^{14}C-dating).

Despite the uncertainties in chronology, there are remarkable similarities between the marine records (Figure 26). Absolute benthic $\delta^{13}C$ minima in core SO75-26KL during H4, before and near the end of H2, and immediately after H1, as well as the secondary $\delta^{13}C$ minima during the late stage of H4 and during H1 are mirrored in planktonic $\delta^{18}O$ minima at Site 609 that occur in the same stratigraphic positions relative to the IRD layers. The structural correspondence thus suggests a close correlation between maximum meltwater flux and decreased thermohaline convection during the 'Heinrich' events. A conspicuous feature in the benthic $\delta^{13}C$ record is the gradual decrease of values that starts 1.5-2.5 ka before the abrupt onset of IRD deposition during H1 and H4. After both events, benthic $\delta^{13}C$ gradually increases over 1.2-3 ka. Assuming a close correlation between the rate of thermohaline circulation and benthic $\delta^{13}C$ levels, the gradual changes in benthic $\delta^{13}C$ mirror gradual changes of thermohaline over-

turn in the North Atlantic that started well before the 'Heinrich' events and lasted much longer than the events.

Successive reduction of oceanic heat flux to the North Atlantic as the conveyor circulation gradually weakened would have led North Atlantic climate to colder conditions. A trend towards colder conditions prior to H4 is documented in increasingly more negative $\delta^{18}O$ maxima of interstadials 11, 10, and 9 in the Greenland ice core $\delta^{18}O$ record (Figure 26). The benthic $\delta^{13}C$ decrease prior to H4 thus is evidence that this cooling was associated with decreasing thermohaline overturn. Warming in the North Atlantic region, on the other hand, occurred abruptly at the end of H4 as is indicated by sudden increases in ice core $\delta^{18}O$ and in marine faunal records from the northern North Atlantic [Dansgaard et al., 1993; Bond et al., 1993] (Figure 26). This is in contrast to the gradual increase in benthic $\delta^{13}C$ that would suggest a gradual strengthening of thermohaline circulation and associated heat flux to the North Atlantic.

A similar pattern of benthic $\delta^{13}C$ change is observed during H1 (Figure 26), but this event occurred during a period of large-scale disintegration of northern hemisphere ice sheets in the course of the last glacial-interglacial transition. The early decrease of benthic $\delta^{13}C$ correlates with the initiation of ice sheet collapse that culminated in a sequence of meltwater pulses and led to a reduction if not complete halt of thermohaline overturn in the North Atlantic [e.g. Keigwin et al., 1991; Lehman and Keigwin, 1992; Sarnthein et al., 1992]. Absolute minima in benthic $\delta^{13}C$ are recorded during H1 and immediately after H1. The second minimum likely corresponds to meltwater pulse 1a (MWP 1a) of Fairbanks [1989]. The gradual increase in benthic $\delta^{13}C$ after MWP 1a documents the transition to the Holocene mode of circulation as meltwater flux decreased and surface circulation assumed its interglacial state. Thus, environmental boundary conditions were different for H1 but the response of deep circulation was similar during H1 and H4 in that the response was more gradual than would have been predicted from the abrupt onset of IRD deposition and the abrupt onset of warming seen in the Greenland ice core record at the end of H1 and H4 (Figure 26).

Benthic $\delta^{13}C$ changes during H2 are more rapid (Figure 26). The $\delta^{13}C$

decline prior to and during H2 is less severe i.e., 0.8‰ compared to 1.0-1.1‰ during H1 and H4. It thus seems that the reduction in thermohaline overturn was less intense during H2, either because glacial meltwater flux was less or not continuously targeted at the site of convection because of variable surface circulation. Apparently, the North Atlantic's conveyor circulation was less inert during H2 allowing thermohaline overturn to respond rapidly to changes in surface forcing.

Whether the inferred changes in thermohaline overturn were caused by gradual increases and decreases of glacial meltwater flux as the Laurentide ice sheet grew, collapsed, and later stabilized, or by changes in surface ocean and/or atmospheric circulation remains speculative. The changes in benthic $\delta^{13}C$ that were associated with the 'Heinrich' events were not monotonous but show subtle maxima and minima (Figure 26). This suggests oscillatory behavior of thermohaline circulation which is also indicated by numerical models that link convective instabilities to changes in surface ocean forcing [Weaver and Hughes, 1994; Rahmstorf, 1994, 1995]. These models also predict convective discontinuities during which thermohaline overturn abruptly jumps to minimum rates as freshwater forcing exceeds critical threshold values. The abrupt depletion of benthic $\delta^{13}C$ that is documented in core SO75-26KL at the culmination of IRD deposition during H1 and H4, and during MWP 1a may be evidence for such discontinuous behavior. The early onset of benthic $\delta^{13}C$ decrease clearly suggests that thermohaline circulation started to spin down well before H4 and that it may have conditioned the North Atlantic region for further ice sheet growth by way of reduced oceanic heat transfer.

Abrupt warming at the end of the 'Heinrich' events that is documented in marine records from the northern North Atlantic [Bond et al., 1993] and in the Greenland ice core record [Dansgaard et al., 1993] could not have been caused by abrupt increases in oceanic heat transfer to the northern North Atlantic. The more gradual increase in benthic $\delta^{13}C$ suggests that thermohaline circulation wound up slowly and resumed its full strength as much as 3 ka after the events. From this it must be concluded that the high-frequency oscillations of North Atlantic climate seen in the Greenland ice core record were at least in part caused by changes outside the ocean system e.g., in atmospheric circula-

tion.

7.7 Mid-Depth Water Mass Oxygenation off Portugal: Provisional Estimates of O_2-Levels From Benthic $\delta^{13}C$

Marked minima in benthic $\delta^{13}C$ at the upper Portuguese margin document significant reductions in ventilation during the 'Heinrich' events. This contention is based on the assumption that $\delta^{13}C$ of total dissolved inorganic carbon ($\delta^{13}C_{\Sigma CO2}$) in ambient sea water is directly correlated to biologically cycled nutrients and oxygen concentrations. In addition to this 'Redfield' fractionation, $\delta^{13}C_{\Sigma CO2}$ and thus, foraminiferal $\delta^{13}C$ that presumably mirrors ambient sea water $\delta^{13}C_{\Sigma CO2}$, is also a function of thermodynamically controlled isotope fractionation during air-sea gas [Mook et al., 1974; Broecker and Maier-Reimer, 1992; Zahn and Keir, 1994]. Thus, benthic $\delta^{13}C$ variations do not trace absolute O_2-concentrations but are a function of O_2-consumption - Apparent Oxygen Utilization (AOU) - during the oxidation of organic matter [Kroopnick, 1985] and temperature-dependent carbon isotope fractionation during gas exchange between the surface ocean and overlying atmosphere.

To estimate absolute O_2-concentrations from benthic $\delta^{13}C$ requires information on 'preformed' O_2-levels, 'preformed' $\delta^{13}C$ (i.e., O_2-concentrations and $\delta^{13}C$ prior to O_2-consumption by organic matter decomposition), and temperature during carbon isotope equilibration of dissolved CO_2 in surface waters with the overlying atmosphere. The 'preformed' O_2-level is best described by the O_2-saturation concentration which is a function of water mass temperature and salinity (T-S) [Weiss et al., 1970]. Using O_2-saturation as a starting point, ambient bottom water O_2-concentrations at a coring site can be derived by subtracting the Apparent Oxygen Utilization (AOU) estimate that has been derived from benthic $\delta^{13}C$ from the saturation O_2 value. The empirical relation between $\delta^{13}C$ of total dissolved carbon (ΣCO_2) and AOU is given by Kroopnick [1985] as

$$\delta^{13}C_{\Sigma CO2} = a - 0.0075 \times AOU \qquad n=1107,\ r=0.95 \qquad \text{equation 5}$$

where AOU is in µmol kg^{-1} and term 'a' describes the 'preformed' $\delta^{13}C_{\Sigma CO2}$ i.e., the zero-AOU intercept of $\delta^{13}C_{\Sigma CO2}$. Typical modern values for 'a' are +1.5‰ PDB for the deep ocean [Kroopnick, 1985] and +1.2‰ to +1.6‰ PDB for the shallow ocean above 1.5 km water depth [Zahn and Keir, 1994].

Using glacial benthic $\delta^{13}C$ for $\delta^{13}C_{\Sigma CO2}$ in equation 5 requires correction of the benthic $\delta^{13}C$ values for changes of the marine carbon reservoir and associated shifts in mean-ocean $\delta^{13}C_{\Sigma CO2}$ that went along with glacial-interglacial climate change [Shackleton, 1977; Curry et al., 1988; Duplessy et al., 1988]. Compilation of benthic $\delta^{13}C$ values from coring sites throughout the global ocean suggest that the mean-ocean $\delta^{13}C_{\Sigma CO2}$ was depleted during the Last Glacial Maximum by 0.32‰ ($\Delta\delta^{13}C_{\Sigma CO2}$=-0.32‰) due to the transfer of ^{12}C-enriched carbon from the terrestrial biosphere to the ocean [Duplessy et al., 1988]. This value takes the presence of ^{13}C-enriched water masses in the glacial-maximum upper ocean into account and is therefore smaller than that of $\Delta\delta^{13}C_{\Sigma CO2}$=-0.46‰ that has been determined by Curry et al. [1988] by using data from deep-ocean sites at water depths below 2.5 km only. The correction value of +0.32‰ has been estimated for glacial-maximum conditions, and not necessarily represents mean-ocean $\delta^{13}C_{\Sigma CO2}$ levels for pre-LGM conditions when benthic $\delta^{13}C$ at deep-ocean sites was less depleted than during the LGM. Yet, I use this value also for mean-glacial conditions with the caveat that 'true' $\delta^{13}C_{\Sigma CO2}$ levels likely were less positive than what is implied by adding 0.32‰ to glacial-benthic $\delta^{13}C$ during oxygen isotope stage 3 and early stage 2.

Mid-depth O_2 concentrations today at the upper Portuguese margin are 4.2 ml L^{-1} as measured in hydrocasts at TTO (Transient Tracers in the Ocean program, TTO [1986]) Station 113 off southern Portugal. The O_2-saturation value is 6.0 ml L^{-1}, according to T-S values of 11°C/36.1 at this depth. Hence, in situ O_2-concentrations of 4.2 ml L^{-1} are 1.8 ml L^{-1} below the saturation value. An AOU of 1.8 ml L^{-1} translates into a $\delta^{13}C_{\Sigma CO2}$ shift of -0.6‰ as defined by the slope of equation 5, assuming that all O_2 has been consumed by oxidation of marine organic matter (Figure 27). Mean Holocene benthic $\delta^{13}C$ in core SO75-26KL is

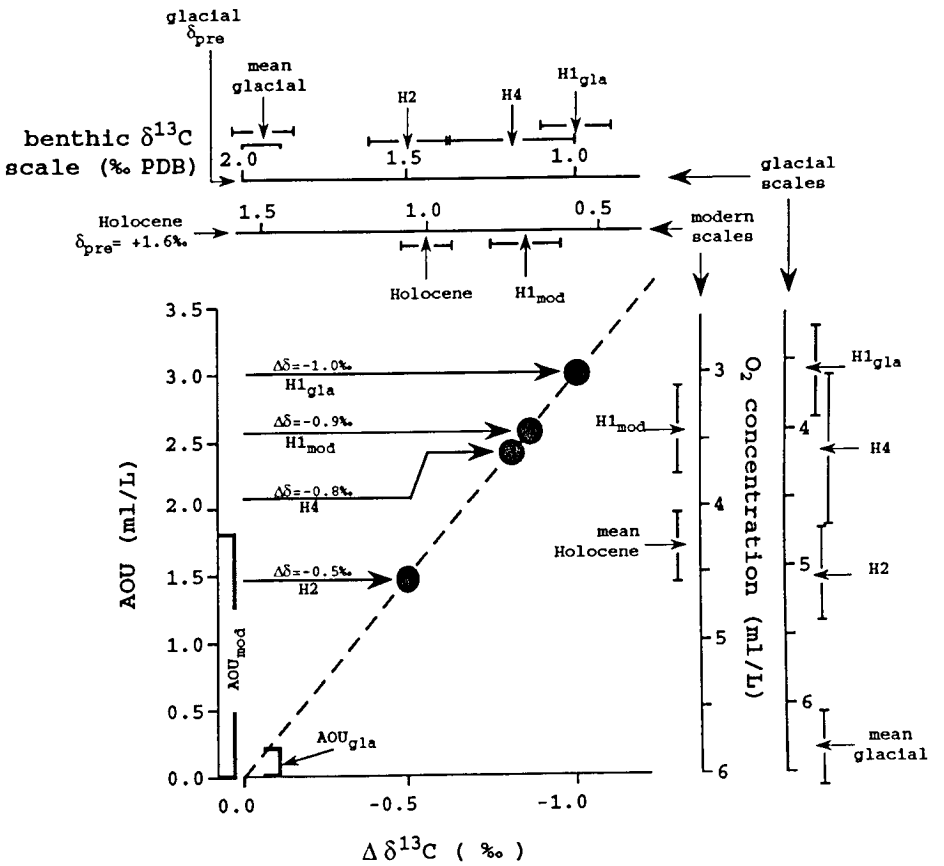

Figure 27. Oxygen concentrations in ambient water masses at the upper Portuguese margin. Oxygen levels are estimated from benthic carbon isotope values. 'Preformed' carbon isotope values and oxygen saturation levels are estimated from the gas saturation and isotope equilibration equations given in Weiss [1970] and Mook et al. [1974]. Temperature and salinity that are needed for the calculations were estimated from benthic oxygen isotopes in cores SO75-6KL and -26KL (Figure 22). It is assumed that the T-S values represent surface ocean conditions in the source region for the mid-depth waters, and that full isotope equilibrium and oxygen saturation were achieved.

+1.0±0.08‰ PDB (n=10, range= 0.8-1.1‰ PDB). This value is the result of $\delta^{13}C$ depletion of 0.6‰ induced by AOU i.e., the mean Holocene benthic $\delta^{13}C$ value in core SO75-26KL is depleted by 0.6‰ relative to the 'original' $\delta^{13}C_{\Sigma CO2}$ value of this water mass before it left the surface layer and got isolated from the atmosphere. Adding this 0.6‰ to the mean Holocene benthic $\delta^{13}C$ of 1.0‰ PDB gives a 'preformed' $\delta^{13}C_{\Sigma CO2}$ value of +1.6‰ PDB. This value agrees well with the 'preformed' $\delta^{13}C_{\Sigma CO2}$ value of +1.56‰ PDB that has been determined for the mid-depth North Atlantic at potential densities of $26.8<\sigma_\phi<27.7$, equivalent to water depths between 0.8-1.5 km [Zahn and Keir, 1994].

Evaluation of benthic $\delta^{18}O$ from upper Portuguese margin cores SO75-6KL and -26KL in T-S-δ_c diagrams (see page 74, Chapter 7.3, *Benthic Foraminiferal $\delta^{18}O$ at the Upper Portuguese Margin*, Figures 21 and 22) suggests that the contribution of mid-depth water masses from the open North Atlantic to the upper Portuguese margin was increased during the last glacial at the expense of Mediterranean Outflow Waters (MOW). A potential shift from a mixture of MOW and North-Atlantic mid-depth waters today (T=11°C, S=36.1) to a water mass that contains major contributions of cold and saline North Atlantic Central Water (T=7.2°C, S=37.1) goes along with an increase in O_2-saturation by 0.5 ml L^{-1}, from 6.0 ml L^{-1} today to 6.5 ml L^{-1} during the last glacial (Figure 27). As temperature also determines the fractionation of carbon isotopes of dissolved carbon in surface waters during air-sea gas exchange (about 0.1‰ increase per 1°C decrease; Mook et al., 1974), a temperature decrease by some 4°C of glacial waters ($T_{Holocene}$=11°C, $T_{glacial}$=7.2°C) would induce an increase in $\delta^{13}C_{\Sigma CO2}$ by about 0.4‰, if isotope equilibrium is achieved during air-sea gas exchange. Glacial 'preformed' $\delta^{13}C_{\Sigma CO2}$ thus is +2.0‰ (PDB) for the last glacial (1.6‰ PDB for modern 'preformed' $\delta^{13}C_{\Sigma CO2}$ plus 0.4‰=2.0‰ PDB; Figure 27). Mean glacial benthic $\delta^{13}C$ is +1.7± 0.06‰ PDB (n=11, range= 1.5-1.7‰ PDB) in core SO75-26KL. Correcting this value for the mean-ocean shift in $\delta^{13}C_{\Sigma CO2}$ by adding 0.32‰, one arrives at a glacial benthic $\delta^{13}C$ value of +2.0‰ PDB for core SO75-26KL. As has been mentioned above, the correction value of +0.32‰ has been estimated for glacial-maximum conditions and does not necessarily represent glacial conditions of stages 3 and early stage 2. The mean $\delta^{13}C_{\Sigma CO2}$ shift likely was reduced during these earlier glacial periods. But even if it was half

the LGM value would the corrected benthic $\delta^{13}C$ value of +1.86‰ PDB (mean glacial benthic $\delta^{13}C$ of 1.7‰ PDB plus 0.16‰) be close to the estimated 'preformed' $\delta^{13}C_{\Sigma CO2}$ plus of 2.0‰ PDB. These considerations imply AOU values of 0-0.3 ml L^{-1} compared to 1.8 ml L^{-1} today (Figure 27) suggesting distinctly higher oxygenation levels, between 6.1-6.5 ml L^{-1} (compared 4.2 ml L^{-1} today) and much higher rates of mid-depth ventilation during the last glacial.

Assuming a glacial 'preformed' $\delta^{13}C_{\Sigma CO2}$ of +2.0‰ PDB (parameter 'a' in equation 5) and glacial O_2-saturation of 6.5 ml L^{-1}, O_2-concentrations during Heinrich events can now be estimated from benthic $\delta^{13}C$ values - once the values are corrected for the mean-ocean $\delta^{13}C_{\Sigma CO2}$ shift - and resultant AOU. In core SO75-26KL, the range of benthic $\delta^{13}C$ is 1.1-1.4‰ PDB with a mean value of +1.2±0.11‰ PDB for H2 (n=6), and 0.5-1.2‰ PDB with a mean value of +0.9±0.19‰ PDB for H4 (n=17). Corrected benthic $\delta^{13}C$ values are +1.5‰ and +1.2‰ PDB for H2 and H4, respectively. Using these values as input into equation 5, O_2-concentrations in ambient bottom waters at the upper Portuguese margin were 4.7-5.6 ml L^{-1} (mean=5.0±0.33 ml L^{-1}) for H2 and 3.0-5.1 ml L^{-1} (mean=4.2±0.57 ml L^{-1}) for H4 (Figure 27). The range of benthic $\delta^{13}C$ during H1 is 0.5-0.8‰ PDB with a mean value of +0.71±0.1‰ PDB (n=12). H1 occurred during the last glacial-interglacial transition when disintegration of northern hemisphere ice sheets led to large-scale reorganization of ocean circulation. Reliable T-S conditions in the North Atlantic region cannot be derived from foraminiferal $\delta^{18}O$ for this period because increased meltwater fluxes conceivably led to significant deviations in the δ_w:S relation that is an essential parameter in paleotemperature equations. Therefore I use both the glacial and mean Holocene parameterization to estimate in situ O_2 levels. 'True' O_2 concentrations may have been somewhere around these estimates.

Correcting the benthic $\delta^{13}C$ value of 0.71‰ PDB for the glacial scenario by adding 0.32‰, one arrives at around +1‰ in $\delta^{13}C$ for H1. Comparing this value with the glacial 'preformed' $\delta^{13}C_{\Sigma CO2}$ of +2.0‰ PDB and an O_2 saturation of 6.5 ml L^{-1}, this suggests an AOU of 3.0 ml L^{-1}, arriving at ambient O_2 concentrations between 3.0-3.9 ml L^{-1} (mean=3.6±0.30 ml L^{-1}, '$H1_{gla}$' in Figure 27). For the alternative interpretation in a Holocene scenario, benthic $\delta^{13}C$ of +0.71 ±0.1‰ is left unchanged. Using a Holocene 'preformed' $\delta^{13}C_{\Sigma CO2}$ of +1.6‰ PDB

and O_2 saturation of 6.0 ml L^{-1}, AOU is estimated to 2.7 ml L^{-1} and absolute O_2 concentrations to 2.8-3.7 ml L^{-1} (mean=3.4±0.30 ml L^{-1}) for this event ('$H1_{mod}$' in Figure 27).

The above estimates suggest that oxygenation during the last glacial was significantly increased at the upper Portuguese margin and that O_2 levels were close to the saturation value implying rapid ventilation with only little 'ageing' of mid-depth water masses. This is in agreement with conceptual models that use enhanced benthic $\delta^{13}C$ levels at shallow ocean coring sites throughout the world ocean as evidence for increased upper ocean ventilation [Zahn et al., 1987; Duplessy et al., 1988; Mix, Pisias, Zahn et al., 1991; Zahn and Pedersen, 1991; Veum et al., 1992; Oppo and Lehman, 1993; Sarnthein et al., 1994; Jung, 1996]. Decreased benthic $\delta^{13}C$ values indicate reductions in O_2 concentrations during 'Heinrich' events. O_2 estimates for H4 and H2 of 4.2 and 5.0 ml L^{-1} are lower than mean-glacial levels (6.1-6.5 ml L^{-1}) but remain above Holocene levels (4.2 ml L^{-1}). Thus ventilation during both 'Heinrich' events was reduced compared to conditions prior to and after both events, but was still increased over Holocene levels. It was only during H1 when O_2 concentrations decreased to 3.4-3.6 ml L^{-1} (using the glacial and Holocene scenarios) that oxygenation sunk below Holocene levels. H1 occurred early in the last glacial-interglacial transition when thermohaline overturn in the North Atlantic wound down and conceivably came to a complete halt in response to large-scale meltwater supply from the disintegration of the Laurentide and Fennoscandian ice sheets [Keigwin and Jones, 1991; Sarnthein et al., 1994; Seidov et al., 1996]. Benthic $\delta^{13}C$ indicates that O_2 concentrations reached the lowest values during this period thus confirming significant convective slow-down during this period.

The estimates of absolute O_2 levels from benthic $\delta^{13}C$ are intrinsically provisional. Variable air-sea gas exchange and potential changes in the $\delta^{13}C$-composition of oxidizable organic matter may modulate the benthic $\delta^{13}C$-data and limit the reliability of benthic $\delta^{13}C$ as a means to estimate changes in O_2-concentration. E.g., the 'Heinrich' events were associated with temperature decreases in the North Atlantic as indicated by the dominance of polar planktonic foraminifera and transfer function SST estimates [Bond et al., 1993;

Maslin et al., 1995]. It appears therefore plausible to assume that 'preformed' $\delta^{13}C_{\Sigma CO2}$ could have been higher than mean-glacial values during the 'Heinrich' events due to the temperature dependent carbon isotope fractionation during air-sea gas exchange [Mook et al., 1974]. Decreased surface temperature would also result in enhanced O_2-saturation levels [Weiss et al., 1970]. On the other hand, reduced air-sea gas exchange due to enhanced stratification of surface-subsurface waters brought about by meltwater-induced salinity reductions could have led to a decrease in 'preformed' $\delta^{13}C_{\Sigma CO2}$ in response to an accumulation of metabolic ^{12}C in the subsurface layer. Reduced surface water PCO_2 in response to lower pCO_2 in the glacial atmosphere would result in reduced carbon isotope fractionation of the marine biota and cause the $\delta^{13}C$-composition of marine organic matter to increase [Jasper and Hayes, 1994; Rau, 1994]. This would cause smaller changes in seawater $\delta^{13}C_{\Sigma CO2}$ per unit change of AOU. The various factors outlined here can only be constrained if independent proxies are used in addition to benthic $\delta^{13}C$ for monitoring ocean change during the last glacial. Benthic Cd/Ca ratios are one such proxy that closely mirrors the distribution of biologically cycled nutrients in the ocean. In contrast to seawater $\delta^{13}C_{\Sigma CO2}$ and to benthic $\delta^{13}C$, Cd/Ca ratios are not influenced by air-sea fractionation or variably atmospheric chemistry and have been successfully used in paleoceanographic research [Boyle, 1992; Boyle, 1994; Lynch-Stieglitz and Fairbanks, 1994; Zahn and Keir, 1994; Lynch-Stieglitz et al., 1996]. Benthic Cd/Ca analyses are currently underway on sediment cores from the upper Portuguese margin and the northern North Atlantic [C. Willamowski, Dissertation in preparation] in an attempt to better constrain ventilation changes during the 'Heinrich' meltwater events.

8.0 MILLENNIAL-SCALE CLIMATE OSCILLATIONS FROM GREENLAND AND ANTARCTIC ICE CORES, AND NORTH ATLANTIC VENTILATION: POSSIBLE INTER-HEMISPHERIC CORRELATION

Climatically sensitive proxy-records along ice cores from Greenland and Antarctica provide clear evidence for rapid climatic oscillations in both hemispheres during the last glacial [Dansgaard et al., 1993; Bender et al., 1994; Grootes et al., 1993; Jouzel et al., 1996]. High-amplitude rapid oscillations in the oxygen isotope composition along the GRIP and GISP2 ice cores have been used to infer that climate in the North Atlantic region was highly instable during the last glacial, shifting rapidly in annual mean temperature by as much as 7°C within few decades [Dansgaard et al., 1993; Grootes et al., 1993]. Coeval oscillations in ice electrical conductivity on time scales of less than 20 years indicate vigorous changes in dustiness, suggesting rapid changes in atmospheric circulation [Taylor et al., 1993].

Similar oscillations are seen in the Vostok ice core record from Antarctica, even though less frequently and reduced in amplitude [Lorius et al., 1985; Jouzel et al., 1987]. Extension of the Vostok paleoclimatic record back to marine oxygen isotope stage 7.5 at 240 cal.-ka (modified "extended glaciological time scale", EGT; Jouzel et al. [1996]) has revealed the existence of similar oscillations during the penultimate glacial (oxygen isotope stage 6; Jouzel et al., [1996]). Spectral analysis of the paleoclimatic records from the Greenland and Vostok ice cores has revealed subtle differences between both cores in the main periodicities of climate change [Yiou et al., 1995], but these likely are due to the lower stratigraphic resolution of the Vostok core. Differences in climatic boundary conditions between Greenland and Antarctica and resultant offsets in snow accumulation - about 23 cm of ice equivalent per year at the Greenland ice core site [Johnsen et al., 1992] compared to 1-3 cm for the Antarctic record [Lorius et al., 1985; Jouzel et al., 1996] - thus limit the degree of certainty with which both ice core records can be correlated. Yet, the Greenland and Antarctic ice records display similar rapid oscillations, suggesting an interhemispheric link between climate change at high northern and southern latitudes [Bender et al., 1994a; Yiou et al., 1995].

The recognition that the climatic oscillations seen in the ice core records must have left their imprints in marine records has triggered a search for evidence for similar oscillations in paleoceanographic proxy records from the northern North Atlantic and the Southern Ocean [Sowers et al., 1993; Bond et al., 1993; Bender et al., 1994b; McManus et al., 1994; Keigwin and Jones, 1994; Yiou et al., 1995; Waelbroeck et al., 1995; Fronval and Jansen, 1996; Labeyrie et al., 1996; Rasmussen et al., 1996]. Detailed correlation between marine and ice core records for most part is hampered by the fact that sedimentation rates in the open ocean are typically in the order of 2-5 cm cal.-ka^{-1} i.e., many orders of magnitude lower than ice equivalent accumulation rates in polar ice cores (ice equivalent accumulation rates are 11 m cal.-ka^{-1} and 460 m cal.-ka^{-1} in the GRIP/GISP and Vostok ice cores respectively, see above). Only if sedimentation rates are exceptionally high are detailed marine versus ice core correlations possible (Lehman and Keigwin [1992]: core TROLL 3.1 from the central Norwegian Channel, sedimentation rates of 5 m ka^{-1}; Keigwin and Jones [1994]: core GPC-5 from the Bermuda Rise, sedimentation rates 20-200 cm ka^{-1}; Rasmussen et al. [1996]: core ENAM93-21 from the Faeroe-Shetland Channel, sedimentation rates 14-30 cm ka^{-1}). Sedimentation rates at the upper Portuguese margin are high, 10-40 cm cal.-ka^{-1} (Figure 5), thus making core SO75-26KL a potential candidate for comparing the mid-depth record of North Atlantic ventilation changes to the ice core records of glacial climatic oscillation.

First, oscillations in the ice-deuterium (δD_{ice}) record from Vostok are compared with stadial-interstadial (Dansgaard-Oeschger) cycles in the Greenland record. The rapid isotope shifts seen in the Greenland record are less pronounced in the Vostok record, but there is a striking resemblance in the sequence of isotope oscillations between both records. As has previously been observed by Bender et al. [1994], the most pronounced interstadials in the Greenland record are also documented in the Vostok record, namely interstadials 8, 12, 14, 16, and 19-23. These interstadials are well known from European pollen records [Woillard, 1978; Küttel, 1989; Kaiser, 1993] and their occurrence on both hemispheres suggests that interstadial warming occurred on a global scale. Finer-scale comparison of isotope oscillations between these dominant

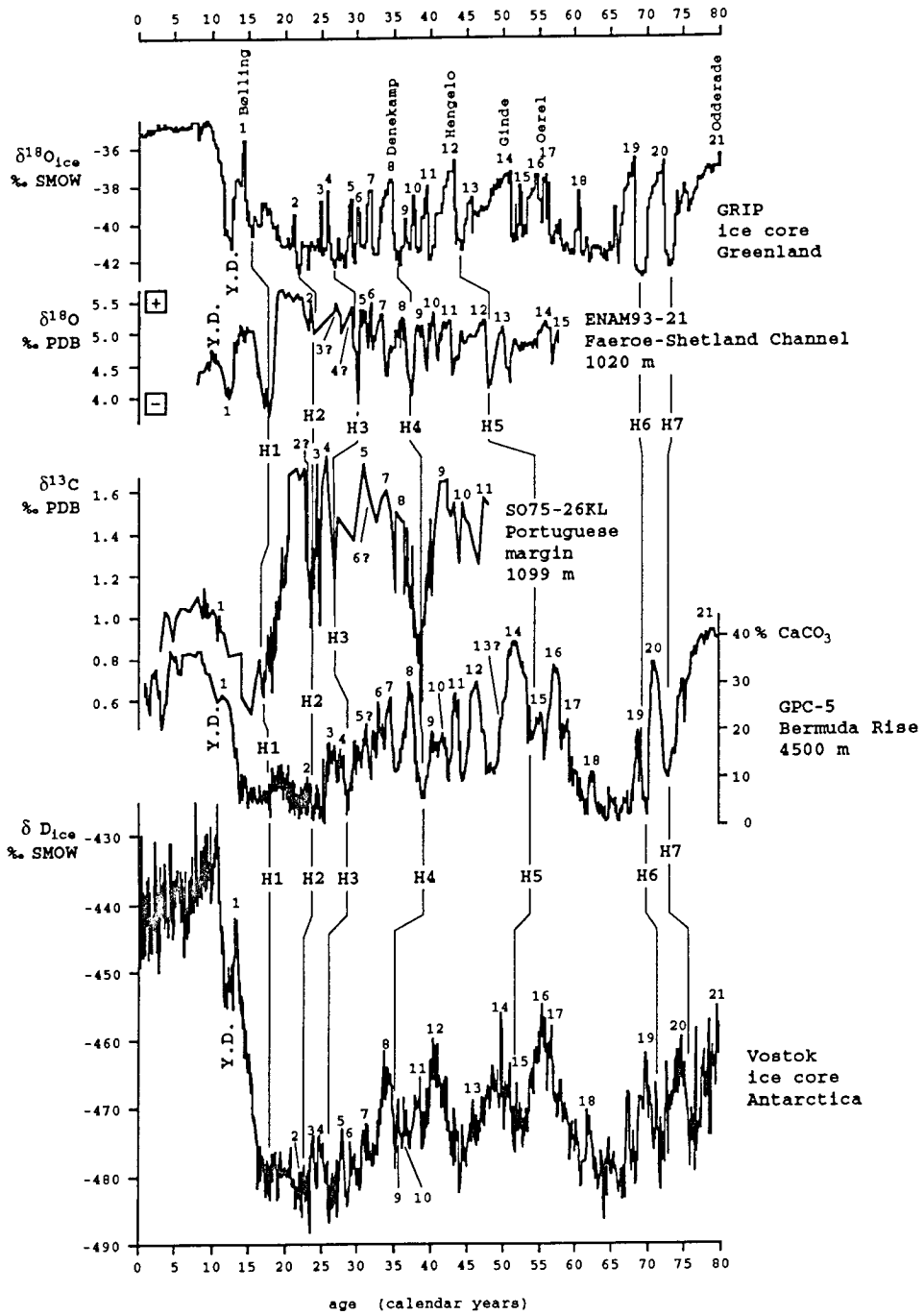

Figure 28. The ice core record from Greenland [Dansgaard et al., 1993; Grootes et al., 1993] shows rapid stadial-interstadial oscillations that are also seen in the Vostok ice core record from Antarctica [Lorius et al., 1985; Jouzel et al., 1996]. The marine records from mid-depth to bottom water core sites in the northern and subtropical North Atlantic [Keigwin and Jones, 1994; Rasmussen et al., 1996b] display similar oscillations suggesting a direct response of thermohaline circulation to surface ocean forcing at high northern and southern latitudes. Stadial-interstadial cycles are tentatively marked along the benthic carbon isotope record from core SO75-26KL.

interstadials reveals that other interstadials which are documented in the Greenland record are also identified in the Vostok record (Figure 28). These "secondary" interstadials are indexed in Figure 28 by transferring interstadial numbers from the GRIP ice core to their apparent counterparts in the Vostok record. In this way the complete sequence of interstadials that is documented in the Greenland $\delta^{18}O_{ice}$ record can be identified in the Vostok record (Figure 28).

As a next step, the high-resolution benthic $\delta^{18}O$ and carbonate records from cores ENAM93-21 (Faeroe-Shetland Channel, northernmost North Atlantic; Rasmussen et al. [1996]) and GPC-5 (Bermuda Rise, subtropical North Atlantic; Keigwin and Jones [1994]) are indexed following the same numeric system as before for the Greenland-Vostok comparison. Both marine records show a striking resemblance to the Greenland and Antarctic ice core records in that they display variations on similar time scales as the stadial-interstadial oscillations seen in the ice core records (Figure 28). As has been discussed by Rasmussen et al. [1996 a, b] the ENAM93-21 isotope and benthic-planktonic faunal records display distinctive cycles that can be directly correlated with the Dansgaard-Oeschger climatic cycles seen in the GRIP ice core. The isotope and faunal changes have been used to infer systematic changes in surface ocean conditions that have led to shifts of convection sites between the Norwegian-Greenland Seas and the northern North Atlantic. Oscillations in percent carbonate along core GPC-5, on the other hand, together with concomitant changes in benthic $\delta^{13}C$ are indicative of high-frequency changes of carbonate dissolution in association with circulation changes of Atlantic deep and bottom waters [Keigwin and Jones, 1994]. Core GPC-5 is located at 4500 m water depth on the lower Bermuda Rise and lies within the transition zone between NADW and AABW. Thus the changes in percent carbonate monitor variable fluxes of North Atlantic versus Southern Ocean water masses during the last glacial. The carbonate variations have been compared to isotope oscillations in the Renland ice core from Greenland [Keigwin and Jones, 1994] using an independent alphanumeric index (*a* through *j*; see Figure 10 in Keigwin and Jones [1994]) for the GPC-5 record. In Figure 28 a direct correlation between the Greenland, Vostok, ENAM93-21 isotope and GPC-5 carbonate records is proposed by using the same interstadial index that is used for the Greenland intersta-

dials.

As a final step, the benthic $\delta^{13}C$ record of core SO75-26KL from the upper Portuguese margin is correlated to the other records. Fix points for interstadial indexing were the pronounced negative $\delta^{13}C$ anomalies during 'Heinrich' events H1, H2, and H4, and the fourth anomaly around 27 cal.-ka that most likely correlates with H3 (Figure 28). H1, H2, and H4 occurred at the culmination of longer-term cooling cycles that were terminated by abrupt warming during interstadials 1 (equiv. Bølling), 2, and 8 (equiv. Denekamp interstadial); H3 occurred during stadial conditions immediately prior to interstadial 4 [Bond et al., 1993; Rasmussen et al., 1996] (see also page 92, Chapter 7.6, *Thermohaline Links Between Mid-Depth Ventilation off Portugal and Northern North Atlantic Surface Conditions*, and Figure 26). Stratigraphic resolution of the SO75-26KL benthic $\delta^{13}C$ record is lower than that of the paleoceanographic records from cores ENAM93-21 and GPC-5 and does not allow correlation to the ice core records in similar detail. E.g., the three $\delta^{13}C$ maxima between the H4 and assumed H3 negative anomalies are facing four interstadials (8-5) in the corresponding stratigraphic section from the ice core record, and the increase of maximum benthic $\delta^{13}C$ of the three maxima between H4 and H3 is in conflict with an opposing trend towards decreasing $\delta^{18}O_{ice}$ maxima from interstadial 8 to 5. Benthic $\delta^{13}C$ maxima, on the other hand, that have tentatively been assigned interstadial numbers 3, 4, and 9 through 11 correlate well with the interstadials from the Greenland ice core record in that benthic $\delta^{13}C$ amplitudes are similar to the ice core $\delta^{18}O_{ice}$ amplitudes (compared to whole-core $\delta^{13}C$ and $\delta^{18}O_{ice}$ variations) and the benthic $\delta^{13}C$ maxima occur at similar stratigraphic positions relative to the benthic $\delta^{13}C$ and ice core $\delta^{18}O_{ice}$ minima during 'Heinrich' events H2 and H4.

Proxy boundary conditions that determine the magnitude and timing of anomalies in the individual records are different, and age models for the marine and ice core records were derived from different analytical techniques. As such, the correlation of marine and ice core records at millennial Dansgaard-Oeschger time scales remains tentative. Yet, variability of the paleoclimatic and paleoceanographic records shown in Figure 28 is strikingly similar and suggests some mechanistic links existed between oscillations of

high-latitude climate as seen in the Greenland and Antarctic ice cores, and ocean circulation as documented in the marine records from the subtropical to northernmost North Atlantic.

As has been discussed by Rasmussen et al. [1996], stadial episodes in the northernmost North Atlantic were associated with an incursion of fully-polar conditions and reduced thermohaline overturn in the Norwegian-Greenland Seas. Coeval migration of benthic foraminiferal fauna that are adopted to warmer intermediate waters from the Atlantic into the southeastern Norwegian Sea implies an advection of Atlantic intermediate waters into the Norwegian Sea and a diminished outflow of deep water through the Faeroe-Shetland Channel into the North Atlantic [Rasmussen et al., 1996b]. The conceptual model of decreased flux of northern source deep waters through the North Atlantic during stadials is supported by minimum carbonate concentrations in core GPC-5 during these periods. Enhanced advection of corrosive AABW in response to reduced flux of NADW would have increased carbonate dissolution and lowered carbonate contents at bottom water coring sites. Benthic $\delta^{13}C$ in core SO75-26KL, although increased during the last glacial suggesting enhanced ventilation of the upper North Atlantic, displays short-term decreases during stadial episodes, implying that even mid-depth ventilation was intermittently reduced during stadials periods (Figure 28).

Decreased planktonic $\delta^{18}O$ (*N. pachyderma* (sin.)) during most stadial periods when surface temperatures were at a minimum as implied by maximum occurrences of polar planktonic foraminifera *N. pachyderma* (sin.) [Bond et al., 1993; Rasmussen et al., 1996] suggests that stadial-interstadial oscillations went along with systematic changes of surface salinity in the northern North Atlantic. The flux of salt through the North Atlantic has been proposed to be a driving force in determining the rate of convection in the North Atlantic which, in turn, determines climates in the North Atlantic region through varying rates of advection of warm subtropical waters to high northern latitudes ('conveyor circulation' hypothesis, Broecker et al. [1990]). The correlation between decreased planktonic $\delta^{18}O$ and cold stadial conditions suggests that salinity variations in the glacial northernmost North Atlantic were directly coupled to Dansgaard-Oeschger climatic oscillations. Variations of minimum

planktonic and benthic $\delta^{18}O$ in the northern North Atlantic (core ENAM93-21), decreased benthic $\delta^{13}C$ in the mid-depth North Atlantic (core SO75-26KL) and minimum carbonate contents in the deep subtropical North Atlantic (core GPC-5) during stadial periods suggest that the Dansgaard-Oeschger cycles and associated changes of surface ocean conditions affected the entire water mass Atlantic circulation, from intermediate to bottom water depths.

The apparent coupling between stadial-interstadial $\delta^{18}O_{ice}$ oscillations in Greenland ice cores and δD_{ice} oscillations in the Vostok record implies rapid climatic communication between both hemispheres. For the longer interstadial episodes (8, 12, 14, 16/17) moderately increased summer-time insolation has been proposed as a cause for these warmer periods [Bender et al., 1994]. The more detailed correlation of stadial-interstadial oscillations that is proposed in Figure 28 together with similar oscillations in paleoceanographic records from the subtropical to northernmost North Atlantic requires additional inter-hemispheric links. For instance, evidence for meltwater surges similar to those that occurred in the North Atlantic during the 'Heinrich' events has also been found in Southern Ocean sediment cores [Labeyrie et al., 1987; Shemesh et al., 1994]. If the surges occurred synchronously on both hemispheres, this would suggest sea level as a further interhemispheric link as a mechansim to destabilize ice sheets on both hemispheres synchronously.

Spectral analysis of paleoceanographic time series that monitor wind-driven divergence in the equatorial Atlantic has revealed the existence of cycles with a period of 7.6 ^{14}C-kyr, roughly in agreement with the period of 'Heinrich' events in the northern North Atlantic [McIntyre and Molfino, 1996]. The period of 7.6 ^{14}C-kyr represents a combination tone of orbital precession and eccentricity which exert primary control on low-latitude insolation. Varying zonality of low-latitude winds, driven by low-latitude insolation, and associated changes in advection of subtropical waters and oceanic heat to the northern North Atlantic have been proposed as a mechanistic link between low-latitude forcing and North Atlantic climate [McIntyre and Molfino, 1996]. Even though orbital forcing during the past 60 kyr has been considered 'atypical' compared to the preceding 300 kyr, this mechanism may provide important clues as to the role of atmospheric circulation in transmitting climatic signals from low to high

latitudes, and possibly on inter-hemispheric scales.

Coeval changes of surface ocean conditions at high northern and southern latitudes would provide a viable explanation for the rapid oscillations that are observed in paleoceanographic proxy records from mid-depth to bottom water coring sites (Figure 28). To determine the timing and magnitude of paleoclimatic oscillations in Antarctica and their temporal relation to the North Atlantic climatic oscillations with more confidence, proxy records from Antarctica are needed at a stratigraphic resolution similar to the Greenland records. Detailed planning to retrieve such cores from coastal sites in West Antarctica where snow accumulation is high is currently underway under the auspices of the WAISCORES program [West Antartic Ice Sheet Cores Program, 1996].

9.0 CONCLUSIONS

Discrete IRD layers on the Portuguese margin have been dated to 13.7 and 21.5 ^{14}C-ka, and an interpolated age of 36.1 ^{14}C-ka. These ages are within the range of published ages for 'Heinrich' events H1, H2, and H4. A marked anomaly in planktonic foraminiferal fauna and benthic δ^{13}C near 25 ^{14}C-ka suggests an association with 'Heinrich' event H3 (dated to 27 ^{14}C-ka; Bond et al. [1993]). IRD deposition did not occur on the southern Portuguese margin during H3, presumably because this event was too small and because the drift paths of icebergs did not touch the Portuguese margin. Planktonic foraminiferal census counts imply SST decreases of 7-10°C during the 'Heinrich' events and suggest that subpolar surface waters reached the Portuguese margin during these periods. Planktonic δ^{18}O does not increase during H2 and H4 as would be expected from the inferred cooling, suggesting that concurrent decreases in salinity compensated for the temperature effects on planktonic δ^{18}O. During H1, similar cooling is inferred, but a marked negative anomaly in planktonic δ^{18}O implies that the salinity decrease during this event was larger than during the previous 'Heinrich' events.

Using planktonic δ^{18}O and inferred SST from the Portuguese margin and the northern North Atlantic (core BOFS-5K, Maslin et al. [1995]), paleosalinity

during the 'Heinrich' events is estimated to decrease by 1.5-3.0 units. These estimates, however, must be regarded tentative as available SST estimates from different transfer function and analogue techniques deviate from each other by as much as 5°C. Together with deviations of 'isotopic' SST (as extracted from planktonic $\delta^{18}O$) from 'true' SST [Duplessy et al., 1991; Weinelt et al., 1996], this imposes uncertainty on surface salinity estimates. Yet, the combined SST and planktonic $\delta^{18}O$ evidence points to significant salinity changes that altered the North Atlantic's density structure and resulted in convective slow-down, as is implied by decreases in benthic $\delta^{13}C$.

The SST estimates do not display the longer-term cooling cycles inferred by Bond et al. [1993] from faunal composition at northern North Atlantic Site 609. Rather, the data suggest that cooling occurred only during the 'Heinrich' events. Concurrent cooling and salinity decreases are observed in sediment cores from the Northwest African margin as far south as Cape Blanc (21°N; Wang et al. [1995], Zhao et al. [1995]) and suggest enhanced export of subpolar waters to the south in the North Atlantic's eastern boundary current.

Evaluating benthic $\delta^{18}O$ in T-S diagrams in conjunction with estimated equilibrium δ_c fractionation implies that the contribution of Mediterranean Outflow Water (MOW) to the upper Portuguese margin was reduced by 50-90% during the last glacial. Reduced advection of MOW to the North Atlantic is also implied by theoretical considerations. A restricted geometry of the Strait of Gibraltar that was caused by a glacially lowered sea level together with an enhanced Atlantic-Mediterranean salinity gradient would reduce the flow of MOW to the North Atlantic [Bryden and Stommel, 1984]. Furthermore, density of MOW was increased because of decreased glacial temperature and increased salinity [Thiede, 1978; Thunell and Williams, 1989]. This would make significant mixing with less saline waters necessary to stabilize MOW at intermediate water depths. These considerations suggest that water masses at the upper Portuguese margin were primarily derived from North Atlantic sources and that MOW played only a minor role in defining the regional mid-depth hydrography during the last glacial.

Benthic $\delta^{13}C$ in cores from the upper Portuguese margin therefore prima-

rily monitors variability of North Atlantic mid-depth water masses and, as such, traces thermohaline overturn in the North Atlantic. Benthic $\delta^{13}C$ at the upper Portuguese margin (1000-1300 m water depth) is increased by 0.5-0.7‰ during the last glacial documenting enhanced ventilation of mid-depth waters that is also seen at other shallow core sites in the northern North Atlantic. Glacial $\delta^{13}C$ similar to that from the upper Portuguese margin is documented in mid-depth core OC205-2-100GGC on the Bahama Rise [Slowey and Curry, 1995] whereas glacial $\delta^{13}C$ at the upper Moroccan margin does not increase above the late Holocene level. From this pattern it is inferred that a hydrographic front existed at 1000-1500 m water depth immediately south of Portugal lending credence to a strong reverse gyre circulation that has been predicted in numerical circulation modelling for the glacial mid-depth North Atlantic [Seidov et al., 1996].

Benthic $\delta^{13}C$ at the upper Portuguese margin displays marked minima that are coeval with 'Heinrich' events H1, H2, and H4 as indicated by the ages of concurrent IRD layers. These minima document marked ventilation decreases during the 'Heinrich' events. A fourth benthic $\delta^{13}C$ minimum at 25 ^{14}C-ka that is not accompanied by an IRD layer likely represents the ventilation decrease during H3 that did not result in the deposition of an IRD layer on the southern Portuguese margin. Enhanced meltwater flux that was associated with the 'Heinrich' events apparently caused convective instabilities in the North Atlantic. Comparison of the benthic $\delta^{13}C$ pattern off Portugal with the planktonic $\delta^{18}O$ pattern from Site 609 implies that slow-down of thermohaline circulation was coupled to enhanced meltwater flux to the North Atlantic during the 'Heinrich' events, and that a thermohaline link existed between the North Atlantic and mid-depth waters at the upper Portuguese margin. Benthic $\delta^{13}C$ at deep water sites off Portugal (>3000 m water depth) does not show significant changes during the 'Heinrich' events. These sites were influenced by Antarctic Bottom Water (AABW) that was already depleted in $\delta^{13}C$. Enhanced northward penetration of AABW during the 'Heinrich' events would thus not cause benthic $\delta^{13}C$ to decrease further.

Using benthic $\delta^{13}C$ in conjunction with T-S changes derived from benthic $\delta^{18}O$ and glacial-interglacial mean ocean $\delta^{13}C_{\Sigma CO_2}$ shift, O_2 concentrations at the

upper Portuguese margin are inferred to be close to saturation. During the 'Heinrich' events, O_2 levels decrease by 1-3 ml L^{-1}. These provisional estimates support the contention that mid-depth waters were vigorously ventilated during the last glacial, and that convection slowed down during the 'Heinrich' events. Minimum O_2 concentrations of 3.4 ml L^{-1} that are inferred for H1 are still too high to suggest a complete shut-down of thermohaline circulation. The values imply that limited convection occurred during H1, presumably outside the region of maximum meltwater flux.

The high-resolution benthic $\delta^{13}C$ record from the upper Portuguese margin allows to determine the timing of ventilation changes in relation to the 'Heinrich' events in more detail. Initial decreases in benthic $\delta^{13}C$ started about 1.5-2.5 ^{14}C-kyr before H1 and H4 suggesting that the North Atlantic's conveyor circulation started to slow down well before the 'Heinrich' events. Coeval reduction in northward oceanic heat transfer likely conditioned North Atlantic climate to enhanced ice sheet growth that ultimately triggered the H4 event. The early spin-down of thermohaline circulation before H1 correlates with the initiation of large-scale ice sheet collapse in the course of the last glacial-interglacial transition.

The Greenland ice core record and marine records from the northern North Atlantic suggest abrupt warming after the 'Heinrich' events [Bond et al., 1993; Dansgaard et al., 1993; Grootes et al., 1993; Rasmussen et al., 1996 a]. The gradual increases of benthic $\delta^{13}C$ that are documented in core SO75-26KL after H4 and H1 imply that thermohaline circulation resumed its full strength between 1.2 and 3 ^{14}C-kyr after the events, disqualifying abrupt increases in oceanic heat transfer to the northern North Atlantic as a driving force for these climatic jumps. From this it must be concluded that changes in atmospheric circulation must have contributed to the climatic oscillations seen in the Greenland record. Benthic $\delta^{13}C$ changes during H2 are more rapid suggesting a less inert North Atlantic conveyor during this period, either because glacial meltwater flux was less or not continuously targeted at the site of convection because of variable surface circulation.

The rapid fluctuations of benthic $\delta^{13}C$ at the upper Portuguese margin

bear some resemblance to oscillations of benthic $\delta^{18}O$ in northernmost North Atlantic core ENAM93-21 [Rasmussen et al., 1996b] and of carbonate content in deep subtropical North Atlantic KNR31-GPC-5 [Keigwin and Jones, 1994]. Using the GRIP $\delta^{18}O_{ice}$ record of climatic oscillation as a 'template', stadial-interstadial oscillations can also be seen in the Vostok dD_{ice} record, even though resolution of the Vostok record is lower than that of the Greenland record because of different climatic boundary conditions in Antarctica. The apparent coupling between climatic oscillations in the Greenland and Vostok ice cores implies rapid climatic communication between both hemispheres. The existence of similar oscillations in paleoceanographic records at intermediate water and bottom water sites that are influenced by water masses forming in the Southern Ocean and the North Atlantic suggests that surface forcing varied nearly simultaneously on both hemispheres. Varying zonality of low-latitude winds on sub-Milankovitch time scales driven by low-latitude insolation may be an important parameter that paces climatic change at low and high latitudes [McIntyre and Molfino, 1996], and possibly on inter-hemispheric scales.

ACKNOWLEDGEMENTS

The results presented in this thesis have been obtained as part of research projects that have been carried out over a period of five years at GEOMAR. I am grateful to my colleagues at GEOMAR, at the Geologisch-Paläontologisches Institut at Kiel University (GPI-Kiel), and at the Sonderforschungsbereich 313 for their continued support and discussions. I am particularly indebted to Profs. Jörn Thiede and Michael Sarnthein for providing their experiences and long-standing paleoceanographic expertises that helped mastering many difficulties, both logistical and scientific.

I am further indebted to Prof. Pieter Grootes, Dr. Helmut Erlenkeuser and Dr. Marie-Jose Nadeau (Leibniz Labor für Isotopen- und Altersforschung, Kiel University) who carried out stable isotope measurements and ^{14}C-AMS datings, and contributed with many long discussions about the significance and limitation of radiocarbon ages. I am also thankful to Dr. Maurice Arnold (Gif-sur-Yvette) for further ^{14}C-AMS datings, and to Dr. Monika Segl (Bremen

University) and Dr. Michael Joachimski (Erlangen University) who carried out more isotope measurements on short notice, when the mass spectrometers at Kiel University were overburdened.

Prof. Dr. Helmut Beiersdorf and Dr. Hermann-Rudolf Kudrass, both at the Bundesanstalt für Geowissenschaften und Rohstoffe (Hannover) invited me to join R/V SONNE Cruise SO75-3 (1991) to the southern Portuguese margin, and provided the Portuguese sediment cores that were used in this thesis. Drs. Uwe Pflaumann (GPI-Kiel) and Devesh Sinha (Varanasi University, India), and Dipl. Geol. Thorsten Kiefer (GPI-Kiel) carried out the planktonic foraminiferal census counts and provided the SST estimates. Drs. Gerard Bond and Jerry McManus (Lamont Dohery Earth Observatory), Drs. William Curry, Lloyd Keigwin, and Scott Lehman (Woods Hole Oceanographic Institution), Prof. Laurent Labeyrie (Gif-sur-Yvette), Dr. Mark Maslin (University College, London), Dr. Tine Rasmussen (University of Copenhagen), Dr. Dan Seidov (SFB 313, Kiel), and Dr. Niall Slowey (Texas A&M University, College Station) contributed with discussions during various scientific meetings, and provided isotope and sedimentologic data. To all of them I owe my sincere thanks.

Special thanks go to my collaborators at GEOMAR, namely to Dr. Joachim Schönfeld who over the years kept track of many logistic ends that needed close attention, and provided his expert knowledge on the various micropaleontologic aspects of this work. Dr. Simon Jung helped me with preparing figures and the final layout in the late stage of completing this thesis. Arnim Allenstein, Angela Harder, Lester Lembke, Manfred Maass, Anja Müller, Myong-Ho Park and many more student workers contributed with untiring laboratory work and prepared the foraminiferal samples for micropaleontologic and isotope analysis.

I am also thankful to Dipl. Chem. Claudia Willamowski and Arndt Stüber, and Dipl. Geol. Heidi Doose, Rita von Grafenstein, and Matthias Hüls who will help with their ongoing doctoral work to extend this paleoceanographic and paleoclimatologic research into the Mediterranean and Caribbean Seas.

Drs. Ralf Tiedemann and Gerald Haug helped me with enthusiastic and stimulating discussions to brave many unforeseen obstacles that occurred in the course of this work.

Ms. Ortrud Runze and Corinna Hoffmann proof-read the text and helped to eliminate the numerous typos that made their way into the text.

I gratefully acknowledge the financial support of the Deutsche Forschungsgemeinschaft to carry out this work and to participate in national and international meetings. The administrative staff at GEOMAR handled the logistics of the research grants with great professionalism and took care of all the special needs with unshakeable patience, for which I am deeply thankful.

Last but not least, my deep appreciation goes to Michaela, Julia, and Jonas for their interest, humor, and the patience - especially during the late stage of completion - with which they followed the progress of this thesis.

REFERENCES

Abrantes, F., L. Gaspar and J. H. Monteiro, Variations on the Paleoceanography/ Paleoproductivity along the Portuguese coast during the last 30 kyrs, Third Report MAST II: European North Atlantic Margin (ENAM): Sediment pathways, processes and fluxes, Lisboa, Portugal, 1995.

Abrantes, F., Increased upwelling off Portugal during the last glaciation: diatom evidence, *Mar. Micropal, 17*: 285-310, 1991

Abrantes, F., Diatom assemblages as upwelling indicators in surface sediments off Portugal, *Mar. Geol., 85*: 15-39, 1988.

Alley, R.B. and D.R. MacAyeal, Ice-rafted debris associated with binge-purge oscillations of the Laurentide Ice Sheet, *Paleoceanography, 9*, 503-511, 1994.

Alley, R. B., D. A. Meese, C. A. Shuman, A. J. Gow, K. C. Taylor, P. M. Grootes, J. W. C. White, M. Ram, E. D. Waddington, P. A. Mayewski and G. A. Zielinski, Abrupt increase in Greenland snow accumulation at the end of the Younger Dryas event, *Nature, 362*, 527-529, 1993.

Ambar, I., L. Armi, M.O. Baringer, A. Bower, A. Fiúza, G.C. Johnson, R. Käse, M. Kennelly, E. Kunze, R. Lueck, P. Lundberg, C.G. Martins, M.D. Prater, J. Price, M. Rhein, T. Sanford, K. Tokos, J. Verrall, and W. Zenk, Outflows and overflows in the Atlantic and their role in the eastern boundary current

system, *Proceedings Internat. Workshop, Lisbon, October 1-4,*, Grupo de Oceanografia, Departmento de Física, Faculdade de Ciências - Universidade de Lisboa, pp. 46, 1992.

Ambar, I., M. R. Howe and M. I. Abdullah, A physical and chemical description of the Mediterranean Outflow in the Gulf of Cadiz, *Deutsche Hydrographische Zeitschrift, 29*(2), 58-68, 1976.

Andrews, J. T. and K. Tedesco, Detritial carbonate-rich sediments, northwestern Labrador Sea: Implications for ice-sheet dynamics and iceberg rafting (Heinrich) events in the North Atlantic, *Geology, 20*, 1,087-1,090, 1992.

Armi, L. and D. Farmer, The internal hydraulics of the Strait of Gibraltar and associated sills and narrows, *Oceanol. Acta, 8*, 37-46, 1985.

Baas, J. H., J. Schönfeld and R. Zahn, Mid-depth oxygen drawdown during Heinrich Events: evidence from benthic foraminiferal community structure, trace fossil tiering, and benthic $\delta^{13}C$ at the Portuguese Margin, *Marine Geology*, (ENAM special issue), submitted.

Bard, E., B. Hamelin, M. Arnold, L. Montaggioni, G. Cabioch, G. Faure, and F. Rougerie, Deglacial sea-level record from Tahiti corals and the timing of global meltwater discharge, *Nature, 382*, 241-244, 1996.

Bard, E., R. G. Fairbanks, M. Arnold, P. Maurice, J. Duprat, J. Moyes, and J.-C. Duplessy, Sea-level estimates during the last deglaciation based on $\delta^{18}O$ and accelerator mass spectrometry ^{14}C ages measured in *Globigerina bulloides, Quat. Res., 31*, 381-391, 1989.

Bard, E., M. Arnold, P. Maurice, J. Duprat, J. Moyes, and J.-C. Duplessy, Retreat velocity of the North Atlantic polar front during the last deglaciation determined by ^{14}C accelerator mass spectrometry, *Nature, 328*, 791-794, 1987.

Bassinot, F., L. Labeyrie and s. scientific party, IMAGES MD 101 - a coring cruise of the R/V Marion Dufresne in the North Atlantic Ocean and Norwegian Sea (29.05.-11.07.1995), cruise report, *96-1, l'Institut Français pour la Recherche et laTechnologie Polaires*, Plouzané, France, 1996.

Bayliss, P., et al., Mineral powder diffraction file-data book, Park Lane, 1390 pp., 1986.

Bender, M., T. Sowers, M.-L. Dickson, J. Orchardo, P. Grootes, P.A. Mayewski, and D.A. Meese, Climate correlations between Greenland and Antarctica during the past 100,000 years, *Nature, 372*, 663-666, 1994.

Berger, W.H., M.K. Yasuda, T. Bickert, G. Wefer, T. Takayama, Quaternary time scale for the Ontong Java Plateau: Milankovitch template for ODP, *Geology, 22*,, 463-467, 1994.

Béthoux, J.P., Paléo-hydrologie de la Méditerranée au cours derniers 20000 ans, *Oceanol. Acta, 7*, 43-48, 1984.

Béthoux, J. P., Budgets of the Mediterranean Sea. Their dependence on the local

climate and on the characteristics of the Atlantic waters, *Oceanol. Acta*, 2, 157-163, 1979.

Bintanja, R. and J. Oerlemans, The effect of reduced ocean overturning on the climate of the last glacial maximum, *Climate Dynamics, 12*, 523-533, 1996.

Biscaye, P.E., Mineralogy and sedimentation of recent deep-sea clay in the Atlantic Ocean and adjacent seas and oceans, *Bull. Geol. Soc. Amer., 76*, 803-832, 1965.

Bond, G., H. Heinrich, W. Broecker, L. Labeyrie, J. McManus, J. Andrews, S. Huon, R. Jantschik, S. Clasen, C. Simet, K. Tedesco, M. Klas, G. Bonani, and S. Ivy, Evidence for massive discharges of icebergs into the North Atlantic ocean during the last glacial period, *Nature, 360*, 245-249, 1992.

Bond, G., W. Broecker, S. Johnson, J. McManus, L. Labeyrie, J. Jouzel, and G. Bonani, Correlations between climatic records from North Atlantic sediments and Greenland ice, *Nature, 365*, 143-147, 1993.

Bond, G.C. and R. Lotti, Iceberg discharges into the North Atlantic on millennial time scales during the last glaciation, *Science, 267*, 1,005-1,010, 1995.

Boyle, E.A., A comparison of carbon isotopes and cadmium in the modern and glacial maximum ocean: can we account for the discrepancies?, in R. Zahn, T.F. Pedersen, M. Kaminski and L. Labeyrie (eds.), *Carbon Cycling in the Glacial Ocean: Constraints on the Ocean's Role in Global Change, NATO ASI Series I, Vol. 17*, 167-194, 1994.

Boyle, E., Cadmium and $\delta^{13}C$ Paleochemical ocean distributions during the stage 2 Glacial Maximum, *Ann. Rev. Earth Planet. Sci. 20*, 245-287, 1992.

Boyle, E.A., Quaternary deepwater paleoceanography, *Science, 249*, 863-870, 1990.

Boyle, E. A., Cadmium: Chemical tracer of deepwater paleoceanography, *Paleoceanography, 3*(4), 471-489, 1988.

Boyle, E. A. and L. D. Keigwin, North Atlantic thermohaline circulation during the past 20,000 years linked to high-latitude surface temperature, *Nature, 330*, 35-40, 1987.

Boyle, E., Paired carbon isotope and cadmium data from benthic foraminifera: Implication for changes in oceanic phosphorus, oceanic circulation and atmospheric carbon dioxide, *Geochimi. Cosmochimi. Acta, 50*, 265-276, 1986.

Brindley, G.W. and G. Brown (eds.), Crystal Structures of Clay Minerals and Their X-Ray Identification, *Mineral. Soc.*, 495 pp., 1984.

Broecker, W.S., Massive iceberg discharges as triggers for global climate change, *Nature, 372*, 421-424, 1994.

Broecker, W.S. and E. Maier-Reimer, The influence of air and sea exchange on the carbon isotope distribution in the sea, *Global Biogeochem. Cyc., 6*, 315-320, 1992.

Broecker, W.S., G. Bond, M. Klas, E. Clark, J. McManus, Origin of the Northern Atlantic's 'Heinrich' events, *Climate Dyn., 6*, 265-273, 1992.

Broecker, W.S., G. Bond, M. Klas, G. Bonani, and W. Wölfli, A salt oscillator in the glacial Atlantic?, 1, the concept, *Paleoceanography, 5*, 459-477, 1990.

Bryan, F., High-latitude salinity effects and interhemispheric thermohaline circulations, *Nature, 323*, 301-304, 1986.

Bryden, H.L. and H.M. Stommel, , Limiting processes that determine the basic features of the circulation in the Mediterranean Sea, *Oceanol. Acta, 7* (3), 289-296, 1984.

Bryden, H.L. and T.H. Kinder, Recent progress in strait dynamics, *Rev. Geophys., Suppl., (U.S. Nat. Rep. Intern. Union Geodesy Geophys. 1987-1990)*, 617-631, 1991.

Clemens, S.C. and W.L. Prell, Late Quaternary forcing of Indian summer-monsoon winds: a comparison of Fourier model and general circulation model results, *J. Geophys. Res., 96*, 22,683-22,700, 1991.

CLIMAP Project Members, Seasonal reconstruction of the Earth's surface at the last glacial maximum, *Geol. Soc. America, Map and Chart Series, MC-36*, 1981.

Comas, M.C., R. Zahn, A. Klaus et al. Proceedings of the Ocean Drilling Program, Vol. 161, Init. Repts., Mediterranean II, The Western Mediterranean, Ocean Drilling Program, College Station, TX, 1023 Seiten, 1996.

Corliss, B. H. and C. Chen, Morphotype patterns of Norwegian Sea deep-sea benthic foraminifera and ecological implications, *Geology, 16*, 716-719, 1988.

Cortijo, E., La variabilité climatique dans l'Atlantique Nord depuis 128 000 ans: relations entre les calottes de glace et l'océan de surface, *Ph.D. thesis, Université de Paris-Sud U.F.R. Scientifique d'Orsay*, 1995.

Crowley, T.J. North Atlantic Deep Water cools the southern hemisphere, *Paleoceanography, 7*, 489-497, 1992.

Curry, W. B., J.-C. Duplessy, L. D. Labeyrie and N. J. Shackleton, Changes in the distribution of $\delta^{13}C$ of deep water ΣCO_2 between the last glaciations and the Holocene, *Paleoceanography, 3*, 317-342, 1988.

Dansgaard, W., J. J. Johnson, B. H. Clausen, D. Dahl- Jensen, N. S. Gundestrup, C. U. Hammer, C. S. Hvidberg, J. P. Steffensen, A. E. Sveinbjørnsdottir, J. Jouzel, and G. Bond, Evidence for general instability of past climate from a 250- kyr ice- core record, *Nature, 364*, 218-220, 1993.

Dansgaard, W., J.W.C. White and S.J. Johnsen, The abrupt termination of the Younger Dryas climate event, *Nature, 339*, 532-534, 1989.

de Menocal, P.B. and D. Rind, Sensitivity of Asian and African climate to variations in seasonal insolation, glacial ice cover, sea surface temperature, and

Asian orography, *J. Geophys. Res., 98*, 7,265-7,287, 1993.

de Menocal, P.B., D.W. Oppo, R.G. Fairbanks, and W.L. Prell, Pleistocene $\delta^{13}C$ variability of North Atlantic Intermediate Water, *Paleoceanography, 7*, 229-250, 1992.

Diester-Haass, L., No current reversal at 10,000 B.P. in the Strait of Gibraltar, *Mar. Geol., 15*, M1-M9, 1973.

Dowdeswell, J.A., M.A. Maslin, J.T. Andrews, and I.N. McCave, Iceberg production, debris rafting, and the extent and thickness of 'Heinrich' layers (H-1, H-2) in North Atlantic sediments, *Geology, 23*, 301-304, 1995.

Duplessy, J.-C., E. Bard, L. Labeyrie, J. Duprat, and J. Moyes, Oxygen isotope records and salinity changes in the northeastern Atlantic ocean during the last 18,000 years, *Paleoceanography, 8*, 341-350, 1993.

Duplessy, J.-C., L. Labeyrie, M. Arnold, M. Paterne, J. Duprat, and T.C.E. van Weering, Changes in surface salinity of the North Atlantic Ocean during the last deglaciation, *Nature, 358*, 485-487, 1992.

Duplessy, J.-C., L. Labeyrie, A. Juillet-Leclerc, F. Maitre, J. Duprat, and M. Sarnthein, Surface salinity reconstruction of the North Atlantic Ocean during the last glacial maximum, *Oceanol. Acta*, 14, 311-324, 1991.

Duplessy, J.-C. and M. Arnold, Radiocarbon dating by accelerator mass spectrometry, in *Nuclear methods of dating*, edited by E. Roth and B. Poty, CEA Paris, 437-453, 1989.

Duplessy, J.-C., N. J. Shackleton, R. Fairbanks, L. Labeyrie, D. Oppo and N. Kallel, Deep water source variations during the last climatic cycle and their impact on the global deepwater circulation, *Paleoceanography, 3*, 343-360, 1988.

Duplessy, J.-C., M. Arnold, P. Maurice, E. Bard, J. Duprat, and J. Moyes, Direct dating of the oxygen-isotope record of the last deglaciation by ^{14}C accelerator mass spectrometry, *Nature, 320*, 350-352, 1986.

Duprat, J., Les foraminiferes planctoniques du quaternaire terminal d'un domaine péricontinental (Golfe de Gascogne, cotes ouest-Ibériques, Mer d'Alboran): écologie - biostratigraphie, *Bull. Inst. Géol. Basin d'Aquitaine, 33*, 71-150, 1983.

Elderfield, H. and E. Thomas, Glacial-Interglacial paleoenvironments of the eastern Atlantic Ocean: The Biogeochemical Flux Study (BOFS) paleoceanography program, *Paleoceanography, 10*(3), 509-511, 1995.

Fairbanks, R. G., A 17,000-year glacio-eustatic sea level record: influence of glacial melting rates on the Younger Dryas event and deep-ocean circulation, *Nature, 342*, 637-642, 1989.

Faugéres, J.C., E. Gonthier and D.A.V. Stow, Contourites drift molded by deep Mediterranean outflow, *Geology, 12*, 296-300, 1984.

Fichefet, T., S. Hovine and J.-C. Duplessy, A model study of the Atlantic thermohaline circulation during the last glacial maximum, *Nature, 372,* 252-255, 1994.

Fiúza, A. F., M. E. Macedo and M. R. Guerreiro, Climatological space and time variation of the Portuguese coastal upwelling, *Oceanol. Acta, 5*(1), 31-40, 1982.

Fiúza, A. F. G., Upwelling patterns off Portugal, NATO conference series, *Coastal Upwelling: Its sedimentary record. Part A: Responses of the Sedimentary Regime to Present Coastal Upwelling, IV: 10a,* E. Suess and J. Thiede (eds.), *Plenum Press* , 85-98, 1981.

Francois, R., and M. Bacon, 'Heinrich' events in the North Atlantic: radiochemical evidence, *Deep-Sea Res., 41,* 315-334, 1994.

Fronval, T. and E. Jansen, Rapid changes in ocean circulation and heat flux in the Nordic Seas during the last interglacial period, *Nature, 383,* 806-810, 1996.

Fronval, T., E. Jansen, J. Bloemendal, and S. Johnsen, Oceanic evidence for coherent fluctuations in Fennoscandian and Laurentide ice sheets on millennium time scales, *Nature, 374,* 443-446, 1995.

Gasse, F. and E. van Campo, Abrupt post-glacial climate events in West Asia and North Africa monsoon domains, *Earth Planet. Sci. Lett., 126,* 435-456, 1994.

Gasse, F., R. Téhet, A. Durant, E. Gilbert, and J.-C. Fontes, The arid-humid transition in the Sahara and the Sahel during the last deglaciation, *Nature, 346,* 141-146, 1990.

Grootes, P.M., M. Stuiver, J.W.C. White, S. Johnsen, and J. Jouzel, Comparison of oxygen isotope records from the GISP2 and GRIP Greenland ice cores, *Nature, 366,* 552-554, 1993.

Grousset, F.E., L. Labeyrie, J.A. Sinko, M. Cremer, G. Bond, J. Duprat, E. Cortijo, and S. Huon, Patterns of ice-rafted detritus in the glacial North Atlantic (40-55°N), *Paleoceanography, 8,* 175-192, 1993.

Grousset, F.E., J.L. Joron, P.E. Biscaye, C. Latouche, M. Treuil, N. Maillet, J.C. Faugéres, and E. Gonthier, Mediterranean outflow through the Strait of Gibraltar since 18,000 years B.P.: Mineralogical and geochemical arguments. *Geomarine Lett., 8,* 25-34, 1988.

Gwiadza, R.H., S.R. Hemming, and W.S. Broecker, Provenance of icebergs during 'Heinrich' event 3 and the contrast to their sources during other Heinrich episodes, *Paleoceanography, 11,* 371-378, 1996.

Hammer, C. U., H. B. Clausen and H. Tauber, Ice-core dating of the Pleistocene/Holocene boundary applied to a calibration of the ^{14}C time scale, *Radiocarbon, 28*(2A), 284-291, 1986.

Harvey, J. G. and A. Theodorou, The circulation of Norwegian Sea overflow water in the eastern North Atlantic, *Oceanol. Acta, 9,* 393-402, 1986.

Haynes, R. and E. D. Barton, A poleward flow along the Atlantic coast of the Iberian Peninsula, *J. Geophysi. Res., 95*(C7), 11,425-11,441, 1990.

Hebbeln, D., T. Dokken, E.S. Andersen, M. Hald, and A. Elverhøi, Moisture supply for northern ice-sheet growth during the last glacial maximum, *Nature, 370*, 357-360, 1994.

Heinrich, H., Origin and consequences of cyclic ice rafting in the Northeast Atlantic Ocean during the past 130,000 years, *Quat. Res., 29*, 143-152, 1988.

Hilgen, F.J., Astronomical calibration of Gauss to Matuyama sapropels in the Mediterranean and implication for the geomagnetic polarity time scale, *Earth Planet. Sci. Lett., 104*, 226-244, 1991.

Hopkins, T.S., The GIN Sea - a synthesis of its physical oceanography and literature review 1972-1985, *Earth-Sci. Rev., 30*, 175-318, 1991.

Howe, M. R., The Mediterranean water outflow in the Gulf of Cadiz, *Oceanogr. Mar. Biol. Ann. Rev., 20*, 37-64, 1982.

Huang, T.-C. and D.J. Stanley, Current reversal at 10,000 years B.P. at the Strait of Gibraltar - a discussion, *Mar. Geol., 17*, 1-7, 1974.

Hurrel, J. W., Decadal trends in the North Atlantic Oscillation: regional temperatures and precipitation, *Science, 269*, 676-679, 1995.

Hut, G., Stable isotope reference samples for geochemical and hydrological investigations, Consultants Group Meeting IAEA, Vienna 16-18 Sept. 1985, Report to the Director General, Intern. Atomic Energy Agency, Vienna, 42 pp., 1987.

Imbrie, J., E.A. Boyle, S.C. Clemens, A. Duffy, W.R. Howard, G. Kukla, J. Kutzbach, D.G. Martinson, A. McIntyre, A.C. Mix, B. Molfino, J.J. Morley, L.C. Peterson, N.G. Pisias, W.L. Prell, M.E. Raymo, N.J. Shackleton, and J.R. Toggweiler, On the structure and origin of major glaciation cycles, 1, Linear responses to Milankovitch forcing, *Paleoceanography, 7*, 701-738, 1992.

Imbrie, J., J.D. Hays, D.G. Martinson, A. McIntyre, A.C. Mix, J.J. Morley, N.G. Pisias, W.L. Prell, and N.J. Shackleton, The orbital theory of Pleistocene climate: support from a revised chronology of the marine $\delta^{18}O$ record, in *Milankovitch and Climate*, edited by A.L. Berger et al., pp. 269-305, 1984.

Jasper, J.P. and J.M. Hayes, Reconstruction of paleoceanic PCO_2 levels from carbon isotopic compositions of sedimentary biogenic components, in R. Zahn, T.F. Pedersen, M. Kaminski, and L. Labeyrie (eds.), *Carbon Cycling in the Glacial Ocean: Constraints on the Ocean's Role in Global Change, NATO ASI Series I, Vol. 17*, 323-341, 1994.

Johnsen, S.J., H.B. Clausen, W. Dansgaard, N.S. Gundestrup, M. Hansson, P. Jonsson, J.P. Steffensen, and A.E. Sveinbjørnsdottir, A "deep" ice core from East Greenland, *Geosci., 29*, 3-22, 1992.

Jouzel, J., L. Waelbroeck, B. Maloize, M. Bender, J. R. Petit, M. Stievenard, N. I.

Barkov, J. M. Barnola, T. King, V. M. Kotlyakov, V. Lipenkov, C. Lorius, D. Raynaud, C. Ritz, and T. Sowers, Climatic interpretation of the recently extended Vostok ice records, *Climate Dyn., 12*, 513-521, 1996.

Jouzel, J., C. Lorius, J.R. Petit, C. Genthon, N.I. Barkov, V.M. Kotlyakov, and V.M. Petrov, Vostok ice core: a continuous isotope temperature record over the last climatic cycle (160,000 years), *Nature, 329*, 403-407, 1987.

Jung, S. J. A., Wassermassenaustausch zwischen dem NE-Atlantik und dem Europäischen Nordmeer während der letzten 300 000/80 000 Jahre im Abbild stabiler O- und C-Isotope, PhD thesis, Kiel University, *Repts. Spec. Res. Progr. 313, "Environmental Variability: northern North Atlantic"*, 104 p., 1996.

Kaiser, K.F., Klimageschichte vom späten Hochglazial bis ins frühe Holozän rekonstruiert mit Jahresringen und Molluskenschalen aus verschiedenen Vereisungsgebieten, Beitragsserie, Eidgen. Forsch.-anst. f. Wald, Schnee u. Landsch., 203 p., 1993 (ISBN-Nr 3 85543 232 5)

Keigwin, L. D. and G. A. Jones, Western North Atlantic evidence for millennial-scale changes in ocean circulation and climate, *J. Geophysi. Res., 99*(C6), 12,397-12,410, 1994.

Keigwin, L.D. and S.J. Lehman, Deep circulation changes linked to 'Heinrich' event 1 and Younger Dryas in a mid depth North Atlantic core, *Paleoceanography, 9*, 185-194, 1994.

Keigwin, L.D., G.A. Jones, and S.J. Lehman, Deglacial meltwater discharge, North Atlantic deep circulation, and abrupt climate change, *J. Geophys. Res., 96*, 16,811-16,826, 1991.

Kroopnick, P.M., The distribution of ^{13}C of ΣCO_2 in the world oceans, *Deep-Sea Res., 32*, 57-84, 1985.

Kudrass, H.R., Sedimentation am Kontinentalhang vor Portugal und Marokko im Spätpleistozän und Holozän, *Meteor Forsch. Ergeb., Reihe C, No.13*, 1-63, 1973.

Kudrass, H.R. and J. Thiede, Stratigraphische Untersuchungen an Sedimentkernen des ibero-marokkanischen Kontinentalrandes, *Geol. Rundsch., 60*, 294-391, 1970.

Kullenberg, B., On the salinity of the water contained in marine sediments, *Göteborgs Kungl. Vetens. Vitter. Handl., Ser. B., 6*, 3-37, 1952.

Küttel, M., Züge der jungpleistozänen Vegetations- und Landschaftsgeschicht der Zentralschweiz, *Rev. Paléobiol., 8*, 525-614, 1989.

Labeyrie, L., M. Labracherie, N. Gorfti, J. J. Pichon, M. Vautravers, M. Arnold, J.-C. Duplessy, M. Paterne, E. Michel, J. Duprat, M. Caralp and J.-L. Turon, Hydrographic changes of the Southern Ocean (southeast Indian sector) over the last 230 kyr, *Paleoceanography, 11*(1), 57-76, 1996.

Labeyrie, L. D., J.-C. Duplessy, J. Duprat, A. Juillet-Leclerc, J. Moyes, E. Michel, N.

Kallel and N. J. Shackleton, Changes in the vertical structure of the North Atlantic Ocean between glacial and modern times, *Quat. Sci. Rev., 11*, 401-414, 1992.

Labeyrie, L. D., J. C. Duplessy and P. L. Blanc, Variations in mode of formation and temperature of oceanic deep waters over the past 125,000 years, *Nature, 327*, 477-482, 1987.

Lautenschlager, M., Simulation of the ice age atmosphere-January and July means, *Geol. Rundsch., 80*(3), 513-534, 1991.

Lautenschlager, M. and K. Herterich, Atmospheric response to Ice Age conditions: climatology near the Earth's surface, *J. Geophys. Res., 95*, 22,547-22,557, 1990.

Leaman, K.D., The formation of Western Mediterranean deep water. In Seasonal and interannual variability of the western Mediterranean Sea, *Coast. Est. Stud., 46*, American Geophysical Union, 227-248, 1995.

Laj, C., A. Mazaud, and J.-C. Duplessy, Geomagnetic intensity and ^{14}C abundance in the atmosphere and ocean during the past 50 kyr, *Geophys. Res. Lett., 23*, 2,045-2,048, 1996.

Lebreiro, S.M., J.C. Moreno, I.N. McCave and P.P.E. Weaver, Evidence for 'Heinrich' layers off Portugal (Torre Seamount: 39°N, 12°W), *Mar. Geol., 131*, 47-56, 1996.

Lehman, S.J. and L.D. Keigwin, Sudden changes in North Atlantic circulation during the last deglaciation, *Nature, 356*, 757-762, 1992.

Lorius, C., J. Jouzel, C. Ritz, L. Merlivat, N. I. Barkov, Y. S. Korotkevitch and V. M. Kotlyakov, A 150 000-year climatic record from Antarctic ice, *Nature, 316*, 591-596, 1985.

Lourens, L.J., Astronomical forcing of mediterranean climate during the last 5.3 million years, Thesis University Utrecht, ISBN 90-393-0754-7, 1994

Lowe, J.J., Late glacial and early Holocene lake sediments from the northern Apennines, Italy - pollen stratigraphy and radiocarbon dating, *Boreas, 21*, 193-208, 1992.

Lynch-Stieglitz, J. and R. G. Fairbanks, A conservative tracer for glacial ocean circulation from carbon isotope and palaeo-nutrient measurements in benthic foraminifera, *Nature, 369*, 308-310, 1994.

MacAyeal, D.R., Binge/purge oscillations of the Laurentide ice sheet as a cause of the North Atlantic's 'Heinrich' events, *Paleoceanography, 8*, 775-784, 1993.

Macdonald, A. M. and C. Wunsch, An estimate of global ocean circulation and heat fluxes, *Nature, 6590*, 436-439, 1996.

Madelain, F., Influence de la topographie du fond sur l'écoulement Méditerranéen entre le Détroit de Gibraltar et le Cap Saint-Vincent, *Cahiers Océanographiques, 22*, 43-61, 1970.

Manabe, S. and R.J. Stouffer, Simulation of abrupt climatic change induced by freshwater input to the North Atlantic Ocean, *Nature, 378*, 165-167, 1995.

Manabe, S. and R. J. Stouffer, Two stable equilibra of a coupled ocean- atmosphere model, *J. Climate, 1*, 841-868, 1988.

Mangerud, J., S. T. Anderson, B. E. Berglund and J. J. Donner, Quaternary stratigraphy of Norden, a proposal for terminology and classification, *Boreas, 3*, 109-128, 1974.

Manighetti, B., I. N. McCave, M. Maslin and N. J. Shackleton, Chronology for climate change: Developing age models for the Biogeochemical Ocean Flux Study cores, *Paleoceanography, 10* (3), 513-525, 1995.

Martinson, D.G., N.G. Pisias, J.D. Hays, J. Imbrie, T.C. More, Jr., and N.J. Shackleton, Age dating and the orbital theory of the ice ages: development of a high-resolution 0 to 300,000-year chronostratigraphy, *Quat. Res., 27*, 1-29, 1987.

Maslin, M.A., Changes in North Atlantic deep-water formation associated with the 'Heinrich' events, *Naturwissenschaften, 82*, 330-333, 1995.

Maslin, M., N. J. Shackleton and U. Pflaumann, Surface water temperature, salinity and density changes in the NE- Atlantic during the last 45.000 years: Heinrich events, deep water formation and climatic rebounds, *Paleoceanography, 10*(3), 527-544, 1995.

McCartney, M. S., Recirculating components to the deep boundary current of the northern North Atlantic, *Progr. Oceanogr., 29*, 283-383, 1992.

McCorkle, D.C., L.D. Keigwin, B.H. Corliss, and S.R. Emerson, The influence of microhabitats on the carbon isotopic composition of deep sea benthic foraminifera, *Paleoceanography, 5*, 161-185, 1990.

McIntyre, A. and B. Molfino, Forcing of Atlantic equatorial and subpolar millennial cycles by precession, *Science, 274*, 1867-1870, 1996.

McManus, J.F., G.C. Bond, W.S. Broecker, S. Johnsen, L. Labeyrie, and S. Higgins, High-resolution climate records from the North Atlantic during the last interglacial, *Nature, 371*, 326-329, 1994.

MEDOC Group, Observation of formation of deep water in the Mediterranean Sea. *Nature, 227*, 1,037-1,040, 1970

Mikolajewicz, U. and E. Maier-Reimer, Mixed boundary conditions in ocean general circulation models and their influence on the stability of the model`s conveyor belt, *J. Geophys. Res., 99*, 633-644, 1994.

Mikolajewicz, U., B. Santer, and E. Maier-Reimer, Ocean response to greenhouse warming, *Nature, 345*, 589-593, 1990.

Milankovitch, M. N., Canon of insolation and the ice-age problem. *Königlich Serbische Akademie, Belgrad* (English translation by the Israel Program for Scientific Translation). U.S. Dept. of Commerce and Nat. Sci. Fnd.,

Washington, D.C., 1941.

Mix, A.C., N.G. Pisias, R. Zahn, W. Rugh, C. Lopez and K. Nelson, Carbon 13 in Pacific deep intermediate waters 0-370 ka: implications for ocean circulation and Pleistocene CO_2, *Paleoceanography, 6*, 205-226, 1991.

Mix, A.C., The oxygen isotope record of glaciation, in *North America and Adjacent Oceans During the Last Deglaciation*, The Geology of North America, Vol. K-3, edited by W. F. Ruddiman and H. E. Wright, 111-135, *Geol. Soc. America*, 1987.

Mix, A.C. and W.F. Ruddiman, Structure and timing of the last deglaciation: Oxygen isotope evidence, *Quat. Sci. Rev., 4*, 59-108, 1985.

Mix, A. C. and R. G. Fairbanks, North Atlantic surface-ocean control of Pleistocene deep-ocean circulation, *Earth Planet. Sci. Lett., 73*, 231-243, 1985.

Molina-Cruz, A. and J. Thiede, The glacial eastern boundary current along the Atlantic Eurafrican continental margin, *Deep Sea Res., 25*, 337-356, 1978.

Mommersteg, H.J.P.M., M.F. Loutre, R. Young, T.A. Wijmstra and H. Hooghiemstra, Orbital forced frequencies in the 975000 year pollen record from Tenagi Phillippon (Greece), *Clim. Dyn., 11*, 4-24, 1995.

Mook, W.G., J.C. Bommerson, and W.H. Staberman, Carbon isotope fractionation between dissolved bicarbonate and gaseous carbon dioxide, *Earth Planet. Sci. Lett., 22*, 169-176, 1974.

Olausson, E., Studies of deep-sea cores, *Rep. Swedish Deep-Sea Expedition, 8 (6)*, 337-391, 1961.

Oppo, D. W. and R. G. Fairbanks, Variability in the deep and intermediate water circulation of the Atlantic Ocean during the past 25,000 years: Northern hemisphere modulation of the southern ocean, *Earth Planet. Sci. Lett., 86*, 1-15, 1987.

Oppo, D. W. and R. G. Fairbanks, Atlantic Ocean circulation of the last 150.000 years: relationship to climate and atmospheric CO_2, *Paleoceanography, 5* (3), 277-288, 1990.

Oppo, D. W. and S.J. Lehman, Mid-depth circulation of the subpolar North Atlantic during the last glacial maximum, *Science, 259*, 1,148-1,152, 1993.

Oppo, D. W. and S.J. Lehman, Suborbital time scale variability of North Atlantic Deep Water during the past 200,000 years, *Paleoceanography, 10* (5), 901-910, 1995.

Östlund, H. G., C. Craig, W. S. Broecker and D. Spencer, GEOSECS Atlantic, Pacific and Indian Ocean Expeditions. Shorebased Data and Graphics, *GEOSECS Atlas Series*, U.S. Government Printing Office, Washington D. C., 200 pp, 1987.

Paillard, D., L. Labeyrie and P. Yiou, Macintosh program performs time-series analysis, *Eos Trans. AGU, 77*, 379, 1996.

Paillard, D. and L. Labeyrie, Role of the thermohaline circulation in the abrupt warming after 'Heinrich' events, *Nature, 372*, 162-164, 1994.

Park, M.-H., Late Quaternary IRD-events in the eastern North Atlantic: mineralogy and foraminiferal stable isotopes from the open North Atlantic and the Portuguese Margin, Diplom Thesis, University of Kiel, 122 pp, 1994.

Pflaumann, U., J. Duprat, C. Pujol, and L.D. Labeyrie, SIMMAX, a modern analog technique to deduce Atlantic sea surface temperatures from planktonic foraminifera in deep-sea sediments, *Paleoceanography, 11*, 15-35, 1996.

Prell, W.L. and J.E. Kutzbach, Sensitivity of the Indian monsoon to forcing parameters and implications for its evolution, *Nature, 360*, 647-652, 1992.

Rahmstorf, S., On the freshwater forcing and transport of the Atlantic thermohaline circulation, *Climate Dynamics, 12*, 799-811, 1996.

Rahmstorf, S., Rapid climate transitions in a coupled ocean-atmosphere model, *Nature, 372*, 82-85, 1994.

Rahmstorf, S., Bifurcations of the Atlantic thermohaline circulation in response to changes in the hydrological cycle, *Nature, 378*, 145-149, 1995.

Rasmussen, T. L., E. Thomsen, L. Labeyrie and T. C. E. van Weering, Circulation changes in the Faeroe-Shetland channel correlating with cold events during the last glacial period (58-10 ka), *Geology, 24* (10), 937-840, 1996a.

Rasmussen, T. L., E. Thomsen, T. C. E. v. Weering and L. Labeyrie, Rapid changes in surface and deepwater-conditions at the Faeroe Margin during the last 58,000 years, *Paleoceanography, 11* (6), 757-771, 1996b.

Rau, G.H., Variations in sedimentary organic $\delta^{13}C$ as a proxy for past changes in ocean and atmospheric CO_2 concentrations, in R. Zahn, T.F. Pedersen, M. Kaminski and L. Labeyrie (eds.), *Carbon Cycling in the Glacial Ocean: Constraints on the Ocean's Role in Global Change, NATO ASI Series I, 17*, 307-321, 1994.

Revel, M., J.A. Sinko, F.E. Grousset, and P.E. Biscaye, Sr and Nd isotopes as tracers of North Atlantic lithic particles: paleoclimatic implication, *Paleoceanography, 11*, 95-113, 1996.

Rohling, E.J., Glacial conditions in the Red Sea, *Paleoceanography, 9*, 653-660. 1994.

Rohling, E.J. and F.J. Hilgen, The eastern Mediterranean climate at times of sapropel formation: a review, *Geol. Mijnbouw, 70*, 253-264, 1991.

Rossignol-Strick, M., African monsoons, an immediate climate response to orbital insolation, *Nature, 304*, 46-49, 1983.

Rossignol-Strick, M., Mediterranean Quaternary sapropels, an immediate response of the African Monsoon to variation of insolation, *Palaeogeogr., Palaeoclimatol., Palaeoecol., 49*, 237-263, 1985.

Ruddiman, W.F. and A. McIntyre, An evaluation of ocean-climate theories on the North Atlantic, in *Milankovitch and Climate*, edited by A.L. Berger et al., *NATO Advanced Study Institute Series, Vol. 126, Part 2*, Reidel Publ. Comp., Dordrecht, 671-686, 1984.

Ruddiman, W.F., Late Quaternary deposition of ice-rafted sand in the subpolar North Atlantic (last 40 to 65 kyr), *Bull. Geol. Soc. Amer., 88*, 1,813-1,827, 1977.

Sarnthein, M. and A.V. Altenbach, Late Quaternary changes in surface water and deep water masses of the Nordic Seas and northern North Atlantic: a review, *Geol. Rundsch., 84*, 89-107, 1995.

Sarnthein, M., E. Jansen, M. Weinelt, M. Arnold, J. C. Duplessy, H. Erlenkeuser, M. Maslin, T. Johannessen, N. Koç, A. Flatøy, G. Johannessen, S. Jung, U. Pflaumann and H. Schulz, Variations in Atlantic surface ocean paleoceanography, 50° - 85° N: A time-slice record of the last 55,000 years, *Paleoceanography*, 10 (6), 1,063-1,094, 1995.

Sarnthein, M., E. Jansen, M. Arnold, J.-C. Duplessy, H. Erlenkeuser, A. Flatøy, T. Veum, E. Vogelsang, and M.S. Weinelt, $\delta^{18}O$ time-slice reconstruction of meltwater anomalies at Termination I in the North Atlantic between 50° and 80°N, in *The Last Deglaciation: Absolute and Radiocarbon Chronologies*, edited by E. Bard and W.S. Broecker, *NATO ASI Ser., 12*, 184-200, 1992.

Sarnthein, M., K. Winn, S. J. A. Jung, J.-C. Duplessy, L. Labeyrie, H. Erlenkeuser, and G. Ganssen, Changes in east Atlantic deepwater circulation over the last 30,000 years: Eight time slice reconstructions, *Paleoceanography, 9* (2), 209-267, 1994.

Sarnthein, M. and R. Tiedemann, Younger Dryas-style cooling events at glacial Terminations I-VI at ODP Site 658: associated benthic $\delta^{13}C$ anomalies constrain meltwater hypothesis, *Paleoceanography, 5*, 1,041-1,055, 1990.

Sarnthein, M., K. Winn and R. Zahn, Paleoproductivity of oceanic upwelling and the effect on atmospheric CO_2 and climatic change during deglaciation times, in *Abrupt Climatic Change*, edited by W.H. Berger and L.D. Labeyrie, *NATO ASI Series, Vol. 216*, Reidel Publ. Comp., Dordrecht, 311-337, 1987.

Sarnthein, M., J. Thiede, U. Pflaumann, H. Erlenkeuser, D. Fütterer, B. Koopmann, H. Lange, and E. Seibold, Atmospheric and oceanic circulation patterns off NW-Africa during the past 25 million years, *in* U. Rad, K. Hinz, M. Sarnthein, and E. Seibold, eds., Geology of the Northwest African Continental Margin, New York, Springer Verlag, p. pp.545-604, 1982.

Sarnthein, M., Sand deserts during glacial maximum and climatic optimum, *Nature, 271*, 43-46, 1978.

Schmitz Jr., W. J. J. and M. S. McCartney, On the North Atlantic Circulation, *Rev. Geophys., 31* (1), 29-49, 1993.

Schrag, D.P., G. Hampt, and D.W. Murray, Pore fluid constraints on the tempe-

rature and oxygen isotopic composition of the glacial ocean, *Science, 272,* 1930-1932, 1996.

Schott, F. and K.D. Leaman, Observations with moored acoustic Doppler current profilers in the convection regime in the Gulf of Lions. *J. Phys. Oceanogr., 21,* 558-574, 1991.

Seidov, D. and M. Maslin, Seasonally ice free glacial Nordic seas without deep water ventilation, *Terra Nova, 8,* 245-254, 1996.

Seidov, D., M. Sarnthein, K. Stattegger, R. Prien and M. Weinelt, North Atlantic Ocean circulation during the last glacial maximum and subsequent meltwater event: A numerical model, *J. Geophys. Res., 101*(C7), 16,305-16,332, 1996.

Shackleton, N.J., Attainment of isotopic equilibrium between ocean water and the benthonic foraminifera genus *Uvigerina*; Isotopic changes in the ocean during the last glacial, *Colloques Int. Centr. Nat. Rech. Sci., 219,* 203-219, 1974.

Shemesh, A., L. H. Burckle and J. D. Hays, Meltwater input to the Southern Ocean during the last glacial maximum, *Science, 266,* 1,542-1,544, 1994.

Slowey, N.C. and W.B. Curry, Glacial-interglacial differences in circulation and carbon cycling within the upper western North Atlantic, *Paleoceanography, 10,* 715-732, 1995.

Sonnenfeld, P., No current reversal at 10,000 yrs B.P. In the Strait of Gibraltar: a discussion. *Mar. Geol., 17,* 339-340, 1974

Sowers, T. and e. al., A 135,000 year Vostok-SPECMAP common temporal framework, *Paleoceanography, 8,* 737-766, 1993.

Spielhagen, R. and H. Erlenkeuser, Stable oxygen and carbon isotopes in planktic foraminifers from Arctic Ocean surface sediments: reflection of the low salinity surface layer, *Mar. Geol., 119,* 227-350, 1994.

Stocker, T. F. and D. G. Wright, A zonally averaged ocean for the thermohaline circulation, II, Interocean circulation in the Pacific-Atlantic Basin system, *J. Phys. Oceanogr., 21,* 1,725-2,739, 1991.

Stommel, H., Thermohaline convection with two stable regimes of flow, *Tellus, 13* , 224-230, 1961.

Stow, D.A.V., J.-C. Faugéres and E. Gonthier, Facies distribution and textural variation in Faro Drift contourites: velocity fluctuation and drift growth, *Mar. Geol., 72,* 71-100, 1986.

Talley, L. D. and M. S. McCartney, Distribution and circulation of Labrador Sea Water, *J. Phys. Oceanogr., 12,* 1,189-1,205, 1982.

Taylor, K. C., C. U. Hammer, R. B. Alley, H. B. Clausen, D. Dahl-Jensen, A. J. Gow, N. S. Gundestrup, J. Kipfstuhl, J. C. Moore and E. D. Waddington, Electrical conductivity measurements from GISP 2 and GRIP Greenland ice cores, *Nature, 366,* 549-552, 1993.

Thiede, J., A glacial Mediterranean, *Nature, 276*, 680-683, 1978.

Thiede, J., Aspects of the variability of the glacial and interglacial North Atlantic eastern boundary current (last 150,000 years), *METEOR Forschungsergebnisse, C*(28), 1-36, 1977.

Thomson, J., N.C. Higgs, and T. Clayton, A geochemical criterion for the recognition of 'Heinrich' events and estimation of their depositional fluxes by the $^{230}Th_{excess}$ profiling method, *Earth Planet. Sci. Lett., 135*, 41-56, 1995.

Thunell, R. C. and D. F. Williams, Glacial-Holocene salinity changes in the Mediterranean Sea: hydrographic and depositional effects, *Nature, 338*, 493-496, 1989.

Thunell, R. C., D. F. Williams and M. Howell, Atlantic-Mediterranean water exchange during the late Neogene, *Paleoceanography, 2*, , 661-678, 1987.

Thunell, R. C., Eastern Mediterranean Sea during the last glacial maximum; an 18,000-years B.P. reconstruction, *Quat. Res., 11*, 353-372, 1979.

Transient Tracers in the Ocean, North Atlantic Study, Shipboard Physical and Chemical Data Report, Physical and Chemical Oceanographic Data Facility, Scripps Institution of Oceanography, University of California, San Diego, 1986.

Trauth, M.H., Bioturbational signal distortion of high-resolution paleoceanographic time-series, PhD thesis (in German), Kiel University, *Repts. Geol.-Paläont. Inst. Univ. Kiel, 74*, 167 pp, 1995.

Vergnaud-Grazzini, C., M. Caralp, J.-C. Faugéres, É. Gonthier, F. Grousset, C. Pujol and J.F. Saliège, Mediterranean outflow through the Strait of Gibraltar since 18000 years BP, *Oceanol. Acta*, 12, 305-324, 1989.

Vergnaud-Grazzini, C., M. Devaux, and J. Znaidi, Stable isotope "anomalies" in Mediterranean Pleistocene records, *Mar. Micropal,. 10*, 35-69, 1986.

Veum, T., E. Jansen, M. Arnold, I. Beyer, and J.-C. Duplessy, Water mass exchange between the North Atlantic and the Norwegian Sea during the past 28,000 years, *Nature, 356*, 783-785, 1992.

Visbeck, M., J. Fischer and F. Schott, Preconditioning the Greenland Sea for deep convection: Ice formation and ice drift, *J. Geophys. Res., 100*(C9), 18,489-18,502, 1995.

Vogelsang, E., Paläo-Ozeanographie des Europäischen Nordmeeres an Hand stabiler Kohlenstoff- und Sauerstoffisotope, Ph.D. thesis, *Repts. SFB 313, 23*, Kiel University, Germany, 136 p., 1990.

Völker, A., M. Sarnthein, and H. Erlenkeuser, 1995, Evolution of the water exchange across the Denmark Strait - a stable isotope record off northern Iceland: ICP-V abstract.

Waelbroeck, A. J., J. Jouzel, L. Labeyrie, C. Lorius, M. Labracherie, M. Stiévenard, N.I. Barkov, A comparison of the Vostok ice deuterium record

and series from Southern Ocean core MD 88-770 over the last two glacial-interglacial cycles, *Climate Dyn., 12*, 113-123, 1995.

WAISCORES (West Antarctic Ice Sheet Cores Program), National Science Foundation, Washington, 1996.

Wang, H. and G.E. Birchfield, Atmospheric water vapor flux, bifurcation of the thermohaline circulation, and climate change, *Climate Dynamics, 8*, 49-53, 1992.

Wang, L., M. Sarnthein, J.-C. Duplessy, H. Erlenkeuser, S. Jung, and U. Pflaumann, Paleo-surface salinities in the low-latitude Atlantic: The $\delta^{18}O$ record of *Globigerinoides ruber* (white), *Paleoceanography, 10*(4), 749-762, 1995.

Weaver, A.J., and T.M.C. Hughes, Rapid interglacial climate fluctuations driven by North Atlantic ocean circulation, *Nature, 367*, 447-450, 1994.

Weaver, A. J., J. Marotzke, P. F. Cummins and E. S. Sarachik, Stability and variability of the thermohaline circulation, *J. Phys. Oceanogr., 23*, 39-60, 1993.

Weinelt, M., Veränderungen der Oberflächenzirkulation im Europäischen Nordmeer während der letzten 60.000 Jahre - Hinweise aus stabilen Isotopen, *PhD thesis, University of Kiel*, 106 p., 1993.

Weinelt, M. S., M. Sarnthein, H. Schulz and S. Jung, Ice-free Nordic Seas during the Last Glacial Maximum? - Potential sites of deepwater formation., *Paleoclimates, 1*, 283-309, 1996.

Weiss, R. F., The solubility of nitrogen, oxygen and argon in water and seawater, *Deep Sea Research, 17*, 721-735, 1970.

Winn, K., M. Sarnthein and H. Erlenkeuser, $\delta^{18}O$ stratigraphy and age control of Kiel sediment cores in the East Atlantic, *Repts. Geol. Paläont. Inst. , 45*, University of Kiel, Kiel, 1991.

Woillard, G.M., Grande Pile peat bog: a continuous pollen record for the last 140.000 years, *Quat. Res., 9*, 1-21, 1978.

Wooster, W. S., A. Bakun and D. R. McLain, The seasonal upwelling cycle along the North Atlantic, *J. Mar. Res., 34*, 131-141, 1976.

Yiou, P., J. Jouzel, S. Johnsen and Ö. E. Rögnvaldson, Rapid oscillations in Vostok and GRIP ice cores, *Geophys. Res. Lett., 22*(16), 2,179-2,182, 1995.

Yu, E.F., R. Francois, and M.P. Bacon, Similar rates of modern and last-glacial ocean thermohaline circulation inferred from radiochemical data, *Nature, 379*, 689-694, 1996.

Zahn, R., J. Schönfeld, H.-R. Kudrass, M.-H. Park, H. Erlenkeuser, and P. Grootes, Thermohaline instability in the North Atlantic during Heinrich events: stable isotope and faunal records from Core SO75-26KL, Portuguese Margin, *Paleoceanography*, 1997, in press.

Zahn, R. and R. Keir, Tracer-nutrient correlations in the upper ocean: observa-

tional and box model constraints on the use of benthic foraminiferal $\delta^{13}C$ and Cd/Ca as paleo-proxies for the intermediate-depth ocean, in R. Zahn, T.F. Pedersen, M. Kaminski and L. Labeyrie (eds.), *Carbon Cycling in the Glacial Ocean: Constraints on the Ocean's Role in Global Change, NATO ASI Series I, Vol. 17*, 195-221, 1994.

Zahn, R. and A. C. Mix, Benthic foraminiferal $\delta^{18}O$ in the ocean's temperature-salinity field: constraints on ice age thermohaline circulation, *Paleoceanography, 6* (1), 1-20, 1991.

Zahn, R., T. F. Pedersen, B. D. Bornhold, and A. C. Mix, Watermass conversion in the glacial subarctic Pacific (59°N, 148°W): physical constraints and the benthic planktonic stable isotope record, *Paleoceanography, 6* (5), 543-560, 1991.

Zahn, R. and T. F. Pedersen, Late Pleistocene evolution of surface and mid-depth hydrography at the Oman Margin: planktonic and benthic isotope records at ODP Site 724, in *Proceedings of the Ocean Drilling Program, Part B: Scientific Results, Leg 117*, edited by W. L. Prell and N. Niitsuma, 291-308, 1991.

Zahn, R., M. Sarnthein and H. Erlenkeuser, Benthic isotope evidence for changes of the Mediterranean outflow during the late Quaternary, *Paleoceanography, 2*, 543-559, 1987.

Zahn, R., K. Winn, and M. Sarnthein, Benthic foraminiferal $\delta^{13}C$ and accumulation rates of organic carbon (*Uvigerina peregrina* group and *Cibicidoides wuellerstorfi*), *Paleoceanography, 1*, 27-42, 1986.

Zenk, W., On the origin of the intermediate double-maxima in T/S profiles from the North Atlantic. *"Meteor" Forsch.-Ergebn.*, A(16), 35-43, 1975.

Zenk, W. and L. Armi, The complex spreading pattern of Mediterranean Water off the Portuguese continental slope, *Deep-Sea Res., 37*, 1805-1823, 1990.

Zhao, M., N.A.S. Beveridge, N.J. Shackleton, M. Sarnthein, and G. Eglinton, Molecular stratigraphy of cores off northwest Africa: sea surface temperature history over the last 80 ka, *Paleoceanography, 10*, 661-675, 1995.